

Localization of BMP receptors in distinct plasma membrane domains and its impact on BMP signaling

**Dissertation zur Erlangung des
naturwissenschaftlichen Doktorgrades
der Bayerischen Julius-Maximilians-Universität Würzburg**

vorgelegt von
Anke Hartung
aus Bleicherode

Würzburg 2006

Eingereicht am:

Mitglieder der Promotionskommission:

Vorsitzender:

1. Gutachter : Prof. Dr. P. Knaus

2. Gutachter: Prof. Dr. G. Krohne

Tag des Promotionskolloquiums:

Doktorurkunde ausgehändigt am:

Holzhacken ist deshalb so beliebt, weil man bei dieser Tätigkeit den Erfolg sofort sieht...

Albert Einstein

Index

1	INTRODUCTION	1
1.1	TRANSFORMING GROWTH FACTOR- β SUPERFAMILY	1
1.2	BONE MORPHOGENETIC PROTEINS.....	1
1.3	BMP2 SIGNAL TRANSDUCTION	3
1.3.1	BMP receptors.....	4
1.3.2	Smad-dependent pathways.....	5
1.3.2.1	Smad proteins.....	5
1.3.2.2	Regulation of Smad proteins	6
1.3.2.3	Smad proteins in the nucleus	7
1.3.3	Smad-independent pathways.....	9
1.3.4	Inhibitors of BMP signaling.....	9
1.3.5	Antagonists of BMPs	10
1.4	DISEASES RELATED TO BMP2 AND ITS RECEPTORS.....	12
1.5	ORGANIZATON OF THE PLASMA MEMBRANE AND ENDOCYTOSIS	14
1.5.1	Models of membrane structure	14
1.5.2	Endocytosis.....	15
1.5.3	Clathrin-mediated endocytosis.....	17
1.5.4	Caveolae-mediated endocytosis	19
1.5.4.1	The caveolin protein family	20
1.5.4.2	Caveolae as “signalosomes”	22
1.5.4.3	Studies of caveolin-1-deficient mice.....	23
1.5.5	Other endocytic routes	24
1.6	ENDOCYTIC REGULATION OF TGF- β SIGNALING	24
1.7	AIM OF THE PROJECT.....	26
2	MATERIAL AND SOLUTIONS.....	27
2.1	CHEMICALS.....	27
2.2	TECHNICAL DEVICES.....	27
2.3	ENZYMES	28
2.3.1	Restriction endonucleases	28
2.3.2	DNA- and RNA- modifying enzymes.....	28

2.4	KITS	28
2.5	OLIGONUCLEOTIDES	28
2.6	EXPRESSION VECTORS	28
2.7	BACTERIAL STRAINS	29
2.8	GROWTH MEDIA AND REAGENTS FOR CELL CULTURE	29
2.9	CELL LINES	30
2.10	GROWTH FACTORS	31
2.11	ANTIBODIES	31
2.12	STANDARDS	34
2.12.1	DNA-standards	34
2.12.2	Protein-standards	34
3	METHODS	35
3.1	MICROBIOLOGICAL METHODS	35
3.1.1	Sterilization	35
3.1.2	Growth media	35
3.1.3	Cultivation and conservation of bacteria	35
3.1.4	Preparation of chemically competent <i>E.coli</i>	36
3.1.5	Transformation of competent <i>E.coli</i> by heat-shock.....	36
3.2	MOLECULAR BIOLOGICAL METHODS	37
3.2.1	Plasmid-DNA amplification and isolation.....	37
3.2.2	Determination of nucleic acid concentrations	37
3.2.3	Agarose gel electrophoresis.....	37
3.2.4	DNA sequencing	38
3.2.5	RNA extraction	38
3.2.6	Reverse transcription	39
3.2.7	Polymerase chain reaction (PCR).....	39
3.2.8	Caveolin-1 knockdown via RNA interference	40
3.3	CELL BIOLOGICAL METHODS	41
3.3.1	Cultivation of eukaryotic cells.....	41
3.3.2	Determination of cell number	41
3.3.3	Cryo-conservation of cells	41
3.3.4	Transfection of eukaryotic cells	42

3.3.4.1	Transfection of 293T cells using Calcium-phosphate coprecipitation	42
3.3.4.2	Transfection of COS-7 cells using DEAE-dextran.....	42
3.3.4.3	Transfection of C2C12 cells using Lipofectamine™	43
3.3.4.4	Transfection using Polyetylenimine (PEI).....	43
3.3.5	Cholesterol depletion.....	44
3.3.5.1	Preparing of lipoprotein-deficient serum	45
3.3.5.2	Lovastatin activation and treatment.....	45
3.3.5.3	Methyl-β-cyclodextrin treatment.....	46
3.3.5.4	Quantitation of cholesterol level.....	47
3.3.6	Inhibition of clathrin-coated pit-mediated endocytosis by chlorpromazine	47
3.3.7	Cellular assays	48
3.3.7.1	Determination of Phospho-Smad1/5	48
3.3.7.2	Determination of Phospho-p38	49
3.3.7.3	Determination of BMP2-induced transcriptional activity using reportergene assay	49
3.3.7.4	Determination of Alkaline phosphatase activity	50
3.3.8	Microscopy.....	51
3.4	PROTEIN CHEMICAL METHODS.....	52
3.4.1	Cell lysis	52
3.4.2	Separation of detergent-resistant membrane fractions	52
3.4.3	Protein precipitation by chloroform-methanol-extraction.....	54
3.4.4	Protein quantification using the BCA assay (Redinbaugh-method)	54
3.4.5	Immunoprecipitation	55
3.4.6	SDS-polyacrylamid gel electrophoresis (SDS-PAGE).....	55
3.4.7	Western blot and detection of immobilized proteins	57
3.4.8	Immunofluorescence	58
3.4.9	Immuno-electron microscopy.....	59
4	RESULTS	61
4.1	CAVEOLIN-1 EXPRESSION AND CAVEOLAE FORMATION IN DIVERSE CELL TYPES ...	61
4.1.1	Caveolin-1 expression.....	61
4.1.2	Caveolae formation.....	63
4.2	LOCALIZATION OF BMP RECEPTORS IN PLASMA MEMBRANE REGIONS.....	64
4.2.1	Isolation and analyses of caveolin-1-enriched membrane fractions	64
4.2.1.1	Establishing the method.....	65
4.2.1.2	Analyses of BMP receptor localization in C2C12 cells.....	66
4.2.1.3	Analyses of BMP receptor localization in 293T cells	69
4.2.2	Co-Immunoprecipitation studies to detect cav-1/BMP receptor interaction	72
4.2.3	Immuno-microscopical techniques to verify colocalization of cav-1 and BMP receptors.....	74
4.2.3.1	Immunofluorescence approach.....	74

4.2.3.2	Immuno-electronmicroscopy approach.....	76
4.3	FUNCTIONAL RELEVANCE OF ENDOCYTIC PATHWAYS ON BMP SIGNALING	77
4.3.1	Influence of cholesterol-sensitive plasma membrane regions on BMP signaling	78
4.3.1.1	Cholesterol depletion decreases cholesterol levels	78
4.3.1.2	Effect of cholesterol depletion on Smad1/5 phosphorylation	80
4.3.1.3	Effect of cholesterol depletion on transcriptional activity.....	81
4.3.1.4	Effect of cholesterol depletion on Alkaline phosphatase activity.....	82
4.3.2	Influence of caveolin-1 overexpression on BMP signaling	83
4.3.2.1	Effect of caveolin-1 overexpression on Smad1/5 phosphorylation.....	83
4.3.2.2	Effect of caveolin-1 overexpression on transcriptional activity.....	85
4.3.2.3	Effect of caveolin-1 overexpression on Alkaline phosphatase activity.....	87
4.3.3	Influence of caveolin-1 knockdown by RNAi on BMP signaling.....	88
4.3.3.1	Effect of caveolin-1 knockdown on Smad1/5 phosphorylation.....	88
4.3.3.2	Effect of caveolin-1 knockdown on transcriptional activity	88
4.3.4	Influence of clathrin-coated pit-dependent endocytosis on BMP signaling.....	89
4.3.4.1	Effect of chlorpromazine on Smad1/5 phosphorylation.....	90
4.3.4.2	Effect of chlorpromazine on transcriptional activity.....	91
4.3.4.3	Effect of chlorpromazine on Alkaline phosphatase activity.....	91
4.3.5	Influence of the Dynamin2 mutant K44A on BMP signaling.....	92
4.3.5.1	Effect of Dynamin 2 mutant K44A on Smad1/5 phosphorylation.....	92
4.3.5.2	Effect of Dynamin 2 mutant K44A on transcriptional activity.....	93
4.3.5.3	Effect of Dynamin 2 mutant K44A on Alkaline phosphatase activity.....	94
5	DISCUSSION.....	96
5.1	LOCALIZATION OF BMP RECEPTORS	97
5.1.1	Evidences for BMP receptor localization in DRM regions and caveolae.....	97
5.1.2	Evidences for BMP receptor localization in clathrin-coated pits	101
5.2	IMPACT OF BMP RECEPTOR LOCALIZATION ON BMP SIGNAL TRANSDUCTION.....	102
5.2.1	Effects on Smad1/5 phosphorylation	103
5.2.2	Effects on BMP2-induced transcription of target genes.....	105
5.2.3	Effects on Alkaline phosphatase production.....	108
5.3	THE CURRENT MODEL OF THE ENDOCYTIC IMPACT ON BMP SIGNALING.....	109
6	SUMMARY – ZUSAMMENFASSUNG	111
7	REFERENCES	113

Appendix

A 1 ABBREVIATIONS I

A 2 SEQUENCES OF RECEPTOR CONSTRUCTS AND OLIGONUCLEOTIDES ... V

DANKSAGUNG IX

LEBENS LAUF XI

SCHRIFTENVERZEICHNIS XII

ERKLÄRUNG.....XIV

Index of Figures

Fig. 1.1 Butterfly-shape structure of BMP2 (Scheufler et al., 1999).....	2
Fig. 1.2 Epitopes of the BMP2 dimer (Kirsch et al., 2000).	3
Fig. 1.3 BMP signal transduction pathways (Nohe et al., 2002).	4
Fig. 1.4 Structural organization of Smad family members (Nishimura et al., 2003).....	6
Fig. 1.5 PPH mutations identified in the gene for BRII (Waite and Eng, 2003).....	12
Fig. 1.6 Models for membrane structure (Engelman, 2005).....	15
Fig. 1.7 Portals of cell entry (Conner and Schmid, 2003).	16
Fig. 1.8 Schematic demonstration of CME (Conner and Schmid, 2003).	17
Fig. 1.9 Schematic demonstration of clathrin- and AP-2-structure (Mousavi et al., 2004).....	18
Fig. 1.10 Schematic representation of the domain structure of dynamin (Peplowska and Ungermann, 2005).....	18
Fig. 1.11 Structure of caveolae and membrane topology of cav-1 (Parton, 2001).	21
Fig. 1.12 Interaction of cav-1 with signaling molecules (Razani et al., 2002c).	22
Fig. 3.1 Structure of Lovastatin (Calbiochem).....	45
Fig. 3.2 Structure of one glucopyranose unit of M β CD (Sigma).....	46
Fig. 3.3 Structure of chlorpromazine (Sigma).....	47
Fig. 4.1 Investigation of cav-1 expression in different cell types by RT-PCR and western blot.....	61
Fig. 4.2 Detection of cav-1-isoforms using different antibodies.	62
Fig. 4.3 Electron microscopy on 293T (A) and C2C12 (B) cells.....	63
Fig. 4.4 Comparison of Triton X-100 and CHAPS extracts.....	65
Fig. 4.5 Summary of the improvements on the separation of DRMs from C2C12 cells.	66
Fig. 4.6 Separation of DRMs from C2C12 cells stably overexpressing BRII-LF.....	67
Fig. 4.7 Separation of DRMs from C2C12 cells stably overexpressing BRII-SF.	67
Fig. 4.8 Separation of DRMs from C2C12 cells stably overexpressing BRII-TC1.	68
Fig. 4.9 Separation of DRMs from C2C12 cells stably overexpressing BRIB.	68
Fig. 4.10 Separation of DRMs from 293T cells transfected with BRIa together with or without cav-1 α	70
Fig. 4.11 Separation of DRMs from 293T cells transfected with BRII-LF together with or without cav-1 α	71
Fig. 4.12 Co-Immunoprecipitation studies between BMP receptors and cav-1 α in C2C12 cells.	73
Fig. 4.13 Co-Immunoprecipitation of BRIa and cav-1 α in 293T cells.....	74
Fig. 4.14 Immunofluorescence approach in C2C12-LF and C2C12-BRIa cells.....	75
Fig. 4.15 Immunofluorescence approach in C2C12-TC1 cells.....	76
Fig. 4.16 Immuno-electronmicroscopy approach in C2C12-LF cells.	77
Fig. 4.17 Examples for cholesterol assays on C2C12 and 293T cells.....	79
Fig. 4.18 Effect of cholesterol depletion on Smad1/5 phosphorylation in C2C12 cells.....	80
Fig. 4.19 Effect of cholesterol depletion on BMP2-dependent transcriptional activity in C2C12 cells. .	81

Index

Fig. 4.20 Effect of cholesterol depletion on ALP activity in C2C12 cells.....	82
Fig. 4.21 Influence of cav-1 α overexpression on Smad1/5 phosphorylation in C2C12 cells.....	83
Fig. 4.22 Influence of cav-1 α overexpression on Smad1/5 phosphorylation in 293T cells.....	84
Fig. 4.23 Effect of EGFP-tagged cav-1 α overexpression on BMP2-induced transcriptional activity using SBE- or BRE-reportergene constructs in C2C12 cells.	85
Fig. 4.24 Influence of the pEGFP-vector backbone on cav-1 effect on BMP signaling.	86
Fig. 4.25 Effect of HA-tagged cav-1 α overexpression on BMP2-induced transcriptional activity in C2C12 cells.	86
Fig. 4.26 Effect of cav-1 α overexpression on ALP activity in C2C12 cells.....	87
Fig. 4.27 Effect of cav-1 knockdown on Smad1/5 phosphorylation.	88
Fig. 4.28 Effect of cav-1 knockdown on BMP2-induced transcriptional activity.....	89
Fig. 4.29 Effect of chlorpromazine on Smad1/5 phosphorylation.....	90
Fig. 4.30 Effect of chlorpromazine on BMP2-induced transcriptional activity.	91
Fig. 4.31 Effect of chlorpromazine on ALP activity.....	92
Fig. 4.32 Effect of dynamin 2 on Smad1/5 phosphorylation.....	93
Fig. 4.33 Influence of dynamin 2 on BMP signaling.	94
Fig. 4.34 Effect of dynamin 2 on ALP activity.....	94
Fig. 5.1 Trajectories of BRIA and BRII overexpressing C2C12 cells (Dr. A. Noskov, Prof. G. Harms, Virchow Center, University of Würzburg; unpublished data).....	98
Fig. 5.2 Summary of main evidences for BMP receptor localization.....	102
Fig. 5.3 Smad1/5 phosphorylation takes place at the cell surface.....	105
Fig. 5.4 Influence of endocytic events on BMP2 signal transduction.....	107
Fig. 5.5 ALP production is influenced by endocytic events.....	109
Fig. 5.6 Summary of the effects of BMP receptor localization on BMP signaling (Hartung et al., submitted).....	110

Index of Tables

Table 2.1 List of first and secondary antibodies, used during this work.....	33
Table 2.2 Molecular Weight Standard SDS-7B.....	34
Table 3.1 PEI-transfection of different cell types.....	44
Table 3.2 Filter sets of the fluorescence microscope.....	51
Table 3.3 Pipetting scheme for SDS-PAGE.....	56
Table 4.1 Quantitative summary of flotation assays in C2C12 cells.....	69
Table 4.2 Quantitative summary of flotation assays in 293T cells.....	71

1 INTRODUCTION

1.1 TRANSFORMING GROWTH FACTOR- β SUPERFAMILY

The Transforming Growth Factor- β (TGF- β) superfamily expresses a large set of structurally and functionally related polypeptides; more than 60 family members have been identified so far (Feng and Derynck, 2005). The family is divided into two general branches: the Bone Morphogenetic Protein (BMP)/Growth and Differentiation Factor (GDF) and the TGF- β /Activin/Nodal branch (Balemans and Van Hul, 2002). A divergent member of that family, which cannot be grouped in one of these subfamilies, is Mullerian Inhibiting Substance (MIS) or Anti-Mullerian Hormone (AMH) (Cate et al., 1986).

The growth factors of this superfamily regulate cell migration, adhesion, differentiation and tissue morphogenesis as well as cell death in a variety of cell types and organisms and are highly conserved during evolution from mammals to *Xenopus*, *Caenorhabditis elegans* to *Drosophila*.

TGF- β superfamily members transmit their signals through two types of transmembrane serine/threonine kinase receptors and diverse nuclear factors, among them the most common are Smads. Upon phosphorylation by the receptors, Smad complexes translocate into the nucleus where they direct gene expression. These processes need to be tightly controlled. Various molecules are involved in the regulation of this signaling cascade, e.g. inhibitors, antagonists, pseudoreceptors, activators or repressors of transcription. Besides Smad-mediated transcription, the activation of different other Smad-independent signaling pathways can be observed, including the p38- and ERK-MAPK pathways (Derynck and Zhang, 2003). However, the mechanisms of how these pathways are initiated and the biological consequences are poorly understood.

So far only five type II and seven type I receptors have been identified (Feng and Derynck, 2005). The number of ligands from this superfamily exceeds the number of associated receptors by far, causing versatility in receptor interactions and ligand binding.

1.2 BONE MORPHOGENETIC PROTEINS

Bone Morphogenetic Proteins (BMPs) are multifunctional growth factors (Hogan, 1996) which were at first discovered by their ability to induce ectopic bone and cartilage formation *in vivo* (Urist, 1965). BMPs are also able to direct cell fate of mesenchymal cells *in vitro* by stimulating osteoblast differentiation and inhibiting differentiation into the myoblast lineage (Katagiri et al., 1994; Vukicevic et al., 1989; Yamaguchi et al., 1991). Today BMPs are known to play also important roles in non-osteogenic developmental processes like ventral mesoderm induction by BMP4 in *Xenopus laevis* (Dale et al., 1992; Jones et al., 1992),

epidermal induction (Munoz-Sanjuan and Brivanlou, 2002) or development of neural crest cells into neuronal phenotypes by BMP2 (Christiansen et al., 2000). BMPs are also involved in key processes in the adult organism: they regulate proliferation, differentiation, chemotaxis as well as apoptosis (Hogan, 1996).

More insight into the functions of BMPs were gained by studies on knock out animals (summarized in: Botchkarev, 2003). Therefore ligands, receptors and adaptor proteins or inhibitors were addressed. Such studies revealed that loss-of-function mutations of the ligands BMP2 or BMP4, the BMP-type Ia receptor or the Smad proteins Smad1, 4 or 5 result in early embryonic lethality due to defects in developing mesoderm, ectoderm and endoderm (Chang et al., 1999; Lechleider et al., 2001; Mishina et al., 1995; Sirard et al., 1998; Tremblay et al., 2001; Winnier et al., 1995; Yang et al., 1999; Yang et al., 1998; Zhang and Bradley, 1996). Gain-of-function mutations cause lethality in later stages of embryonic development, as for example constitutive deletion of BMP antagonist noggin leads to abnormalities in brain and skeletal development (Brunet et al., 1998; McMahon et al., 1998). The pleiotropic functions of BMPs implicate a strong need for regulation of BMP signaling. Inhibitors of BMP signaling molecules or antagonists of BMP ligands are potent effectors for regulation (see 1.3.4 and 1.3.5).

The ligand BMP2 is secreted as a pre-propeptide in which the N-terminal signal sequence indicates the precursor molecule for the secretory pathway. The prodomain that is also situated N-terminally, is responsible for the correct folding and activity of the signal molecule. The C-terminal mature peptide with a length of 114 amino acids is released upon furin-mediated cleavage (Bottner et al., 2000).

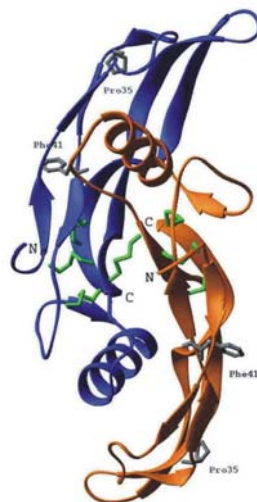


Fig. 1.1 Butterfly-shape structure of BMP2 (Scheufler et al., 1999).

BMP2 represents a dimer of two identical monomers, here depicted in blue and orange. The cystine-bridge connecting the two monomers and the cystine bridges of the cystine-knot motif are depicted in green.

The physiological active molecule is a dimer with a molecular weight of 25,8 kD. The crystal structure of mature human BMP2 was resolved by X-ray analyses at 2,7 Å resolution (Scheufler et al., 1999). BMP2, like every member of the TGF- β superfamily, comprises the cystine-knot motif. One of the seven cysteine residues is used for covalent inter-chain disulfide bridging; the others form an intramolecular ring, known as the cystine-knot configuration, which drives the molecules to undergo dimerization resulting in highly stable dimeric proteins with a butterfly-shape structure (Fig. 1.1) (Scheufler et al., 1999).

1.3 BMP2 SIGNAL TRANSDUCTION

BMP2 binds to two transmembrane serine/threonine kinase receptors, the BMP-type I and – type II receptors (BRI, BRII). It was shown that BMP2 contains two symmetrical pairs of juxtaposed epitopes: the wrist and the knuckle epitope. While the wrist epitope binds BRI with high affinity and consists of residues from both BMP2 monomers, the knuckle epitope resembles the low affinity site for BRII and comprises residues from only one monomer (see Fig. 1.2) (Kirsch et al., 2000; Knaus and Sebald, 2001; Nickel et al., 2001).

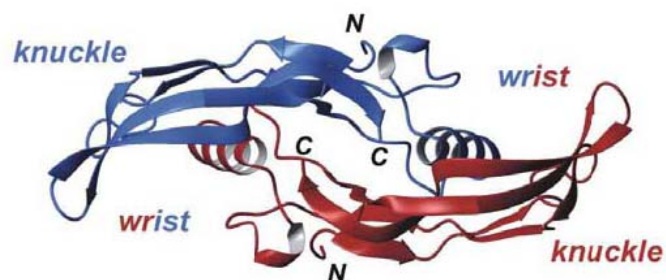


Fig. 1.2 Epitopes of the BMP2 dimer (Kirsch et al., 2000).

The wrist epitope binds BRI with high affinity, the knuckle epitope binds BRII.

BMP receptor activation occurs upon ligand binding to preformed receptor complexes (PFCs) or BMP2-induced signaling complexes (BISCs) composed of BRI and BRII. Binding of BMP2 to PFCs results in activation of the Smad pathway, whereas BISCs initiate the activation of Smad-independent pathways resulting in induction of Alkaline phosphatase (ALP; see Fig. 1.3) (Nohe et al., 2002). On the one hand, Smad proteins (R-Smads) are recruited to and phosphorylated by the receptors, on the other hand p38-MAPK, Ras and ERK pathways get activated upon BMP receptor stimulation.

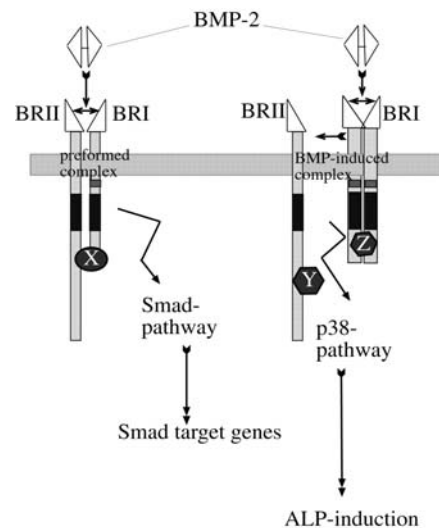


Fig. 1.3 BMP signal transduction pathways (Nohe et al., 2002).

1.3.1 BMP receptors

BMPs bind with different affinities to BMP type I- and type II receptors. So far, ALK3/BRIa, ALK6/BRIb and ALK2/ActRI are described to be BMP type I receptors and BRII (short form – SF and long form – LF; as described in Rosenzweig et al., 1995), ActRII and ActRIIb to be BMP type II receptors. BRIa, BRIb and BRII are BMP-specific receptors, whereas ActRI, ActRII and ActRIIb are also transmitting signals from Activins.

Type I receptors exhibit a molecular weight of about 50 kD and show an extracellular ligand-binding domain, a single transmembrane domain and a cytoplasmatic serine/threonine kinase domain. Type II receptors are similarly organized like type I receptors, but since they are more glycosylated, their molecular weight is around 75 kD. As a speciality, BRII-LF exhibits a long C-terminal extension, called the tail domain, following the kinase domain, resulting in a molecular weight of about 170 kD.

In response to ligand binding, type I receptors get trans-phosphorylated by the constitutive active kinase of type II receptors at their GS-box, a glycine/serine (SGSGSG) rich region preceding the kinase domain (Wrana et al., 1994). Phosphorylation of the GS-box triggers Smad-binding to type I receptors and contributes to the strength and stability of this interaction (Chen and Massague, 1999; Wu et al., 2001). However, the specificity of signaling is achieved through the L45 loop, a 9 amino acid sequence within the kinase domain of type I receptors, which binds to the L3 loop in the MH2 domain of the respective R-Smads (Chen et al., 1998b; Lo et al., 1998). This allows the type I receptor kinase to phosphorylate the C-terminal SSXS-motif of R-Smads resulting in a conformational change in and dissociation of the activated Smad, followed by heteromerization with Smad4. Smad1, 5 and 8 are substrates for BRIa, BRIb, ALK1 (which binds TGF- β type II receptor) and

ALK2/ActRI, whereas Smad2 and 3 are activated by TGF- β type I receptor, ALK4/ActRIb and ALK7.

As mentioned before, signaling responses depend on the ligand and receptor combinations, but also differential Smad-activation as well as distinct ligand-induced internalization and routing of the receptor complexes contribute to the regulatory mechanisms. Different signaling responses are initiated for example by BRIa and BRIb. While BRIa promotes adipogenic differentiation, BRIb is more potent in osteoblast differentiation (Chen et al., 1998a).

Recently, DRAGON, a GPI-anchored protein, was described as a coreceptor for BMPs. DRAGON directly interacts with ligands and receptors to facilitate BMP signaling (Samad et al., 2005). In addition, the same group published evidences for a second coreceptor: repulsive guidance molecule (RGM), a homologue of DRAGON, seems to be similarly involved in the BMP signaling pathway (Babitt et al., 2005).

Mutations in BRII have been found in patients with familial primary pulmonary hypertension (PPH; see 1.4), which is a rare autosomal dominant disorder (Deng et al., 2000; Lane et al., 2000; Newman et al., 2001). Null mutation of the BRIa gene in mice causes embryonic lethality due to lack of mesoderm formation in the developing embryo (Mishina et al., 1995). Mice lacking BRIb are viable, exhibiting a markedly reduced proliferation of prechondrogenic cells and chondrocyte differentiation as well as defects in the appendicular skeleton (Yi et al., 2000). These examples manifest the importance of BMP receptors and BMP signaling on developmental processes in mammals.

1.3.2 Smad-dependent pathways

The Smad pathway is the best characterized and understood pathway involved in signaling of TGF- β superfamily members. In TGF- β -induced Smad signaling a specialized protein (SARA = Smad anchor for receptor activation) links Smads to the receptor and the Smad pathway to endosomes (Di Guglielmo et al., 2003; Tsukazaki et al., 1998). Such a protein is not yet known for the other members of this family. Another speciality was observed in BMP-Smad signaling. It was shown that Smad signaling is specifically initiated at PFCs, whereas Smad-independent signaling requires activation via BISCs (see Fig. 1.3) (Nohe et al., 2002).

1.3.2.1 Smad proteins

Smads are structurally related signaling effector molecules. Eight vertebrate Smads are known so far which can be divided by their function into three subclasses: the receptor associated Smads (R-Smads: Smad1, 2, 3, 5 and 8) that become phosphorylated by type I receptors, the common-mediator Smad4 (Co-Smad) which oligomerizes with activated R-

Smads and the inhibitory Smads (I-Smads, Smad6 and 7) which get also activated upon ligand stimulation (Fig. 1.4).

R-Smads are released from the receptor complex to form a heterotrimeric complex of two R-Smads and Smad4 that in turn translocates to the nucleus. I-Smads are structurally divergent and exert a negative feedback effect by marking the receptors for degradation and by competing with R-Smads for receptor interaction.

R- and Co-Smads contain a conserved MAD-homology (MH) 1 and C-terminal MH2 domain, flanking a linker segment. I-Smads instead have only a MH2 domain (Fig. 1.4).

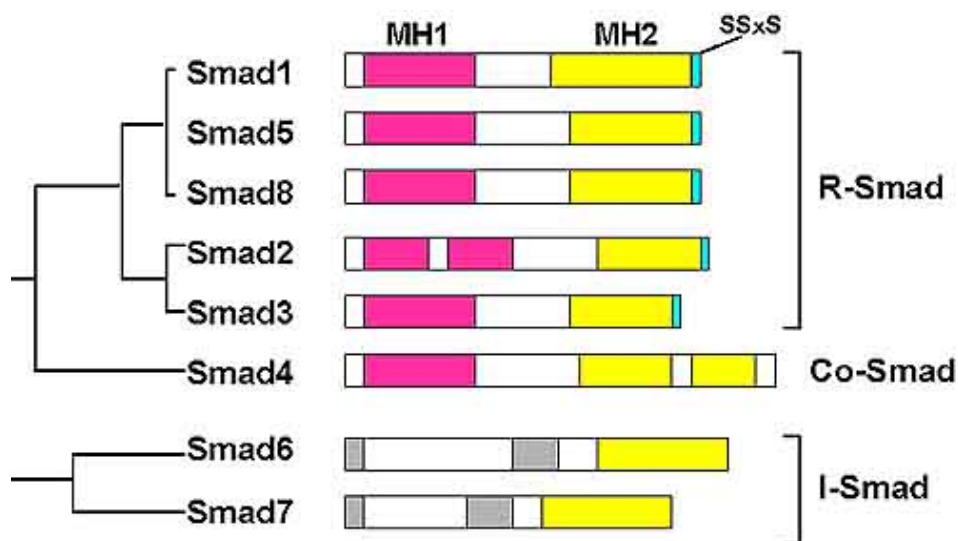


Fig. 1.4 Structural organization of Smad family members (Nishimura et al., 2003).

Receptor-associated Smads (R-Smads), common-mediator Smad (Co-Smad) and inhibitory Smads (I-Smads) are depicted. R-Smads contain a specific phosphorylation motif, SSXS, in the C-terminal region.

MH1 and MH2 domains interact with sequence-specific transcription factors. While MH1 domains (except the one of Smad2) can bind DNA, MH2 domains of R-Smads alone can recruit the related coactivators CREB-binding protein (CBP) or p300 and mediate Smad oligomerization as well as Smad-receptor interaction (Itoh et al., 2000; Massague, 2000; Moustakas et al., 2001).

1.3.2.2 Regulation of Smad proteins

Because of their key position in signaling of TGF- β family members, expression levels and activation of Smad proteins need to be tightly regulated by several mechanisms. Expression levels of I-Smads are controlled by extracellular signals, representing an auto-inhibitory feedback mechanism for ligand-induced signaling. The levels of R-Smads are post-translationally regulated by ubiquitin-proteasome-mediated degradation. Hereby, Smad-ubiquitination-regulatory factor (Smurf) 1 and 2 (see 1.3.4) interact with R-Smads and target

them for degradation (Arora and Warrior, 2001). Proteasomal degradation can regulate R-Smad levels also after translocation into the nucleus (Fukuchi et al., 2001; Lo and Massague, 1999). Sumoylation was observed for Smad4 which enhances the stability of this protein (Lee et al., 2003).

Several proteins are known to interact with Smad proteins and thereby regulate their activity and signaling features. One example is the Smad anchor for receptor activation (SARA), which specifically interacts with Smad2 and the TGF- β receptor complex. SARA and the adaptor protein disabled (Dab) 2, which also binds Smad2 and the receptors, are enriched in endosomes and clathrin-coated vesicles (CCVs) and promote Smad phosphorylation and TGF- β signaling (Di Guglielmo et al., 2003; Hocevar et al., 2001). SARA forms a bridge between the receptor complex and non-activated Smad2 and assists in phosphorylation of Smad2 by the TGF- β type I receptor (Tsukazaki et al., 1998). Furthermore, it inhibits nuclear import of Smad2 (Xu et al., 2000a). For the BMP7 signaling cascade CD44, a hyaluronan receptor, was reported to bind Smad1 and influence its nuclear translocation (Peterson et al., 2004). Another example is the interaction of un-phosphorylated Smad2 and 3 with microtubule filaments which prevents the R-Smads from phosphorylation and activity (Dong et al., 2000). Another mechanism to regulate the activation of R-Smads is provided by binding of the MH2 domain of I-Smads to type I receptors. This interaction prevents the recruitment and phosphorylation process of R-Smads. Additionally, Smad6 interferes with the heteromerization of BMP-activated R-Smads with Smad4 (see 1.3.4).

Smad proteins can also be regulated by other kinase pathways. ERK-MAPK, MEKK1, JNK, Ca²⁺/calmodulin-dependent protein kinase (CamKII) and PKC influence R-Smads by specific phosphorylation (Brown et al., 1999; Funaba et al., 2002; Kretzschmar et al., 1999; Wicks et al., 2000; Yakymovych et al., 2001). In contrast, mammalian Co-Smad4 is not regulated by phosphorylation, but I-Smads are also phosphorylated independent of TGF- β stimulation (Pulaski et al., 2001).

These mechanisms are described in more detail and completeness in several review articles (Derynck and Zhang, 2003; Feng and Derynck, 2005; Moustakas et al., 2001).

1.3.2.3 Smad proteins in the nucleus

There are several proteins which interact with Smads in the nucleus and therefore regulate Smad-dependent transcriptional activity. Among these are DNA-binding transcription factors, co-activators and co-repressors (reviewed in Derynck and Zhang, 2003; Feng and Derynck, 2005; Moustakas et al., 2001). Additionally the nuclear translocation after activation and oligomerization of R-Smads is tightly regulated and organized.

Inactive R-Smads localize completely to the cytoplasm and are imported into the nucleus after ligand and type I receptor-induced phosphorylation of two serine residues in their MH2 domain. This results in conformational changes, exposing the lysine-rich nuclear localization sequence (NLS) in their MH1 domain to allow importin- β binding, thus nuclear import (Kurisaki et al., 2001; Xiao et al., 2001; Xu et al., 2000a). Due to the presence of the unique exon3 in the MH1 domain of Smad2, Smad2 nuclear import is importin- β -independent, requiring instead a region of the MH2 domain (Kurisaki et al., 2001; Xu et al., 2000a; Yagi et al., 1999).

In contrast, Co-Smad4 shuttles continuously between cytoplasm and nucleus, conferring to a constitutively active NLS in its MH1 domain and a nuclear export signal (NES) in the linker region, its activity regulated by the nuclear transport receptor CRM1 (Inman et al., 2002; Watanabe et al., 2000).

I-Smads are constitutively imported to the nucleus and can act as transcription co-factors, as for example Smad7 is interacting with the co-activator CBP/p300 (Gronroos et al., 2002). The export of Smad7 is induced by TGF- β , maybe via an interaction with Smurf1 or 2 (Hanyu et al., 2001), whereas Smad6 export is BMP-induced (Itoh et al., 2001).

In the nucleus R-Smads get constantly dephosphorylated, resulting in dissociation of the Smad complex and export of the inactive Smads to the cytoplasm (Inman et al., 2002; Xu et al., 2002).

Interestingly, the nuclear export of R-Smads is regulated in different ways. Smad1 contains a NES in its MH1 domain, resulting in constitutive export (Xiao et al., 2001), whereas no NES could be identified in Smad2 and 3 which exit the nucleus only after prolonged treatment with the ligand TGF- β (Pierreux et al., 2000).

Smads are weak DNA-binding proteins, thus their function needs to be enhanced and regulated by a large number of sequence-specific DNA-binding transcription factors as well as co-activators and co-repressors (reviewed in Derynck and Zhang, 2003; Feng and Derynck, 2005; Moustakas et al., 2001).

After entering the nucleus, Smad complexes (except for Smad2, again due to the unique exon3 in its MH1 domain) selectively bind to Smad-binding elements (SBEs) 5'-CAGAC-3', sequences located in promoters of target genes of members of the TGF- β superfamily (Jonk et al., 1998; Kusanagi et al., 2001; Zawel et al., 1998). Alternatively, Smad1 is able to bind to a GC-rich motif (GCCG) in promoters, referred to as the BMP-responsive element (BRE) (Korchynskyi and ten Dijke, 2002; Kusanagi et al., 2000).

1.3.3 Smad-independent pathways

The best characterized Smad-independent pathways are mediated by mitogen-activated protein kinases (MAPK) like p38, extracellular signal-regulated kinase (ERK) and c-Jun N-terminal kinase (JNK). However, the mechanisms involved in these activities and the biological consequences are poorly characterized so far.

After ligand binding these pathways can be activated directly or indirectly. A direct activation is rapid (5-15 min) and independent from transcription, whereas the indirect stimulation is a slow process, requiring (mostly Smad-dependent) transcriptional activity (Derynck and Zhang, 2003; Massague, 2000). To differentiate between these two processes the use of Smad4-deficient cells or dominant-negative Smads is of great importance (Engel et al., 1999).

It was shown that BMP2 stimulates the phosphorylation of p38, leading to upregulation of type I collagen, fibronectin, osteopontin, osteocalcin and ALP (Lai and Cheng, 2002; Nohe et al., 2002). In the phosphorylation of p38 the BRI-interacting protein X-chromosome linked inhibitor of apoptosis (XIAP) is involved. XIAP links the TGF- β -activated kinase (TAK) 1 and the TAK-binding protein (TAB) to the receptor. TAB stimulates TAK1 which in turn activates p38 (through MAP kinase kinase [MKK] 3 or 6) and other factors.

Our group could show that p38 phosphorylation and ALP production are initiated at BISCs. BMP2 binds to the high affinity type I receptor, which leads to the recruitment of BRII into the complex (=BISC) and activation of the Smad-independent signaling cascade via p38 (Nohe et al., 2002).

ERK phosphorylation results in the stimulation of fibronectin and osteopontin (Lai and Cheng, 2002) and is mediated by the Ras-MEK1-ERK1/2 pathway (Lou et al., 2000; Palcy and Goltzman, 1999).

Furthermore, it was shown that BMP2 induces phosphoinositol-3-kinase (PI3K) in C2C12 cells (Vinals et al., 2002) as well as protein kinase C (PKC) and protein kinase D (PKD) (Hay et al., 2001; Lemonnier et al., 2004).

The crosstalk between the different pathways is complex and needs to be further investigated.

1.3.4 Inhibitors of BMP signaling

BMP activity can be suppressed by different mechanisms including expression of pseudoreceptors, I-Smads, intracellular Smad-binding proteins, Smurfs, extracellular antagonists and so forth (Canalis et al., 2003).

BAMBI (BMP and Activin membrane-bound inhibitor) serves as a pseudoreceptor for BMP signal transduction (Onichtchouk et al., 1999). This transmembrane protein exhibits an

extracellular domain with sequence similarity to type I receptors of the TGF- β superfamily, thus binds BMP ligands and hinders signaling by forming heterodimers with normal and constitutive active (due to mutations in GS-box) type I receptors. Its intracellular region lacks the kinase domain, therefore signaling can not be transmitted.

Smad6 and 7, the I-Smads (see 1.3.2.1), inhibit TGF- β -, BMP- and Activin signaling. Smad7 inhibits R-Smad phosphorylation by occupying type I receptors. Low concentrations of Smad6 compete with Smad4 for specific binding of receptor-activated Smad1 which leads to an inactive Smad1-Smad6 complex, thus inhibition of the BMP signaling cascade. Overexpression of Smad4 overcomes this effect and rescues BMP signaling (Hata et al., 1998). At higher levels Smad6 mimics Smad7 action and affects BMP and TGF- β signaling.

C-ski blocks BMP signaling by binding to the MH2 domain of Smad1, 4 and 5, but it associates even stronger with Smad2 and 3 (Luo et al., 1999; Wang et al., 2000). Skip (ski-interacting protein) augments (Leong et al., 2001), whereas sno (ski-related novel protein) and ski itself inactivate BMP signaling. These proteins are critical mediators in embryonic development, morphogenesis of the central nervous system and cranofacial structures (Berk et al., 1997).

Tob (transducer of Erb-B2) decreases BMP2-induced transcriptional activity by binding to the MH2 domain of Smad1, 5 and 8, thereby modifying their activity and intracellular localization (Yoshida et al., 1997). It blocks bone formation like c-ski which was shown in tob null mice. These mice are viable but exhibit an increased number of osteoblasts and a higher bone formation rate (Yoshida et al., 2000).

Smurf1 and 2 are E3 ubiquitin ligases which specifically bind to R- and I-Smads, triggering their ubiquitination and proteasomal degradation. Smurf1 preferentially interacts with Smad1 and 5, blocking specifically BMP-mediated signaling. Both Smurfs exhibit two WW domains which mediate binding to the PPXY motif in the linker region of R- and I-Smads (Smad4 lacks the PPXY motif, thus binds not to Smurfs) (Zhang et al., 2001; Zhu et al., 1999).

1.3.5 Antagonists of BMPs

BMP signaling and function is also regulated on the extracellular site by ligand-binding proteins. These molecules prevent ligand access to the signaling receptors and therefore antagonize BMP-dependent developmental processes. BMP antagonists exhibit the cystine-knot motif like all members of the TGF- β superfamily (see 1.2) and can be divided into three subgroups based on the size of their cystine ring: CAN-family (eight-membered ring), twisted gastrulation (tsg; nine-membered ring) and chordin and noggin (ten-membered ring) (Avsian-Kretchmer and Hsueh, 2004).

The CAN-family (also named: DAN/cerberus family) consists of *drm/gremlin*, *PRDC*, *cerberus*, *coco*, *DAN*, *USAG-1*, *sclerostin*, *dante* and *caronte* (among others). Some of these proteins are described below (reviewed in Canalis et al., 2003; Massague and Chen, 2000).

DAN (differential screening-selected gene aberrant in neuroblastoma) was initially identified as inhibitor of tumorigenic activity of *src*-transformed fibroblasts (Enomoto et al., 1994), whereas most of the other molecules of this family are described as regulators of developmental processes.

Cerberus is concentrated in the Spemann's organizer of the *Xenopus* early embryo (Bouwmeester et al., 1996). Microinjection of *cerberus*-mRNA induces ectopic heads, neuralizes the ectoderm, duplicates heart and liver and suppresses trunk-tail mesoderm (Bouwmeester et al., 1996). It binds with high affinity to BMP4, but is also able to bind *Xnr-1* (mesoderm-inducing factor) as well as *Xwnt8* (inducer of secondary axis) (Glinka et al., 1997; Piccolo et al., 1999). Because of that, *cerberus* is known to antagonize coordinately three trunk-forming pathways, namely the BMP, nodal and wnt pathways (Massague and Chen, 2000).

Caronte controls the BMP-nodal counterbalancing system to regulate left-right asymmetry in the chick and mouse embryo by a complex network of molecules including *Lefty-1* or *Lefty-2*, nodal, sonic hedgehog (*Shh*), *FGF-8*, BMP and *ActRII* (Rodriguez Esteban et al., 1999; Yokouchi et al., 1999).

Sclerostin (*SOST*) inhibits BMP6 and 7 (Kusu et al., 2003). The responsible gene was cloned from families exhibiting sclerosteosis (Brunkow et al., 2001).

Tsg, the only member of the nine-membered ring subgroup, forms a ternary complex together with *chordin/sog* and BMP4 and inhibits efficiently BMP signaling. Interestingly, it has also the potential to exhibit BMP agonistic activity by competing with the residual anti-BMP activity of *chordin* (Canalis et al., 2003; Chang et al., 2001; Ross et al., 2001; Scott et al., 2001).

Noggin, a 32 kD glycoprotein, binds specifically BMPs (Piccolo et al., 1996; Zimmerman et al., 1996). The antagonism by *noggin* was shown to be critical for proper skeletal development, thus *noggin* null mice exhibit excess cartilage and lack initiation of joint formation (Brunet et al., 1998; McMahon et al., 1998). Dominant mutations of *noggin* are linked to two human genetic disorders: proximal symphalangism and multiple synostoses syndrome which are characterized by bony fusions of joints (Gong et al., 1999).

Chordin is a large (120 kD) protein and its structural and functional homolog in *Drosophila* is short gastrulation (*sog*) (Holley et al., 1996). *Chordin* plays a key role in dorsalizing early vertebrate embryonic tissues by binding to ventralizing BMPs and sequestering them in complexes (Millet et al., 2001; Piccolo et al., 1996). There are also antagonists of BMP antagonists known which are linked to *chordin* called *Tolloid* (*Drosophila*)/*Xolloid*

(*Xenopus*)/BMP-1 or hTld1 (human) (Finelli et al., 1994; Takahara et al., 1994). These molecules are secreted metalloproteases which are able to interact with BMPs and thereby shaping morphogenetic gradients. Xolloid for example cleaves chordin at two specific sites, so that it is unable to antagonize BMP activity. Furthermore, it can cleave chordin also in already existing chordin/BMP-inactive complexes to release biological active BMP (Piccolo et al., 1997).

1.4 DISEASES RELATED TO BMP2 AND ITS RECEPTORS

Because of the variety of processes which are regulated by BMPs, mutations in genes which are involved in the complex BMP signal transduction pathways are linked to several, severe diseases. Three of them are discussed below: primary pulmonary hypertension (PPH), juvenile polyposis (JPS) and fibrodysplasia ossificans progressiva (FOP).

PPH is a rare autosomal dominant disorder with decreased penetrance and female predominance which was mapped to chromosome 2q33. PPH patients suffer from monoclonal plexiform lesions of proliferating endothelial cells in their pulmonary arterioles which lead to elevated pulmonary artery pressure, right ventricular failure and death (Chen et al., 2004). By genotyping multiple PPH families, several mutations in the *BRII* gene were found to cause the disease (see Fig. 1.5) (Deng et al., 2000; Lane et al., 2000; Newman et al., 2001).

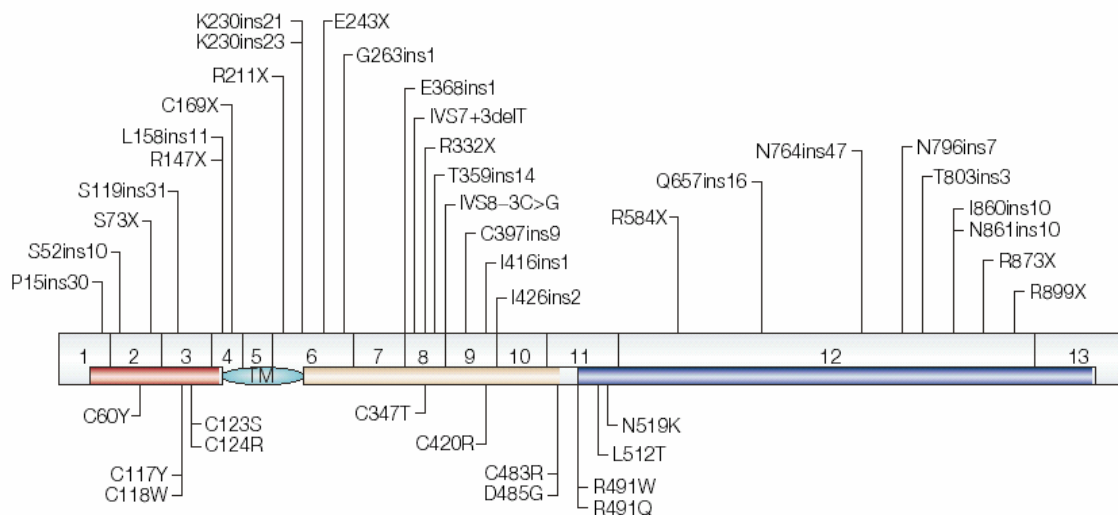


Fig. 1.5 PPH mutations identified in the gene for *BRII* (Waite and Eng, 2003).

The domain structure of *BRII* is depicted as follows: extracellular domain in red, transmembrane domain (TM) in light blue, kinase domain in yellow and tail domain in dark blue. Truncating mutations are displayed above and missense mutations below. ins = insertion

Only 13 of the 41 known distinct mutations are missense mutations, being situated predominantly outside of the tail domain. Truncating mutations are more distributed over the

gene, although 75% of these mutations lie in the ligand binding and kinase domain (Waite and Eng, 2003). It was predicted that loss-of-function mutations in the *BRII* gene interrupt downstream signaling pathways and increase proliferation. This fact was supported by studies which showed that pulmonary vascular endothelial hyperproliferation was observed in patients with germline mutations in the *BRII* gene (Atkinson et al., 2002; Waite and Eng, 2003). Furthermore, a reduced *BRII* expression is reported for PPH patients (Atkinson et al., 2002). However, it is not known, how exactly receptor mutants contribute to the development of PPH.

A recent study links the occurrence of PPH to caveolae (see 1.5.4), by giving evidence for an at least partial localization of *BRII* in these membrane invaginations (Ramos et al., 2006). They conclude that the presence of *BRII* in caveolae on the apical and basal surfaces of endothelial cells may contribute to a potential role for caveolar-mediated distribution of the receptors in vascular responses (Ramos et al., 2006). Furthermore, a microarray analysis revealed that PPH patients have reduced caveolin expression levels (Geraci et al., 2001). Another evidence for that is that caveolin-1 (*cav-1*) null mice develop proliferative vascular abnormalities reminiscent of PPH lesions (Razani et al., 2001a) as well as dilated cardiomyopathy and pulmonary hypertension (Zhao et al., 2002).

Another autosomal dominantly inherited disease is linked to mutations in BMP signaling molecule genes. JPS belongs to hamartoma polyposis syndromes, characterized by gastrointestinal hamartomatous juvenile polyps and a 10-50% risk of getting gastrointestinal, mostly colorectal cancers (Coburn et al., 1995; Howe et al., 1998a; Jarvinen and Franssila, 1984). It was discovered that germline mutations in the gene for *Smad4* and for *BRIa* are responsible for JPS development (Howe et al., 2001; Howe et al., 1998b). Mutations in the gene for *Smad4* affect mostly the C-terminal half of the gene which is highly conserved and encodes the *Smad4* homo-oligomerization and transcriptional activation domains. This observed inability to form homo- and hetero-oligomers results in a loss of TGF- β -induced signaling responses (Shi et al., 1997). Mutations in the *BRIa* gene result mainly in truncated receptors. Missense mutations occur in highly conserved residues and affect ligand-binding or kinase activity (Zhou et al., 2001).

FOP is an extremely rare and disabling genetic disorder and is characterized by congenital malformations of the great toes and progressive, heterotopic, endochondral ossification in predictable anatomical patterns. Ectopic expression of *BMP4* was found to cause this disease, accompanied by deficiency of the BMP antagonist *noggin* (Gannon et al., 1997; Xu et al., 2000b). A recently developed therapy applies the engineered *noggin* mutein *hNOGDeltaB2* which should prevent the *BMP4*-induced heterotopic ossification (Glaser et al., 2003).

Furthermore, overexpression of BMP2, BMP4 and BMP5 as well as BRIA is associated with malignancy of the oral epithelium (Jin et al., 2001). Other studies show an implication of overexpression of BMP3 and BMP2 in prostate cancer cells (Harris et al., 1994).

1.5 ORGANIZATION OF THE PLASMA MEMBRANE AND ENDOCYTOSIS

The plasma membrane separates the cell from its surroundings and exhibits a barrier for molecules which enter or exit the cell, serving as a checkpoint to control efflux and influx efficiently. It is composed of lipids and proteins (see 1.5.1). To communicate with the extracellular environment, integral membrane protein pumps as well as ion channels are embedded in the plasma membrane. Only small molecules like sugars, amino acids or ions can pass via these structures, whereas larger molecules need to be carried into the cell via vesicles derived by invagination and pinching-off of part of the plasma membrane using different kinds of endocytosis (see 1.5.2).

1.5.1 Models of membrane structure

In the 19th century the first model of membranes simply suggested that they were layers of lipid, but this model did not account for how a lipid layer could remain stable in contact with the water of the cell and the environment. Chemical analyses and experiments on isolated membranes in the early 20th century revealed that membranes were largely made of amphiphilic phospholipids and cholesterol, forming a stable double layer of molecules in water. Thereby the water soluble heads of each layer were supposed to be oriented outward toward the water and the lipid soluble tails were oriented inward toward each other. Furthermore, it was discovered that proteins are involved in membrane structure. A new model, proposed by the scientists Davson and Danielli in 1934, suggested that the phospholipid bilayer was coated on both sides with water-soluble proteins, in a kind of lipoprotein sandwich. Early electron micrographs revealed a three layered structure, confirming the Davson-Danielli model which remained the accepted view until 1972, when the scientists Singer and Nicolson proposed the fluid mosaic model of membrane structure (Singer and Nicolson, 1972). This model suggests that the molecules of the phospholipid bilayer are not bonded to one another, but float freely to form a viscous, two-dimensional solvent into which proteins are inserted and integrated. The hydrophobic parts of the proteins are in contact with the hydrophobic tails of the lipid molecules and the polar groups jut out from the membrane (Singer and Nicolson, 1972). In our days membranes are seen as a mosaic of different compartments and domains, since in 1997 Simons and Ikonen constituted the lipid raft hypothesis (Simons and Ikonen, 1997).

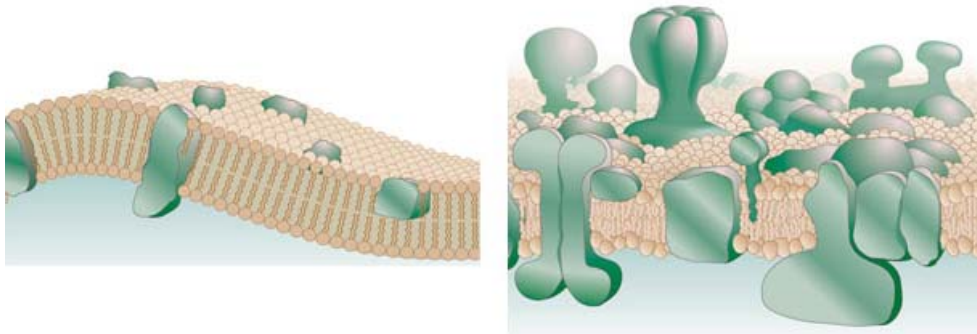


Fig. 1.6 Models for membrane structure (Engelman, 2005).

The Singer-Nicolson fluid mosaic model (left side) is compared to an up-to-date version (right side). Today it is suggested that membranes are more crowded by proteins and that the bilayer vary considerably in thickness than Singer and Nicolson proposed in 1972.

Lipid rafts (see also 1.5.5) are proposed to be small structures enriched in cholesterol, sphingolipids and other highly ordered saturated lipids which are laterally mobile in the plane of the fluid (= disordered) bilayer of mostly unsaturated lipids (Brown and London, 1998; Simons and Ikonen, 1997). Lipids can be present in three phases: the gel phase (immobile lipids, fully extended fatty acids), the liquid or fluid phase “ld” (loosely packed lipids, high lateral mobility, disordered fatty acid structures) or the liquid ordered phase “lo” (intermediate, high lateral mobility and ordered structure with extended fatty acids). It was found that in membranes different phases coexist in a temperature- and composition-dependent manner (Helms and Zurzolo, 2004) and that lipid rafts are in the lo-phase “swimming” in the ld-phase. More lately the lipid shell hypothesis proposed that the molecular address for proteins targeted to lipid domains are lipid shells, small dynamic assemblies in the plane of the membrane for which raft proteins have a high affinity (Anderson and Jacobson, 2002).

Moreover, rafts are especially sensitive to cholesterol depleting reagents because of their high cholesterol content (Hailstones et al., 1998; Rothberg et al., 1992; Schnitzer et al., 1994).

Taken together the image of the plasma membrane today is that of a mosaic with segregated regions of structure and function (Engelman, 2005).

1.5.2 Endocytosis

Endocytosis is an active process, necessary for the uptake of macromolecules into the cell. It plays a crucial role in development, immune response, neurotransmission, intercellular communication, signal transduction and cell and organismal homeostasis (Conner and Schmid, 2003) and itself is highly regulated. Recently a genome-wide analysis has been revealed that a high number of human kinases is involved in and modulate endocytic events (Pelkmans et al., 2005).

Several diverse mechanisms are known to internalize particles into transport vesicles derived from the plasma membrane. On the one hand, phagocytosis, a process known as “cell eating”, i.e. uptake of large particles, is restricted to specialized mammalian cells such as macrophages, monocytes and neutrophils. The function of this process is to clear large pathogens or debris (Aderem and Underhill, 1999). The mode of action is normally determined by the particle to be ingested and the receptors recognizing these particles, but involves usually activation of Rho-family GTPases. Activated Cdc42 and Rac triggers actin assembly and the formation of cell surface-extensions that zipper up the cargo to engulf it (Fig. 1.7) (reviewed in Conner and Schmid, 2003). On the other hand, there is pinocytosis known as “cell drinking”, i.e. uptake of fluids and solutes, which occurs in all cells. Four kinds of mechanisms of pinocytosis are described: macropinocytosis, clathrin-mediated endocytosis (CME; see 1.5.3), caveolae-mediated endocytosis (see 1.5.4) and clathrin- and caveolae-independent endocytosis (see 1.5.5) (Fig. 1.7).

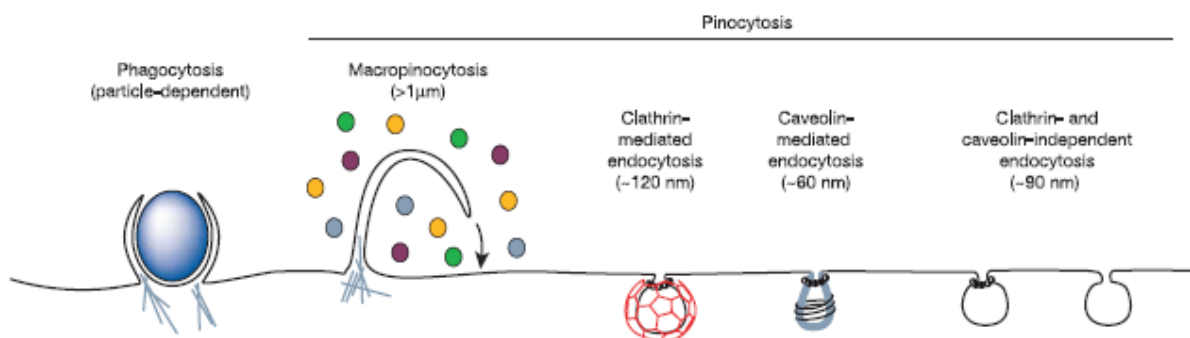


Fig. 1.7 Portals of cell entry (Conner and Schmid, 2003).

The pathways vary in vesicle size, cargo and mechanisms of vesicle formation.

Macropinocytosis is also induced via Rho-family GTPase signaling cascades, triggering the actin-driven formation of membrane protrusions. But unlike the mechanism of phagocytosis, these “membrane noses” fuse with the plasma membrane (Fig. 1.7) to generate large endocytic vesicles (= macropinosomes) carrying the cargo together with extracellular milieu (Conner and Schmid, 2003). Functions of macropinocytosis include downregulation of activated signaling molecules, e.g. platelet-derived growth factor (PDGF), as well as directed cell migration via activation of Rac and p21-activated kinase (PAK) (Ridley, 2001).

The remaining three types of pinocytosis are characterized by different mechanisms of vesicle formation and smaller pinocytic vesicles and are described in more detail in the following chapters.

1.5.3 Clathrin-mediated endocytosis

Clathrin-mediated endocytosis (CME) occurs in all mammalian cells and is the most important mechanism for the uptake of essential nutrients like low-density lipoprotein (LDL) particles or transferrin (Tfn) (Brodsky et al., 2001; Schmid, 1997). It modulates signal transduction pathways by controlling the level of signaling receptors at the cell surface and by mediating recycling processes of activated receptors. It functions to concentrate high-affinity transmembrane receptors and their bound ligands into coated pits, formed by assembly of cytosolic coat proteins. They invaginate and pinch-off, forming endocytic vesicles (CCVs) which are encapsulated by a polygonal clathrin-coat (see Fig. 1.8) (Conner and Schmid, 2003).

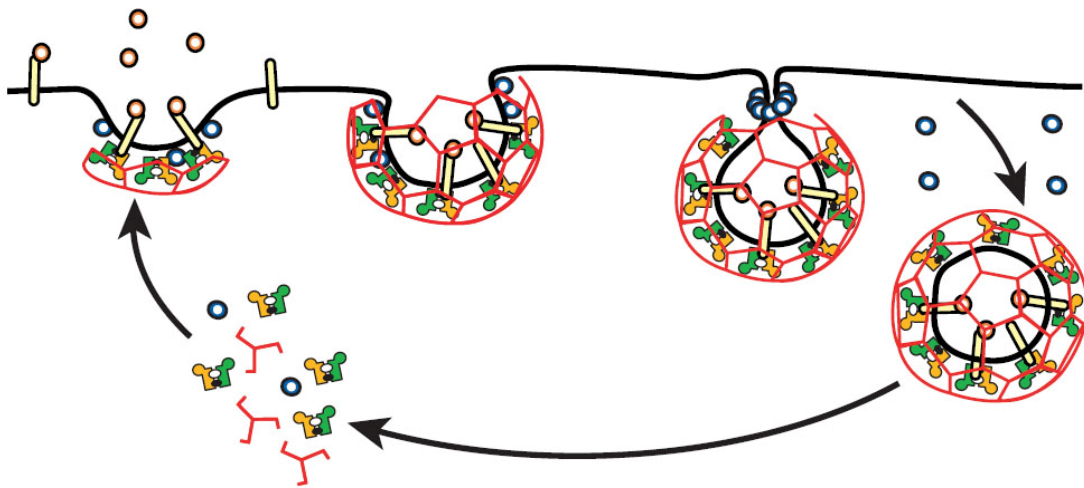


Fig. 1.8 Schematic demonstration of CME (Conner and Schmid, 2003).

Cargo molecules (ligands) bind to their receptors. Clathrin triskelien (in red) assemble, supported by AP-2 (in yellow/green), to form a basket-like, invaginated structure called clathrin-coated pit. Dynamamin (in blue) forms a “collar” around the neck of a deeply invaginated coated pit and catalyzes the fission of the CCV into the cytoplasm of the cell. CCVs uncoat and the components of the endocytic machinery are recycled back to the plasma membrane.

Clathrin is the main coat protein and has a three-legged structure called “triskelion” which is formed by three clathrin heavy chains associated with the respective light chains (see Fig. 1.9) (Brodsky et al., 2001; Kirchhausen, 2000). The assembly of clathrin in a cage- or basket-like structure is supported by assembly proteins (APs). The only monomeric AP (AP180) is expressed specifically in neurons, but an ubiquitously-expressed isoform was also discovered in mammals (Lindner and Ungewickell, 1992; Tebar et al., 1999). Four structurally-related AP-complexes are known, working at distinct subcellular locations (Brodsky et al., 2001; Kirchhausen, 1999; Robinson and Bonifacino, 2001). AP-2 is the only AP involved in endocytic CCV formation and is structurally composed of two large subunits (α - and β 2-adaptins), a medium subunit μ 2 and a small subunit σ 2 (see Fig. 1.9). α -adaptin specifies the site of clathrin assembly by targeting the AP-2 complex to the plasma

membrane. The β -subunits of all AP complexes interact with clathrin and trigger clathrin assembly. The μ 2-subunit binds tyrosine-based internalization motifs on receptors and the σ 2-subunit exhibits a structural role in stabilizing the core domain (Collins et al., 2002). Thus the functions are clearly allocated, showing that clathrin drives the membrane invagination, whereas the AP-2 complex directs clathrin assembly into curved lattices and couples it to cargo recruitment (Brodsky et al., 2001; Kirchhausen, 1999).

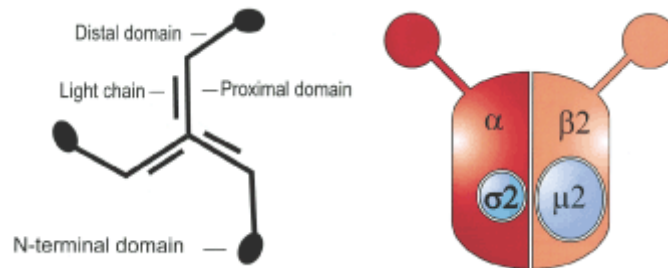


Fig. 1.9 Schematic demonstration of clathrin- and AP-2-structure (Mousavi et al., 2004).

The clathrin triskelion consists of three heavy chains and three tightly associated light chains (left side). The AP-2-complex is composed of four subunits: the α - and β 2-adaptins and the μ 2- and σ 2-subunits (right side).

Furthermore, the GTPase dynamin plays a crucial role in CME, but also in phagocytosis, caveolae-mediated endocytosis as well as in some clathrin- and caveolae-independent endocytic pathways (Hinshaw, 2000; Sever et al., 2000). Dynamin structure includes five distinct domains with special functions: the GTPase and a middle domain, the pleckstrin homology (PH) domain for binding to phosphatidylinositol-4,5-biphosphate, the GTPase effector domain (GED) for the dynamin-self assembly process (in that the GTPase and middle domain are supporting) and a proline/arginine rich domain (PRD) for the interactions of dynamin with other endocytic components (see Fig. 1.10) (Conner and Schmid, 2003).



Fig. 1.10 Schematic representation of the domain structure of dynamin (Peplowska and Ungermann, 2005).

Dynamin consists of five domains: GTPase domain, middle domain, PH (pleckstrin homology) domain, GED (GTPase effector domain) and PRD (proline/arginine rich domain).

Dynamin encodes for its own GTPase activating protein (GAP) within the GED. GAP is required for the self assembly of dynamin into helical rings and stacks which leads to an up to 100fold GED-mediated GTPase activity. In the late stages of CCV formation, dynamin self assembles into a "collar" at the neck of invaginated coated pits, carrying out the pinching-off of CCVs inside of the cell. For that process it must undergo GTP hydrolysis-driven conformational changes (Song and Schmid, 2003).

There are a lot of accessory proteins which spatially and temporally regulate CME as well as link CME to distinct cell processes and aspects of cell physiology, e.g. Eps15/Eps15R, epsin, endophilin, amphiphysin or intersectin (reviewed in Brodsky et al., 2001; Slepnev and De Camilli, 2000). Most of these proteins mediate their actions by binding to clathrin, AP-2 and/or dynamin. CME is spatially organized at “hotspots” which are at least partly constrained by the actin cytoskeleton (Gaidarov et al., 1999). Actin itself is spatially and temporally coordinated with the recruitment of dynamin just before CCVs are released into the cytosol (Merrifield et al., 2002). Interactions of components of the CME machinery with lipids are also essential for CME and are reported to be involved in the generation of membrane curvature and to destabilize the lipid bilayer to initiate membrane fission (Conner and Schmid, 2003). Furthermore, the phosphorylation of subunits of AP-2 by CCV-kinases regulates AP-2 recruitment to the plasma membrane, AP-2 interaction with cargo proteins as well as AP-2-clathrin co-assembly (Fingerhut et al., 2001; Olusanya et al., 2001; Wilde and Brodsky, 1996). In receptor-mediated endocytosis via CME, different receptors use diverse mechanisms for their uptake into CCVs. For example Tfn and LDL receptors exhibit different endocytic sorting motifs. In the Tfn receptors the motif $YX\psi\phi$ (X = any amino acid, ψ = bulky hydrophilic amino acid, ϕ = hydrophobic amino acid) is recognized by the $\mu 2$ -subunit of AP-2 (Kirchhausen, 1999). A special $\mu 2$ kinase was found to regulate the affinity of AP-2 for this motif (Conner and Schmid, 2002). The sorting motif which is located in the LDL receptors is FXNPXY and was shown to be recognized by Dab2 which also binds AP-2 and mediates clathrin assembly (Mishra et al., 2002; Morris and Cooper, 2001). The TGF- β type II receptor was shown to be continuously endocytosed via CME (Ehrlich et al., 2001). This process was reported to be dependent on a short sequence (IIL) which corresponds to the di-leucine family of internalization signals (Ehrlich et al., 2001). The TGF- β type I receptor contains in its C-terminus the NANDOR-box (nonactivating non downregulating-box) which links TGF- β receptor activation and signaling with endocytosis of the receptor complex (Garamszegi et al., 2001). Other signaling receptors use different mechanisms for directing their internalization by CME like for example G-protein coupled receptors which bind the AP-2-interacting protein β -arrestin (adaptor-like molecule) (Miller and Lefkowitz, 2001); or others which use ligand-induced mono-ubiquitination (Hicke, 2001).

1.5.4 Caveolae-mediated endocytosis

Caveolae were discovered by early electron microscopists in the 1950s to be around 50 nm small, mostly flask-shaped pits in the plasma membrane (Palade, 1953; Yamada, 1955). Almost 40 years later a major protein-constituent of caveolae, caveolin-1 (cav-1) or VIP-21, was identified (Kurzchalia et al., 1992; Rothberg et al., 1992). Today caveolae are known to

be involved in and important for a variety of cellular functions and processes including endocytosis, cholesterol and lipid homeostasis, signal transduction (see 1.5.4.2) and tumor suppression. Their physiological role seems to be adapted to the cell type and organ system of an organism, as well as their morphology can differ in different cell types and tissues. Certain cell types have an extraordinary abundance of caveolae as for example adipocytes, endothelial cells, type I pneumocytes, fibroblasts, smooth muscle cells and striated muscle cells (Palade, 1953; Gabella, 1976; Gil, 1983; Mobley and Eisenberg, 1975; Napolitano, 1963), whereas others lack caveolae at all, e.g. central nervous system neurons, lymphocytes and many tumor cells (Cameron et al., 1997; Fra et al., 1994). Caveolae exhibit the same biochemical properties like lipid rafts, being composed mainly of sphingolipids and cholesterol (see 1.5.1) (Brown and London, 1998; Simons and Toomre, 2000). These membrane regions are insoluble in some detergents like Triton X-100 or CHAPS at 4°C and can be separated from other membrane regions and cell contents by sucrose density gradient ultracentrifugation (Brown and Rose, 1992; Lisanti et al., 1994).

It was shown that the shape and structural organization of caveolae are conferred by cav-1, a 22 kD protein. The caveolin protein family contains also cav-2 and cav-3 (see 1.5.4.1) (Scherer et al., 1996; Tang et al., 1996; Way and Parton, 1995). More insight into the function and role of cav-1 and caveolae were obtained in studies using cav-1-deficient mice (see 1.5.4.3). These mice are viable, but show some interesting phenotypes. An important observation among others is that the absence of cav-1 and cav-3, but not cav-2, leads to a complete loss of caveolae in the respective tissue (Drab et al., 2001; Galbiati et al., 2001; Razani et al., 2001a; Razani et al., 2002c).

1.5.4.1 The caveolin protein family

The family of caveolins consists of three members, cav-1, cav-2 and cav-3. Furthermore, for cav-1 and cav-2 smaller isoforms exist in addition to the full length proteins (α -isoform). The β -isoform of cav-1 is derived from an alternative translational start site, resulting in a 32 amino acid truncated form (Scherer et al., 1995); the β - and γ -isoforms of cav-2 were not analyzed till now. The three caveolins exhibit a caveolin signature motif with highest identity, but still unknown function, as well as the membrane-spanning, oligomerization and scaffolding domains. Cav-1 and cav-2 are mainly expressed in the same cell types, like adipocytes, endothelial cells, pneumocytes and fibroblasts, whereas cav-3 expression is limited to muscle cell types (Scherer et al., 1994; Tang et al., 1996). Cav-1 inserts into the inner leaflet of the plasma membrane as a loop, C- and N-termini facing the cytoplasm (Dietzen et al., 1995; Dupree et al., 1993; Li et al., 1996; Monier et al., 1995) and is palmitoylated at three cysteine residues on the C-terminus to further strengthen its

membrane association (Dietzen et al., 1995). The structure of caveolae and cav-1 is presented in Fig. 1.11.

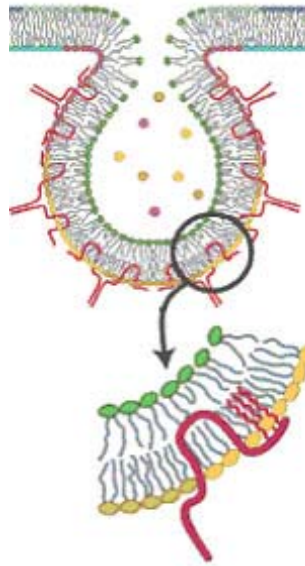


Fig. 1.11 Structure of caveolae and membrane topology of cav-1 (Parton, 2001).

Cav-1 (red) is inserted into the inner leaflet of the membrane (yellow) as a “double-pass membrane-spanning protein” (Razani et al., 2002c) and is palmitoylated at three cysteine residues on the C-terminus.

Cav-1 oligomerizes to a highly stable homo-oligomer of approximately 14 to 16 monomers (Li et al., 1996; Monier et al., 1995; Sargiacomo et al., 1995). Amino acids 61-101 were discovered to be responsible for this oligomerization tendency and called the oligomerization domain (Sargiacomo et al., 1995; Song et al., 1997b). Furthermore, it was shown that cav-1 can form higher ordered interactions with cav-2 (Scherer et al., 1997) and that this association is mediated by the membrane-spanning domains of cav-1 and cav-2 (Das et al., 1999). While cav-2 is not able to form large homo-oligomers and exists instead in a monomeric/dimeric form (Scherer et al., 1996), cav-3 oligomers of 350-400 kD could be found (Tang et al., 1996). Overexpression of cav-1 in cells which lack endogenous cav-1 and caveolae leads to *de novo* production of caveolae (Fra et al., 1995). The inverse experiment, i.e. down-regulating cav-1 expression, resulted in loss of caveolae (Galbiati et al., 1998; Liu et al., 2001). These results manifest the structural importance of cav-1 for the formation of the invagination in which also cholesterol is involved (Hailstones et al., 1998). Furthermore, cav-1 binds cholesterol and sphingolipids, the major lipid components of lipid rafts (Fra et al., 1995; Murata et al., 1995; Thiele et al., 2000).

1.5.4.2 Caveolae as “signalosomes”

Caveolae and cav-1 play an important role in transcytosis, endocytosis, potocytosis, cholesterol homeostasis and transport, signal transduction, as targets of oncogenes and tumor suppressor. There are excellent reviews discussing the involvement of caveolae/cav-1 in these processes in detail (Parton and Richards, 2003; Razani et al., 2002c; Simons and Toomre, 2000). In the following it will be focused on the importance of caveolae for signaling processes.

Caveolae represent compartments of the plasma membrane which serve as platforms for the aggregation and concentration of (signaling) proteins. In this context, Razani et al. used the term “signalosomes” to reveal the importance of compartmentalizing by caveolae on signaling (Razani et al., 2002c). Proteins which are located in caveolae can be identified by their insolubility in detergents at 4°C and their buoyancy in sucrose gradients. Using this method numerous proteins were found, the majority of them being signal transduction molecules (Sargiacomo et al., 1993). Several of the signaling molecules identified contain lipid modifications, e.g. H-Ras, Src-family tyrosine kinases, heterotrimeric G-protein α -subunits and endothelial nitric oxide synthase (eNOS) (Feron et al., 1996; Garcia-Cardena et al., 1996; Li et al., 1995; Song et al., 1996; Song et al., 1997a). In addition, caveolin proteins might also act as scaffolding proteins by interacting with signaling molecules and modulating thereby their activity.

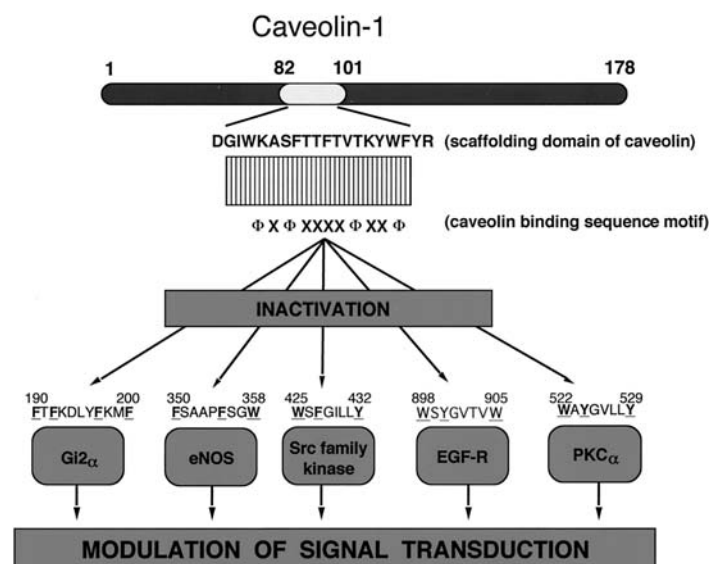


Fig. 1.12 Interaction of cav-1 with signaling molecules (Razani et al., 2002c).

The caveolin scaffolding domain (CSD) of cav-1 recognizes the caveolin binding motif, which is located in several signaling proteins. In most cases, cav-1 interaction leads to the inactivation of the respective signaling cascade and modulate signal transduction thereby.

The 20 amino acid long caveolin scaffolding domain (CSD; amino acids 82-101) selectively bind diverse signaling molecules (see Fig. 1.12) (Engelman et al., 1998; Li et al., 1995;

Okamoto et al., 1998; Smart et al., 1999). In the search of similarities in the sequences of caveolin-associated proteins the following putative caveolin-binding motifs were identified: $\phi X\phi XXXX\phi$, $\phi XXXX\phi XX\phi$, $\phi X\phi XXXX\phi XX\phi$ (ϕ = aromatic residue, X = any amino acid) (Couet et al., 1997a). Most of the signaling cascades have been shown to be inhibited by cav-1.

1.5.4.3 Studies of caveolin-1-deficient mice

Cav-1-null mice are viable but exhibit a lot of defects in several tissues. These mice were generated and analyzed by two groups in parallel (Drab et al., 2001; Razani et al., 2001a). The mice developed no caveolae in cav-1-null tissues, proving the finding from cell culture that cav-1 is required for caveolar invagination. In all cav-1-null tissues the expression of cav-2 is extremely reduced, due to destabilization and proteasomal degradation of cav-2 when cav-1 is absent. Razani et al. used primary cultured mouse embryonic fibroblasts (MEFs) to reveal that cav-1-null cells display a more active cell cycle profile than wildtype cells resulting in hyperproliferation. This supports the finding of tumor suppressor qualities of caveolins, although cav-1-deficient mice did not exhibit accelerated tumor development (Razani et al., 2001a). In terms of endocytosis, it was found that the uptake of albumin was completely disrupted in cav-1-null MEFs, pointing to caveolae as the predominant pathway by which the major serum albumin is endocytosed (Razani et al., 2001a; Schubert et al., 2001). Most likely other pathways must at least partially compensate for caveolae *in vivo*, otherwise the viability and benign phenotype of cav-1-null mice could not be explained. Above all other organs the lung was especially affected by the lack of cav-1 and caveolae, because up to 70% of the total plasma membrane in a typical septa is composed of caveolae in normal mice (Gumbleton, 2001). Loss of lung caveolae resulted in hypercellularity and thickened alveolar septa suggesting an endothelial cell proliferation phenotype in these mice. Furthermore, increased deposition of extracellular matrix was found (Drab et al., 2001; Razani et al., 2001a) leading commonly to restrictive lung diseases like acute respiratory distress syndrome, idiopathic pulmonary fibrosis and pneumoconiosis. As a result of the cav-1/eNOS connection, cav-1-null mice exhibit a decreased vascular tone. Moreover, cav-1 was shown to play an important role in lipid homeostasis, as older cav-1-null mice exhibit significantly smaller body sizes, resistance to diet-induced obesity, a lean appearance, dramatically smaller fat pads as well as histologically reduced adipocyte cell diameters (Razani et al., 2002a).

Also cav-2- and cav-3-null mice are available, exhibiting different phenotypes (reviewed in Razani et al., 2002b).

1.5.5 Other endocytic routes

Lipid rafts have been proposed to function in protein trafficking and sorting inside of the cell. They can be internalized via different endocytic vesicles. Shiga toxin and nonaggregated cholera toxin for example which bind to raft-associated glycolipids are both endocytosed by CCVs (Sandvig et al., 1989; Thomsen et al., 2002). The best-studied proteins in this context are GPI-anchored proteins which are internalized via distinct mechanisms, namely caveolae, coated pits as well as a dynamin-independent pathway (Anderson, 1998; Conese et al., 1995; Sabharanjak et al., 2002; Sunyach et al., 2003; Triantafilou et al., 2001). Which mechanism is chosen by GPI-anchored proteins depends on the interactions with other surface components. The dynamin-independent route leads the internalized receptors to Rab5-negative early endosomes, lacking the normal markers of clathrin- or caveolin-mediated pathways and is dependent on raft integrity shown by cholesterol depletion experiments (Sabharanjak et al., 2002). Interleukin 2 receptor β (IL2R β), also a resident of lipid rafts (Goebel et al., 2002), is endocytosed preferentially via a dynamin-dependent route (Lamaze et al., 2001). By studying cholera toxin entry in cav-1-null MEFs in comparison to wildtype cells it was found that this toxin (often used as caveolae marker) was internalized mostly caveolin-independent in both cell types. New uncoated tubular- or ring-shaped structures were described as carriers, which turned out to be clathrin-, cav-1- and dynamin-independent, but cholesterol-dependent (Kirkham et al., 2005). Furthermore, Simian Virus 40 (SV40), commonly known to entering host cells via caveolae and caveosomes, was shown to use additionally a cav-1-independent pathway. This route turned out to be cholesterol- and tyrosine kinase-dependent, but independent of clathrin, dynamin and ARF6 and was carried out by small, tight-fitting vesicles (Damm et al., 2005). The latter two endocytic routes, used by cholera toxin and SV40, involve neither clathrin nor caveolae and are also active in the presence of cav-1.

Moreover, raft lipids, e.g. glycosphingolipids (GSLs), are internalized clathrin-independent by a caveolar-related mechanism, but then merge immediately with the endosomal compartment to be transported to the Golgi apparatus (Pagano, 2003; Sharma et al., 2003).

1.6 ENDOCYTIC REGULATION OF TGF- β SIGNALING

The level and localization of signaling events are regulated by endocytic sorting processes of signaling receptors and other molecules. Traditionally, endocytosis was thought to be a down-regulating mechanism, but recent work has shown that it modulates signaling via multiple mechanisms. Signaling may be increased by associating internalized receptors with signaling targets in endosomes or it may be decreased by sorting receptors to the lysosome for degradation (Seto et al., 2002).

The regulation of TGF- β signaling by endocytic processes has recently been under fierce investigation and discussion by several groups. The discovery of SARA, a FYVE-domain-containing protein (and therefore situated at endosomal membranes) which binds Smad2 and the TGF- β receptor complex linked TGF- β signaling to endocytic events (Tsukazaki et al., 1998). By using several immuno-microscopical methods the receptors and SARA could be localized to early endosomes (Hayes et al., 2002). The same group and others could show that the disruption of SARA localization resulted in inhibition of TGF- β -induced Smad2 nuclear translocation (Hayes et al., 2002; Penheiter et al., 2002). However, this question remains controversial because other groups found evidences against internalization-dependent Smad2 phosphorylation (Lu et al., 2002; Runyan et al., 2005). If Smad2 is phosphorylated only after internalization via clathrin-coated pits (CCPs) into early endosomes, it is obvious that endocytosis is required for propagation of TGF- β signaling via Smads.

Another publication demonstrates that the TGF- β type I receptor interacts with cav-1 in detergent-resistant membranes (DRM)/caveolae (Razani et al., 2001b; Schwartz et al., 2005). But controversy remains which function the caveolar localization fulfills and whether the receptors are also internalized via the caveolar pathway (Di Guglielmo et al., 2003; Mitchell et al., 2004). One study claims that Smad signaling occurs in early endosomes, whereas the receptor complex is degraded while internalized via caveolae/caveosomes (Di Guglielmo et al., 2003). Therefore the TGF- β receptor complex, SARA and Smad2 could be localized to EEA1-positive vesicles, whereas Smad7 and Smurf2 were found together with the receptors in cav-1-positive vesicles (Di Guglielmo et al., 2003). However, another study found no link to caveolae, neither a colocalization of TGF- β receptors with cav-1 nor an effect of nystatin (to disrupt caveolae by cholesterol sequestration) on receptor internalization could be detected (Mitchell et al., 2004). Rather, they argue that recycling, downregulation and degradation occurs most likely clathrin-dependent (Mitchell et al., 2004).

Comparable studies are still missing for the BMP receptors. Lately, it was found that BRII is associated with cav-1 in A431 cells and that caveolae seem to be involved in the downregulation of Smad signaling (Nohe et al., 2005). Another study confirmed this finding by detecting BRII in DRMs and in caveolae using biochemical methods and immuno-electronmicroscopy (Ramos et al., 2006). Moreover DRAGON, a recently discovered BMP coreceptor and GPI-anchored protein, could be localized to DRMs by using immunocytochemistry and gradient sucrose ultracentrifugation (Xia et al., 2005).

The present study was initiated to answer the still open questions about BMP receptor localization and the influence of distinct internalization events on BMP signaling pathways.

1.7 AIM OF THE PROJECT

Endocytosis of growth factor receptors is a highly regulated process and in turn modulates numerous signal transduction pathways. Prerequisite for the controlled internalization of receptors is their localization in specialized regions of the plasma membrane.

The present study was set up to elucidate BMP receptor localization in distinct plasma membrane domains. Therefore the contribution of cholesterol- and sphingolipid-enriched regions like lipid rafts and caveolae as well as clathrin-coated pits (CCPs) was investigated.

Previous studies demonstrated that BMP receptors constitute different oligomerization patterns at the cell surface leading to the activation of two distinct signaling pathways. Smad-dependent BMP signaling was triggered at PFCs, whereas BISCs initiated Smad-independent BMP signaling via p38-MAPK resulting in the production of functional ALP (Nohe et al., 2002).

On that account, the second aim of the present study was to shed light on the question whether the different signaling pathways are initiated in discrete plasma membrane regions. To follow up this issue the contribution of endocytic pathways on diverse steps of BMP signaling as well as on Smad-dependent and Smad-independent BMP signaling should be investigated.

2 MATERIAL AND SOLUTIONS

2.1 CHEMICALS

Basic chemicals of highest purity were purchased from Merck, Roth, Serva and Sigma.

All solutions were prepared using deionized water of Millipore quality.

Cell culture reagents were obtained from Biochrom, Bio Whittaker, Falcon, Greiner, Invitrogen, Nunc, Merck and Sigma.

Substances used for preparation of bacteria growth media were supplied by Roth and Difco.

2.2 TECHNICAL DEVICES

Agarose gel electrophoresis		Institute's workshop
Balance	2001 MP2	Sartorius
Balance	1264 MP	Sartorius
Centrifuge	Megafuge 1.0	Heraeus
Centrifuge	J2-21	Beckman
Clean bench	HLB 2472	Heraeus
Confocal microscope	Leica DMR	Leica
Electrophoresis power supply	E831	CONSORT
Electron microscope	Zeiss EM10	Zeiss
Fluorescence microscope	Axiovert 25	Zeiss
Incubator	HERA cell	Heraeus
Light microscope	Leitz DM IL	Leica
Luminometer	FB12	Berthold
Microplate reader	MR5000	DYNATECH
Table centrifuge	Centrifuge 5415 C	ependorf
PCR cycler	GeneAmp PCR System 2400	Perkin Elmer
pH meter	pH523	WTW
Potter	Potter S	B.Braun
Protein Blotting	Mini-V 8.10	BIO-RAD
Protein gel electrophoresis	Mini-PROTEAN II	BIO-RAD
Shaker	Rockomat	TECHNO MARA
Spectrophotometer	CARY 50 Bio	VARIAN
Thermal table		MEDAX
Ultracentrifuge	L8M	Beckman
UV-transilluminator		UVP Inc.
X-Ray developing machine	COMPACT 35	PROTEC

2.3 ENZYMES

2.3.1 Restriction endonucleases

Restriction enzymes were purchased from MBI and NEB.

2.3.2 DNA- and RNA- modifying enzymes

RNase	Roth
RNasin™	Promega
MMLV reverse transcriptase	Promega
T4 DNA-ligase	Promega
DNA polymerase	Promega

2.4 KITS

Plasmid-DNA preparation	Qiagen
Dual Luciferase Assay Kit	Promega
RNeasy Kit	Qiagen
Amplex Red Cholesterol Assay Kit	Molecular Probes
CEQ 2000 DTCS Quick Start Kit	Beckmann
Taq CORE Kit 10	Q-BIOgene

2.5 OLIGONUCLEOTIDES

Oligonucleotides were synthesized and purchased by Interactiva/ThermoHybaid in HPLC quality.

Primers used for PCR reactions are listed in the appendix (A 2).

2.6 EXPRESSION VECTORS

pcDNA1 (Invitrogen)	mammalian expression vector for high level constitutive expression driven from a CMV promoter; the plasmid encodes the tRNA suppressor F gene kinase which demands transformation in specific bacterial strains that harbor the P3 episome (i.e. MC1061/P3); sensitivity to tetracycline and ampicillin is generated by suppression of the amber mutations
pcDNA3 (Invitrogen)	mammalian expression vector for high-level constitutive expression driven from a CMV enhancer promoter

pcDNA3.1 (Invitrogen)	mammalian expression vector for high-level constitutive expression driven from a CMV enhancer promoter; similar to pcDNA3 but differs in the multiple cloning site
pEGFP-C1 (Clontech)	mammalian expression vector for high-level constitutive expression of a fusion protein with EGFP from a CMV enhancer promoter; encodes a red-shifted variant of wild-type GFP which has been optimized for brighter fluorescence and higher expression; Excitation maximum = 488 nm; Emission maximum = 507 nm
pCB6 (ATCC)	E.coli plasmid vector for cloning
pGL3 basic (Promega)	(<i>Firefly</i>) Luciferase Reporter Vector for analyzing factors that potentially regulate mammalian gene expression
pRLTK (Promega)	Luciferase Reporter Vector for low-level expression of <i>Renilla</i> luciferase driven from a thymidine kinase promoter

2.7 BACTERIAL STRAINS

<i>E.coli</i> DH5 α	<i>deoR</i> , <i>endA1</i> , <i>gyrA96</i> , <i>hsdR17</i> ($r_k^- m_k^+$), <i>recA1</i> , <i>relA1</i> , <i>supE44</i> , <i>thi-1</i> , $\Delta(lacZYA-argFV169)\Phi80lacZ\Delta M15$, F ⁻ (Hanahan, 1983)
<i>E.coli</i> C600	<i>lacY1</i> , <i>leuB6</i> , <i>mcrB+</i> , <i>supE44</i> , <i>thi-1</i> , <i>thr-1</i> , <i>tonA21</i> , F ⁻ (Young and Davis, 1983)
<i>E.coli</i> MC1061/P3	<i>araD139</i> , <i>galK</i> , <i>galU</i> , <i>hsdR2</i> ($r_k^- m_k^+$), <i>rpsL</i> , <i>thi-1</i> , $\Delta ara-leu$ 7696, $\Delta lacX74$, F-[P3 <i>kan</i> ^r amber <i>amp</i> ^r amber <i>tef</i>] (Invitrogen)
<i>E.coli</i> JM109	<i>endA1</i> , <i>recA1</i> , <i>gyrA96</i> , <i>thi</i> , <i>hsdR17</i> ($r_k^- m_k^+$), <i>relA1</i> , <i>supE44</i> , $\Delta(lac-proAB)$, [F', <i>traD36</i> , <i>proAB</i> , <i>lacI</i> ^q Z Δ M15] (Stratagene)

2.8 GROWTH MEDIA AND REAGENTS FOR CELL CULTURE

DMEM (GIBCO)	<u>D</u> ulbecco's <u>M</u> odified <u>E</u> agle <u>M</u> edium was prepared according to manufacturers' instructions and sterilized by filtration
FCS (Life Technologies)	<u>F</u> etal <u>C</u> alf <u>S</u> erum was heat-inactivated for 30 min at 56°C before use

G418 (PAA)	additive to cell culture media, aminoglycosid-antibiotic for selecting neomycin-resistant cells (final concentration: 0,1 – 2 mg/ml)
L-Glutamine (Biochrom)	additive to cell culture media (final concentration: 1 mM)
Nu-serum (Becton Dickinson)	was heat-inactivated for 30 min at 56°C before use
Penicillin (Biochrom)	additive to cell culture media (final concentration: 100 U/ml)
RPMI1640 (Biochrom)	sterile fluid media
Streptomycinsulfat (Biochrom)	additive to cell culture media (final concentration: 100 µg/ml)
Trypan Blue (Biochrom)	was diluted 1:4 with PBS
Trypsin (Biochrom)	500 mg Trypsin and 200 mg EDTA were dissolved in PBS and sterilized by filtration

2.9 CELL LINES

(HEK-) ad293	human embryonic kidney cell line transformed with adenovirus 5 DNA (CRL-1573, ATCC), semi-adherent
(HEK-) 293T	human embryonic kidney cell line transformed with the large T-antigen from the SV40 virus (DuBridge et al., 1987), adherent clone
COS7	african green monkey kidney fibroblast-like cell line (CRL-1651, ATCC), adherent
C2C12	murine muscle myoblast line, described to differentiate to myotubes under serum starvation and to osteoblasts under BMP treatment (CRL-1772, ATCC), adherent
HeLa	malignant cervix cells removed from the cervix of <u>Henrietta Lacks</u> , a 31 year old black woman from Baltimore in 1951, Henrietta Lacks died eight months later from cervical cancer, adherent
AGS	stomach adenocarcinoma cell line, adherent

2.10 GROWTH FACTORS

BMP2 recombinant BMP2 was a generous gift from Prof. W. Sebald, Würzburg

2.11 ANTIBODIES

Antibodies used in the studies and the corresponding conditions are listed in the table below (Table 2.1).

Antibody	Dilution for WB	Dilution for IF	Conc. for IP	Blocking	Type, origin	Epitope, recognition
1st Antibody						
anti-HA (Roche)	1:1000 in TBS-T (0,1%)	1:100 1:200	1 µg	5% BSA in TBS-T (0,1%)	monoclonal, mouse	12CA5, haemagglutinin protein (YPYDVPDYA)
anti-HA (Santa Cruz)	1:1000 in TBS-T (0,1%)	1:50	-	1,5% BSA in TBS-T (0,1%)	polyclonal, rabbit, Y-11	12CA5, haemagglutinin protein (YPYDVPDYA)
anti-cav-1 α (Santa Cruz)	1:1000 in TBS-T (0,1%)	0,5 µg	1 µg	5% BSA in TBS-T (0,1%)	polyclonal, rabbit	epitope mapping at the N-terminus of cav-1, cav-1 α -specific
anti-cav-1 (BD Transduction Laboratories)	1:500 in blocking	2,5 µg	-	3% BSA in TBS-T (0,1%)	monoclonal, mouse	immuno. FEDVIAEP, clone 2297, recognizes both isoforms of cav-1
anti-PSmad1/5/8 (Cell signaling)	1:500 in TBS-T (0,1%) + 5% BSA	1:100	-	5% milk in TBS-T (0,1%)	polyclonal, rabbit	C-terminally phosphorylated form of Smad1/5 (Ser463, 465, KKKNPISSVS) and Smad8 (Ser426, 428)
anti-PSmad1/5 (P. ten Dijke, Leiden) (Persson et al., 1998)	1:1000 in TBS-T (0,5%)	-	-	5% milk in TBS-T (0,5%)	polyclonal, rabbit	C-terminal phosphorylated form of Smad1 (Ser463/465, KKKNPISSVS), crossreacts with P-Smad3

Material and solutions

Antibody	Dilution for WB	Dilution for IF	Conc. for IP	Blocking	Type, origin	Epitope, recognition
1st Antibody						
anti-Smad1/5 (P. ten Dijke, Leiden) (Persson et al., 1998)	1:1000 in TBS-T (0,5%)	-	-	5% milk in TBS-T (0,5%)	polyclonal, rabbit	region in the MH2 domain of Smad1 (QWLDKLTQ MGSPHNPISSVS)
anti-β-Actin (Sigma)	1:10000 in TBS-T (0,1%)	-	-	2% milk in TBS-T (0,1%)	monoclonal, mouse	Slightly modified β-cytoplasmic actin N-terminal peptide Ac-DDDIAALVIDNGSGL conjugated to KLH, clone AC-15
anti-GFP (Santa Cruz)	1:1000 in TBS-T (0,1%)	-	-	5% milk in TBS-T (0,1%)	monoclonal, mouse	immunogen: aa 1-238, clone B-2
anti-P-p38 (Promega)	1:2000 in TBS-T (0,1%)	-	-	1% BSA in TBS	polyclonal, rabbit	phosphorylated form of human p38 (pTGpY), the catalytic core T180 and Y182
anti-Eps15R (Abgent)	1:100 in TBS-T (0,1%)	-	1 µg	5% milk in TBS-T (0,1%)	polyclonal, rabbit	immunogen: synthetic peptide within the region of aa 800-815 of human Eps15R, conjugated to KLH
anti-Eps15R (Coda et al., 1998)	1:1000 in blocking	-	-	5% milk in TBS	polyclonal, rabbit	immunogen: region between EH2 – and EH3 domain (aa 216-266)
anti-Clathrin (Sigma)	-	1:20 1:50	-	-	polyclonal, goat, whole antiserum	immunogen: clathrin from bovine brain coated vesicles, wide interspecies cross-reactivity
anti-EEA1	1:500 in TBS-T (0,1%)	1:100	-	3% milk in TBS-T (0,1%)	monoclonal, mouse	immunogen: aa 3-281 from human EEA1, clone 14

Material and solutions

Antibody	Dilution for WB	Dilution for IF	Conc. for IP	Blocking	Type, origin	Epitope, recognition
1st Antibody						
anti-GD1a (Lunn et al., 2000)	Dotblot: 1:1000 in TBS-T (0,1%)	0,1 µg/ml	-	3% milk in TBS-T (0,1%)	monoclonal, mouse	immunogen: GD1a conjugated to KLH, knockout mice with a disrupted gene for GM2/GD2 synthase
2nd Antibody						
goat-anti-rabbit (Dianova)	1:20000 in TBS-T (0,1% or 0,5%)	-	-	-	polyclonal, goat	heavy – and light chains of rabbit IgGs, HRP-conjugated
goat-anti-mouse (Dianova)	1:20000 in TBS-T (0,1%)	-	-	-	polyclonal, goat	heavy – and light chains of mouse IgGs and IgMs, HRP-conjugated
goat-anti-rabbit (Dianova)	-	1:200	-	-	polyclonal, goat	heavy – and light chains of rabbit IgGs, Cy2-conjugated
goat-anti-mouse (Dianova)	-	1:200	-	-	polyclonal, goat	heavy – and light chains of mouse IgGs, Cy3-conjugated
goat-anti-mouse (Dianova)	-	1:1000	-	-	polyclonal, goat	heavy – and light chains of mouse IgGs, Cy2-conjugated
goat-anti-rabbit (Molecular Probes)	-	1:200	-	-	polyclonal, goat	heavy – and light chains of rabbit IgGs, Alexa546-conjugated

Table 2.1 List of first and secondary antibodies, used during this work.

TBS-T
 10 mM TRIS/HCl pH 8,0
 150 mM NaCl
 0,1 or 0,5% Tween-20

2.12 STANDARDS

2.12.1 DNA-standards

100 bp standard (NEB)	1500 bp – 1200 bp – 1000 bp – 900 bp – 800 bp – 700 bp – 600 bp – 500 bp – 400 bp – 300 bp – 200 bp – 100 bp
1 kb standard (NEB)	10 kb – 8 kb – 6 kb – 5 kb – 4 kb – 3 kb – 2 kb – 1,5 kb – 1 kb – 0,5 kb

2.12.2 Protein-standards

SDS-7B (Sigma)

The molecular weight of standard proteins varies slightly between different batches of the product.

Protein	Molecular weight [kD]
A ₂ -Macroglobulin	172,5
β-Galactosidase	112,5
Fructose-6-phosphate kinase	86
Pyruvate kinase	62,5
Fumarase	53
Lactic dehydrogenase	33,5
Triosephosphate isomerase	31,5

Table 2.2 Molecular Weight Standard SDS-7B.

Precision Plus Protein standards, all blue (BIO-RAD)

Recombinant proteins are designed to get convenient and consistent sizes. Three reference bands are three times as intense as the other bands (25, 50 and 75 kD).

250 kD – 150 kD – 100 kD – 75 kD – 50 kD – 37 kD – 25 kD – 20 kD – 15 kD – 10 kD

3 METHODS

3.1 MICROBIOLOGICAL METHODS

3.1.1 Sterilization

All solutions, buffers and media were sterilized by autoclaving at 120°C and 1,1 bar for 20 min. Solutions that contain heat-sensitive components were sterilized by filtration using sterile 0,2 µm filters.

3.1.2 Growth media

Luria-Bertani-medium (LB) 10 g/l Trypton
 5 g/l Yeast-extract
 10 g/l NaCl
 adjust pH 7,4 and autoclave

SOB-medium 20 g/l Trypton
 5 g/l Yeast-extract
 0,5 g/l NaCl
 0,83 mM KCl
 adjust pH 7,0 and autoclave

SOC-medium 1 ml SOB-medium
 10 µl 1M MgCl₂
 10 µl 1M MgSO₄
 10 µl 40% glucose

LB-agar plates supplement LB-medium with 15 g/l agar
 autoclave and cool down to 40°C
 add antibiotic(s) in appropriate concentration
 pour fluid LB-agar in plates to gel

3.1.3 Cultivation and conservation of bacteria

For cultivating bacteria plain LB-medium or LB-medium containing appropriate concentrations of antibiotics were used. Cultivation was carried out over night at 37°C under permanent shaking.

For long-term conservation of bacteria 500 µl of a freshly prepared bacteria suspension were mixed with 200 µl 86% sterile glycerol solution and stored in cryo-vials at -80°C.

3.1.4 Preparation of chemically competent *E.coli*

For the transformation of *E.coli* via heat-shock it was necessary to treat bacteria cells chemically, so that they would be able to accept plasmid DNA.

Therefore 200 ml LB-medium without antibiotics were inoculated with a 2 ml LB-over night culture until an optical density of $OD_{550\text{ nm}} = 0,2 - 0,3$ was reached. Afterwards bacteria were incubated on ice for 5 min and centrifuged for 10 min at 2500 rpm and 4°C. The pellet was resuspended in 40 ml ice-cold Tfb1-buffer. Following a second centrifugation for 10 min at 3000 rpm and 4°C, the pellet was resuspended thoroughly in 4 ml ice-cold Tfb2-buffer and incubated on ice for 15 min. Aliquots of 200 µl were transferred to sterile cryo-vials, immediately frozen in liquid nitrogen and stored at -80°C.

To determine the transformation rate of competent bacteria, 1 ng of a plasmid was transformed in 100 µl of competent bacteria suspension and the number of grown colonies was calculated as colonies per µg plasmid DNA. A good competence is reached when the transformation rate is $\geq 10^7$ colonies per µg plasmid DNA.

Tfb1-buffer

30 mM KAc
100 nM RbCl
10 mM $\text{CaCl}_2 \cdot 2\text{H}_2\text{O}$
50 mM $\text{MnCl}_2 \cdot 4\text{H}_2\text{O}$

dissolve in 300 ml dH_2O
adjust pH 5,8
add 75 ml 86% glycerol
add dH_2O to reach a final volume of 500 ml
autoclave

Tfb2-buffer

10 mM MOPS
75 mM $\text{CaCl}_2 \cdot 2\text{H}_2\text{O}$
10 mM RbCl

dissolve in 50 ml dH_2O
adjust pH 6,5 with 1 M KOH
add 15 ml 86% glycerol
add dH_2O to reach a final volume
of 100 ml
autoclave

3.1.5 Transformation of competent *E.coli* by heat-shock

At least 1 – 10 ng of plasmid DNA were added to 100 µl of competent bacteria which were thawed on ice. Following incubation on ice for 30 min, the heat-shock was accomplished at 42°C for 90 s, allowing DNA uptake into the bacteria cells. After 1 – 2 min on ice bacteria

were resuspended in 1 ml SOC-medium and incubated for 30 – 60 min at 37°C (or at appropriate temperature for the respective bacteria strain) in a shaker. The bacteria solution was centrifuged and the cell pellet resuspended in 100 µl LB-medium. To select transformed bacteria, 10 µl or 50 µl were plated on a LB-agar plate containing the appropriate antibiotics and incubated over night at the suitable temperature.

3.2 MOLECULAR BIOLOGICAL METHODS

3.2.1 Plasmid-DNA amplification and isolation

To amplify transformed bacteria a 2 ml LB-over day culture was inoculated to 100 ml of LB-medium containing appropriate antibiotics. The isolation of plasmid DNA was carried out according to manufacturers' instructions from the *Qiagen Plasmid Maxi Kit*, which is based on the principle of alkaline lysis, followed by binding of plasmid DNA to an Anion-Exchange Resin under low-salt and pH conditions. The DNA is purified from RNA, proteins and other impurities by a medium-salt wash and eluted in a high-salt buffer. Finally, the DNA is concentrated and desalted by isopropanol precipitation.

3.2.2 Determination of nucleic acid concentrations

The concentration of nucleic acids can be determined by measuring the absorption of an aqueous solution at a wavelength of 260 nm using a spectrophotometer.

DNA was diluted 1:100 in dH₂O and the absorption spectrum was measured in the range of 240 – 320 nm after having calibrated the photometer with pure dH₂O. The concentration of the original solution can be calculated by comprising the dilution factor as follows:

cDNA	$c = 33 \times A_{260 \text{ nm}} \times \text{dilution factor} [\mu\text{g/ml}]$
DNA	$c = 50 \times A_{260 \text{ nm}} \times \text{dilution factor} [\mu\text{g/ml}]$
RNA	$c = 40 \times A_{260 \text{ nm}} \times \text{dilution factor} [\mu\text{g/ml}]$

3.2.3 Agarose gel electrophoresis

The electrophoretic separation of DNA and DNA-fragments was achieved, depending on its molecular weight, in 1 – 2% agarose gels containing 1 µg/ml Ethidium Bromide (EtBr; final concentration) in TAE-buffer. Nucleic acid containing samples were mixed with 6 x DNA sample buffer and loaded onto the gel. The gel run was carried out at 100 V. Visualization of DNA is possible because of intercalation of EtBr into the double-helix of the DNA and fluorescence stimulation using the UV-transilluminator at a wavelength of 254 nm.

Methods

10 x TAE	400 mM TRIS/acetate, pH 8,5 10 mM EDTA
6 x DNA sample buffer	0,25% Bromphenolblue 0,25% Xylencyanol 30% glycerol dissolve in dH ₂ O and store in aliquots at 4°C
EtBr	10 mg/ml

3.2.4 DNA sequencing

Sequencing of DNA constructs was carried out by Dr. W. Feichtinger (Physiological Chemistry I, Biocenter, Würzburg) using the automated CEQ™ 8000 sequencer (Beckmann Coulter). The reaction is based on the chain-terminating method according to Sanger (Sanger et al., 1977) with fluorescently labeled dideoxynucleotids.

For sample preparation the *CEQ 2000 Terminator Cycle Sequencing – Quick Start Kit* (Beckmann) was used. The results were analyzed by the mean of the computer program *CEQ 2000*.

3.2.5 RNA extraction

10⁵ C2C12 cells/well or 3 x 10⁵ 293T cells/well were seeded on a 6-well plate. After washing the cells with 1 x PBS, cell lysis was carried out by adding 1 ml TriFast (PeqLab)/well. To extract RNA, 200 µl chloroform were added, vortexed for 15 s and incubated 3 – 10 min at RT. Centrifugation for 5 min at 12000 rpm and RT leads to the formation of 3 phases, from which the upper, aqueous phase contains exclusively RNA and was transferred to a new tube. Most of the DNA is found in the interphase whereas proteins could be extracted from the organic phase. The RNA-containing phase was mixed with 500 µl isopropanol, incubated for 5 – 15 min at RT and centrifuged for 10 min at 12000 rpm and 4°C for RNA-precipitation. The pellet was washed two times with 75% ethanol at 4°C, air dried and dissolved in 30 µl RNase-free dH₂O.

As an alternative, total RNA was isolated using the *RNeasy Mini Kit* (Qiagen) according to manufacturers' instructions.

Yield and quality of the RNA were verified by spectrophotometry.

1 x PBS	10 g/l NaCl
	0,25 g/l KCl
	1,45 g/l Na ₂ HPO ₄
	0,25 g/l KH ₂ PO ₄
	dissolve in dH ₂ O

3.2.6 Reverse transcription

Starting from 2 µg of total RNA, single-stranded cDNA was synthesized by using a reverse transcriptase (MMLV, from *Moloney Murine Leukemia Virus*) and Oligo-dT primers. For that 2 µg RNA, 0,5 µg Oligo-dT primers and RNase-free water were mixed and denatured for 5 min at 70°C. Afterwards 0,4 mM dNTPs, 1 x MMLV-buffer, 1,6 U RNase inhibitor and 8 U MMLV-reverse transcriptase were added and the reaction mix was filled up with RNase-free water to reach a final volume of 25 µl. The mixture was incubated for 50 min at 42°C followed by 15 min incubation at 70°C to inactivate the enzyme. The generated cDNA could be used directly in polymerase chain reactions or stored at -20°C.

3.2.7 Polymerase chain reaction (PCR)

To amplify small amounts of DNA- or cDNA-fragments, the polymerase chain reaction is used. For this purpose double stranded DNA is at first denatured, then primers are allowed to anneal. In a third step, the elongation phase, the synthesis of DNA is completed by means of a DNA-polymerase.

A standard PCR reaction is performed by using the following reaction mix and PCR cyler program:

Reaction mix	1 x <i>Taq</i> incubation mix with MgCl ₂
	0,2 mM dNTPs
	1 pmol/µl 5' primer
	1 pmol/µl 3' primer
	0,05 U <i>Taq</i> DNA-polymerase
	2 µl template cDNA or 1 – 10 ng template DNA
	ad 50 µl with dH ₂ O

Methods

Standard cycler program	Initial denaturation	95°C	5 min	1 x
	Denaturation	95°C	30 s	} 30 x
	Annealing	50 – 60°C	30 s	
	Elongation	72°C	30 s – 1 min	
	Final extension	72°C	10 min	1 x

For special template – primer combinations the program has to be adapted that is in terms of Annealing temperature or Elongation time. Sometimes it was necessary to use a biphasic PCR by converging gradually to the required Annealing temperature for two cycles each. The Annealing temperature is dependent on the composition of the primers and the resultant melting temperature (T_D). T_D can be calculated by the following formula:

$$T_D = [(C_n + G_n) \times 4 + (A_n + T_n) \times 2]^\circ\text{C}$$

The duration of the Elongation phase is dependent on the length of the fragment which is amplified and on the processivity of the DNA-polymerase used.

3.2.8 Caveolin-1 knockdown via RNA interference

RNA interference (RNAi) is a cell mechanism which influences gene expression of cells at the post-transcriptional level (PTGS = post-transcriptional gene silencing). RNAi was at first described in *petunia* and other plants, but in the last few years it has become clear that it occurs also in animals and important functions like viral defense and transposon silencing have been reported (Hammond et al., 2001). This mechanism can be used to knockdown specifically genes which gives a more detailed view on the physiological importance of the respective gene. This technique was successfully accomplished for the first time on mammalian cells by Elbashir et al. (Elbashir et al., 2001).

RNAi is initiated by the introduction of double-stranded RNA (dsRNA) which is digested into 21 – 23 nucleotides small interfering RNAs (siRNAs) by an enzyme called Dicer, a member of the RNase III family of dsRNA-specific ribonucleases. The siRNA duplexes bind to a nuclease complex to form the RNA-induced silencing complex (RISC) which is activated by an ATP-dependent unwinding of the duplexes. Active RISCs target the homologous transcripts and cleave the corresponding mRNA (www.ambion.com).

In practice, it is possible to generate specific siRNA by oneself or to purchase tested oligonucleotides ready-for-use from a company.

siRNA specified against cav-1 was bought from Santa Cruz and transfected into C2C12 cells to knockdown endogenous cav-1 expression and by that affecting caveolae formation. 10^5 C2C12 cells per well were seeded in a 6-well plate and grown over night in the incubator. The next day cells were transfected with 10 μ M cav-1 siRNA (Santa Cruz) or fluorescently labeled scrambled siRNA probe (Qiagen) using the Lipofectamin™-method (see 3.3.4.3) and incubated at 37°C over night. The transfection efficiency can be checked by means of the fluorescently labeled control siRNA and the fluorescence microscope. The transfected cells can be used in different cellular assays to verify and examine the effect of the downregulation of the cav-1 gene.

3.3 CELL BIOLOGICAL METHODS

3.3.1 Cultivation of eukaryotic cells

Depending on the cell line, cells were grown in DMEM (C2C12, 293T, 293, COS-7, HeLa) or RPMI (AGS) medium supplemented with 5 or 10% FCS, 1% glutamine and antibiotics in an incubator at 37°C, 95% humidity and 5 or 10% CO₂.

For subcultivation, adherent cells were detached from the cell culture flask using 2 x Trypsin. Addition of fresh FCS-containing medium blocks the activity of trypsin.

3.3.2 Determination of cell number

For determining the cell number per ml medium a Neubauer counting chamber was used. The cell suspension was mixed with Trypan Blue solution at a 1:1 ratio. This dye can only enter dead cells, so that it is possible to identify dead cells by blue staining and count only the unstained, living cells. Normally, two out of four quadrants were counted and the cell concentration (cell number/ml) calculated by multiplying the chamber factor 10^4 .

3.3.3 Cryo-conservation of cells

For long-term conversation of cells, about $10^6 - 10^7$ cells are resuspended in growth medium containing 10% DMSO, transferred to a cryo-vial, kept at -80°C over night and stored in liquid nitrogen (-196°C).

Thawing of cells was carried out rapidly at 37°C. The cells were immediately transferred to growth medium and cultivated at corresponding conditions.

3.3.4 Transfection of eukaryotic cells

3.3.4.1 Transfection of 293T cells using Calcium-phosphate coprecipitation

This transfection method was carried out in 6 cm - (or 6 well) plates. The day before transfection, 10^6 (3×10^5) cells were seeded. Prior to transfection the medium was replaced by 4 ml (2 ml) of fresh growth medium and the cells were returned to the incubator for pH adjustment. 10 μ g (5 μ g) DNA were mixed with dH₂O to reach a final volume of 438 μ l (219 μ l) and 62 μ l (31 μ l) of 2 M CaCl₂ was added. After mixing the solution, 500 μ l (250 μ l) 2 x HBS were added by “bubbling” and the mixture is immediately distributed drop by drop on the cells. Following incubation for 7 – 10 h at 37°C and 5% CO₂, the transfection medium is replaced by fresh growth medium. 24 - 48 h post transfection, cells could be used for further experiments.

2 x HBS	50 mM HEPES 10 mM KCl 12 mM α -D-glucose 280 mM NaCl 1,5 mM Na ₂ HPO ₄ dissolve in dH ₂ O adjust pH 7,0 – 7,1 using 1 M NaOH autoclave and store in aliquots at -20°C
2 M CaCl ₂	dissolve CaCl ₂ in dH ₂ O autoclave and store in aliquots at -20°C

3.3.4.2 Transfection of COS-7 cells using DEAE-dextran

This transfection method was carried out in 10 cm plates in which around 10^6 COS-7 cells were seeded the day before transfection to reach a confluency of about 50 – 70%. 10 μ g plasmid DNA were dissolved in transfection buffer to reach a final volume of 1140 μ l and 60 μ l of freshly prepared DEAE-dextran (10 mg/ml) were added. After washing the cells three times with prewarmed transfection buffer, the cells were incubated with the DNA/DEAE-dextran mixture for 30 min at 37°C. Subsequently, 14 ml Chloroquine-Nu-medium was added to the transfection mixture on the cells and the cells were incubated for 2,5 – 3 h at 37°C and 5% CO₂. Following this incubation time, a DMSO-shock was performed to facilitate DNA uptake. For that, the transfection medium was aspirated and the cells were treated for exactly 2,5 min with 3 ml of growth medium containing 10% DMSO. Afterwards the cells

were washed with growth medium and subsequently cultivated under appropriate conditions. 48 h post transfection, cells could be used for further experiments.

Transfection buffer	250 mM NaCl 2,3 mM NaH ₂ PO ₄ 7,7 mM Na ₂ HPO ₄ dissolve in dH ₂ O adjust pH 7,5 and autoclave
DEAE-dextran	10 mg/ml in sterile dH ₂ O
Chloroquine	20 mg/ml (40mM) in sterile dH ₂ O
Chloroquine-Nu-medium	10% Nu-serum 80 µM Chloroquine in DMEM without supplements

3.3.4.3 Transfection of C2C12 cells using Lipofectamine™

Lipofectamine™ transfection was performed as to manufacturers' instructions (Life Technologies). The day before transfection, C2C12 cells were seeded on a 6-well plate in a density of 10⁵ cells per well. 1 – 3 µg DNA per well were dissolved in DMEM containing 0,2% FCS (without antibiotics) to reach a final volume of 100 µl. In parallel, 10 µl Lipofectamine™ Reagent were mixed with 100 µl DMEM without supplements in a separate tube. The two solutions were combined and incubated for 30 min at RT. After that 800 µl DMEM without supplements were added to the transfection mixture and distributed on the cells. Following incubation for 5 h in the incubator at 37°C and 10% CO₂, the transfection medium was replaced by growth medium and the cells could be used for further experiments 24 – 48 h later.

3.3.4.4 Transfection using Polyetylenimine (PEI)

PEI (Aldrich) is an organic macromolecule with very high cationic-charge-density potential and is described in the literature as a versatile vector for gene delivery to the nucleus of mammalian cells (Boussif et al., 1995; Florea et al., 2002). Acid-catalyzed polymerization generates a highly branched network that is able to act as a proton-sponge to ensnare DNA. Its efficiency seems to rely on its ability to buffer the low pH in the lysosome which protects DNA from nuclease degradation. The PEI/DNA complex is released into the cytoplasm and

It can not be ruled out that also other membrane regions are affected by some of these treatments.

Because of that, two different classes of raft-disrupting agents were used in this study and extensively tested concerning the concentration and treatment time periods. The success of cholesterol depletion was measured by determination of the cholesterol concentration of a depleted probe in comparison to a non-treated sample (3.3.5.4).

3.3.5.1 Preparing of lipoprotein-deficient serum

During treatment of the cells with cholesterol depleting agents, lipoprotein-deficient serum (LPDS) instead of normal FCS was used. Thereby it is prevented that the cells compensate their cholesterol loss by lipids out of the serum.

20 g solid KBr was completely dissolved in 50 ml FCS and filled in ultracentrifuge tubes. The mixture was ultracentrifuged for 48 h at 40000 rpm and 4°C. The upper phase (20 – 25% of the volume) was removed and the serum was dialyzed against 500 ml of TNE-buffer to get rid of remaining celltoxic KBr. The buffer is changed 5 – 6 times over a period of 10 – 16 h. Afterwards the volume of the serum was adjusted back to 50 ml with TNE-buffer. Finally the serum was sterile filtered using a 0,2 µm filter, aliquoted and stored at -20°C.

TNE-buffer	2 mM TRIS/HCl pH 7,4
	150 mM NaCl
	0,01% Na-EDTA

3.3.5.2 Lovastatin activation and treatment

The active form of Lovastatin (C₂₄H₃₆O₅) is a principal metabolite and potent inhibitor of 3-hydroxy-3-methylglutaryl-coenzyme A (HMG-CoA) reductase which catalyzes an early and rate limiting step in the biosynthesis of cholesterol, namely the conversion of HMG-CoA to mevalonate. Because it is initially an inactive lactone, it has to be activated by hydrolysis to the corresponding β-hydroxyacid form. It is sparingly soluble in ethanol, methanol and acetonitrile, but not in water.

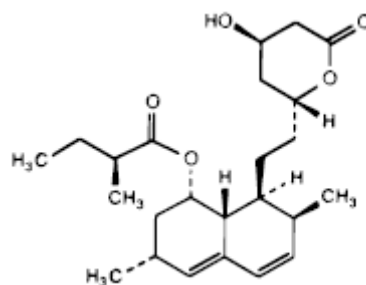


Fig. 3.1 Structure of Lovastatin (Calbiochem)

90 mg of Lovastatin (Calbiochem) were dissolved in 1,8 ml ethanol which was preheated to 55°C. 0,9 ml of 0,6 M NaOH and subsequently 18 ml dH₂O was added. The dilution was incubated for 30 min at RT and it was checked with pH paper that the pH is 8. If the pH was higher, it had to be adjusted with HCl. To reach a final concentration of 4 mg/ml (0,01 M), dH₂O is added until a volume of 22,5 ml was obtained. Finally the solution was sterile filtered by a 0,2 µm filter and stored in aliquots for up to 3 month at -20°C.

To start the inhibition reaction of Lovastatin, catalytical amounts of mevalonate, the product of the reaction, had to be added. Mevalonic acid lactone (Sigma) was dissolved in 1 x PBS to a slightly higher concentration than 2 M. The pH was calibrated to pH 7,2 using HCl and the volume was adjusted to reach a final concentration of 2 M. The solution was sterile filtered by a 0,2 µm filter and stored in aliquots at -20°C.

To prepare the cells for the treatment, an appropriate amount of each cell type was seeded in a cell culture plate and grown over night in the incubator in growth medium. The next day cells were washed once with 1 x PBS and starved with DMEM containing 0,5% LPDS for different time periods depending on the following experiment. Subsequently, the cells were incubated for 16 h in starving medium containing 50 µM Lovastatin and 50 µM mevalonate. Finally, the cells were harvested and treated for the particular experiment.

3.3.5.3 Methyl-β-cyclodextrin treatment

Methyl-β-cyclodextrin (MβCD) is a naturally occurring, cyclic oligosaccharide consisting of 7 glucopyranose units and is commonly used as a complexing agent. The molecule assumes the shape of a torus and this hydrophobic cavity is well-suited for use with molecules the size of hormones or vitamins. In several publications it is mentioned as a cholesterol sequestering agent.

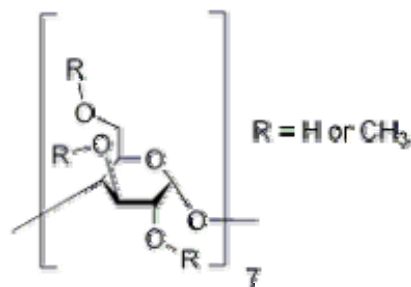


Fig. 3.2 Structure of one glucopyranose unit of MβCD (Sigma)

The solubility of MβCD is 50 mg/ml in dH₂O what is equivalent of 38 mM stock solution. This stock solution was sterile filtered and stored at 4°C.

To deplete cholesterol from the membrane, an appropriate amount of cells were seeded in a cell culture plate and grown over night in growth medium in the incubator. The next day cells

were washed once with 1 x PBS and starved with DMEM containing 0,5% LPDS for different time periods depending on the following experiment. Subsequently the cells were incubated in starving medium containing 2,5 – 10 mM M β CD. For a 30 min – 1 h incubation period 10 mM were used and for 16 h or longer time periods of treatment 2,5 mM M β CD were applied. Finally the cells were harvested and treated for the particular experiment.

3.3.5.4 Quantitation of cholesterol level

To verify the reduction of cholesterol levels by Lovastatin and M β CD, the *Amplex Red Cholesterol Assay Kit* (Molecular Probes) was used according to manufacturers' instructions. The principle of this assay is based on the oxidation of cholesterol by a provided cholesterol oxidase to H₂O₂ and the corresponding ketone product. The amount of H₂O₂ can be determined by a colorimetric analysis via Resorufin fluorescence which is produced after adding the *Amplex Red Reagent* (10-acetyl-3,7-dihydroxyphenoxazine) and horseradish peroxidase (HRP). Resorufin has absorption and fluorescence maxima of 563 nm and 587 nm. The reaction was measured against a cholesterol calibration curve (2 μ g/ml – 4 μ g/ml - 6 μ g/ml – 8 μ g/ml) and together with a H₂O₂-positive control in the microplate reader (reference filter: 630 nm, test filter: 550 nm).

3.3.6 Inhibition of clathrin-coated pit-mediated endocytosis by chlorpromazine

Chlorpromazine (CP) is a cationic amphiphilic drug which interferes with the recycling machinery of endocytosed molecules. The exact mechanism of this inhibition is not known, but it is reported that treatment with 100 μ M CP for 30 min at 37°C causes clathrin-coated pits (CCPs) to disappear from the cell surface by affecting the AP-2 binding to the plasma membrane (Wang et al., 1993).

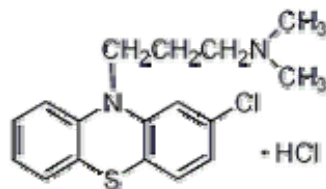


Fig. 3.3 Structure of chlorpromazine (Sigma)

To inhibit specifically CCP-mediated endocytosis, an appropriate amount of cells were seeded in a cell culture plate and grown over night in growth medium in the incubator. The next day cells were washed once with 1 x PBS and starved with DMEM containing 0,5% FCS for different time periods depending on the following experiment. Subsequently, the cells were incubated in starving medium containing 5 μ M CP. In pretests it was shown that higher

CP-concentrations affected the cell viability (C2C12, 293T and COS7 cells). Finally, the cells were harvested and treated for the particular experiment.

3.3.7 Cellular assays

3.3.7.1 Determination of Phospho-Smad1/5

To detect the level of phosphorylated Smad1/5 in C2C12 (293T) cells in dependence on different overexpressed genes or inhibitors, 10^5 (3×10^5) cells were seeded in 6-well plates, grown over night at 37°C and 10% (5%) CO₂ and starved for 24 h in starving medium. Following stimulation of the cells with 20 nM BMP2 in starving medium for 30 min, cells were lysed in 100 µl of TNE-Tx buffer per well supplemented with protease- and phosphatase inhibitors. Afterwards the protein concentration was determined using the Redinbaugh method (see 3.4.4). By loading the same protein amount per lane, an immunoblot was performed and incubated with an antibody which specifically detects the phosphorylated form of Smad1/5 (see Table 2.1).

starving medium	DMEM + 0,5% FCS + antibiotics
TNE-Tx buffer	25 mM TRIS, pH 7,5 150 mM NaCl 3 mM EDTA 1% Triton X-100
Protease inhibitors	25 x Protease inhibitor cocktail (Roche) 1 tablet dissolved in 2 ml dH ₂ O, store at -20°C working concentration: 1 x 100 x PMSF 100 mM phenylmethylsulfonylfluoride dissolved in isopropanol, store at -20°C working concentration: 1 x
Phosphatase inhibitors	200 mM Na ₃ VO ₄ working concentration: 2 mM 200 mM Na ₂ P ₂ O ₇ in dH ₂ O working concentration: 20 mM

1 M NaF in dH₂O
working concentration: 20 mM

3.3.7.2 Determination of Phospho-p38

To detect the level of phosphorylated p38 in C2C12 cells in dependence on different overexpressed genes or inhibitors, 10⁵ cells were seeded in 6-well plates, grown over night at 37°C and 10% CO₂. The starving time for this assay needs to be established every time new to get a sufficient stimulation effect and varied between 1 h and 8 h. Following stimulation of the cells with 20 nM BMP2 in starving medium for 1 h, cells were lysed in 100 µl of TNE-Tx buffer per well supplemented with protease- and phosphatase inhibitors. Afterwards the protein concentration was determined using the Redinbaugh method (see 3.4.4). By loading the same protein amount per lane, an immunoblot was performed and incubated with an antibody which specifically detects the phosphorylated form of p38 (see Table 2.1).

3.3.7.3 Determination of BMP2-induced transcriptional activity using reporter gene assay

By applying reporter gene assays, it is possible to study gene regulatory elements and their ability to be regulated by soluble growth factors in dependence on different overexpressed genes or inhibitors.

A responsive promoter element is cloned in front of a luciferase gene, firefly luciferase (*Photinus pyralis*), and transfected into responsive cells.

The reporter gene assay was performed transfecting cells with 1 µg per 6-well of two different firefly luciferase constructs:

pSBE-luc (Smad Binding Element) (Jonk et al., 1998)

pBRE-luc (BMP Response Element) (Korchynskiy and ten Dijke, 2002)

The pSBE reporter consists of four Smad binding elements that are cloned in front of an adenoviral minimal promoter and the luciferase gene. It serves as readout for TGF-β as well as for BMP signaling.

The BRE-reporter is composed of BMP-responsive regions in the Id1-promoter upstream of a minimal adenoviral major late promoter (MLP) reporter construct. It responds specifically to BMP-mediated signals.

To normalize the firefly signal and to control transfection efficiency, 0,3 µg of a constitutively active luciferase gene per well, renilla luciferase (*Renilla reniformis*), were cotransfected. The next day, cells were incubated for 5 h in starving medium (see 3.3.7.1) and subsequently

stimulated with 10 nM (for SBE) or 1 nM (for BRE) BMP2 for 16 - 24 h. Cell lysis and luciferase measurements were carried out according to manufacturers' instructions of the *Dual Luciferase Assay System* (Promega). Luciferase activity was recorded in relative light units (RLU) by calculating the quotient between firefly- and renilla-activity. Because of the higher transfection efficiency 293T cells lysates were diluted to a final volume of 10 ml with dH₂O and measured as described.

3.3.7.4 Determination of Alkaline phosphatase activity

For quantitative analysis of Alkaline phosphatase (ALP) activity in dependence on different overexpressed genes or inhibitors, 3×10^3 C2C12 cells per well were seeded in a 96-well plate and grown over night. The next day cells were starved in ALP-starving medium for 5 h and subsequently stimulated with 50 nM or 100 nM BMP2 in ALP-starving medium for 72 h. Following cell lysis by applying 100 μ l of ALP1 (1 h rocking plate, RT), the enzymatic reaction was started by adding 100 μ l of ALP2 directly onto the 96-well plate. Enzymatic activity was measured using a microplate reader with test filter at 405 nm and reference filter at 550 nm.

ALP-starving medium	DMEM + 2% FCS + antibiotics
ALP1	0,1 M glycine, pH 9,6 1% NP-40 1 mM MgCl ₂ 1 mM ZnCl ₂
ALP2	0,1 M glycine, pH 9,6 1 mM MgCl ₂ 1 mM ZnCl ₂ 20 mg/ml p-nitrophenyl-phosphate (pNPP)
pNPP	1 tablet (20 mg) dissolved in 0,1 M glycine, pH 10,4 1 mM MgCl ₂ 1 mM ZnCl ₂

3.3.8 Microscopy

Three kinds of microscopy were used in this work.

At first **light microscopy** was applied - predominantly to control cell morphology after inhibitors of endocytosis were added or to count cells in the Neubauer counting chamber. For that the *Leitz DM IL* Light microscope from Leica was used with the 5 x or 10 x objective resulting in a 50 to 100 times magnification.

The second applied method was **fluorescence and confocal microscopy** to localize specific proteins in the cell or at the cell membrane. On the one hand, a DNA-GFP fusion can be transfected and the distribution of the protein-of-interest can be detected directly with a fluorescence microscope via the GFP fluorescence. On the other hand, immunofluorescence experiments can be used to detect endogenous proteins by means of specific antibodies and fluorescently labeled secondary antibodies. This method is described in detail in chapter 3.4.8. The analyses were accomplished with the Fluorescence microscope *Axiovert 25* from Zeiss by using three different filter sets:

Fluorochrome	Excitation [nm]	Emission [nm]
Hoechst 33258	345	487
Propidium Iodide;	536, 538;	617;
Cy3; Alexa546	552, 554; 556, 557	570; 572, 573
GFP; Cy2	475; 489	509; 506

Table 3.2 Filter sets of the fluorescence microscope

To achieve a magnification of 400 times a 40 x inverted objective was used.

To obtain a more detailed picture of the distribution of a molecule in the cell, the confocal laser scanning microscope (CLSM) *Leica DMR* from Leica was used. The same filter sets (except for the Hoechst filter which was not available for this microscope) and a 63 x objective (water, 630 times magnification) were used.

As a third method **electron microscopy** was employed.

For electron microscopy the cells were plated on coverslips (diameter: 12 mm, *CELLocate*, when transfected cells should be analyzed) which were put in a well of a 6-well plate. 5×10^4 C2C12 or 10^5 293T cells per well were seeded and grown over night in the incubator. The next day cells were transfected or directly fixed. For that coverslips were put on ice and covered with one drop (about 50 μ l) of 2,5% glutaraldehyde for 45 min. Following a wash step with 0,05 M cacodylate-buffer, every subsequent step had to be accomplished at the flue with appropriate protective clothing to avoid direct contact with toxic substances (above all OsO_4). The cells were fixed with 2% OsO_4 -solution buffered with 0,05 M cacodylate-buffer for 60 min. Following a wash step in dH_2O they were incubated in 0,5% uranyl acetate at 4°C over night. The next day cells were washed three times each for 5 min with dH_2O and

dehydrated by incubating the cells in gradually increasing alcohol concentrations on ice (50%, 70%, 90%, two times 100% EtOH). Following an incubation in propylenoxid (two times each for 5 min) and 2 – 4 h incubation in an 1:1 propylenoxid-EPON-mixture, cells were incubated in EPON (Serva) over night. The next day cells were embedded in EPON and after polymerization at 60°C for at least 24 h they were ultrathin sectioned. Sections were analyzed with a *Zeiss EM10* electronmicroscope (Zeiss).

These experiments were mainly carried out in the lab and under supervision of Prof. G. Krohne (Department of Electron Microscopy, University of Würzburg) by Daniela Bunsen and Elisabeth Meyer-Natus.

Glutaraldehyde solution	2,5% glutaraldehyde
	50 mM cacodylate pH 7,2
	50 mM KCl
	2,5 mM MgCl ₂

3.4 PROTEIN CHEMICAL METHODS

3.4.1 Cell lysis

Depending on the following assay, different lysis buffers were used for cell lysis. The composition and use of the buffers is mentioned in the description of the respective methods. At first the cells were washed with 1 x PBS, an appropriate volume of lysis buffer were added and the cells were scraped into an eppendorf-tube. Following 30 – 60 min incubation on the shaker at 4°C, lysed cells were centrifuged for 20 min at 13000 rpm and 4°C to precipitate insoluble cell contents and debris. The supernatant was transferred to a fresh tube, denatured by adding 6 x SDS-sample buffer and boiling for 5 min at 95°C and used for further analysis.

6 x SDS-sample buffer	125 mM TRIS/HCl, pH 6,8
	30% glycerol
	10% SDS
	0,6 M DTT
	0,012% Bromphenolblue

3.4.2 Separation of detergent-resistant membrane fractions

Caveolae and lipid rafts are insoluble in detergents like Triton X-100 or CHAPS at 4°C (Fra et al., 1994). The insolubility contributes to their high sphingolipid content.

Under such conditions these special plasma membrane domains form so called detergent-resistant membranes (DRMs) which can be separated from soluble cell contents by gradient centrifugation (Brown and Rose, 1992; Sargiacomo et al., 1993). Because of their high lipid content, DRMs float to a low density in sucrose or OptiPrep™ gradients. With this method it is possible to identify caveolae- and lipid rafts-associated proteins.

C2C12 cells which stably overexpress HA-tagged BMP receptors or truncation variants of BRII were seeded in 15 cm plates ($1,3 \times 10^6$ per plate) and grown in the incubator until a confluency of about 90 – 100% was reached. Another possibility was to transfect COS7 or 293T cells in 15 cm plates using PEI (see 3.3.4.4 and Table 3.1) and to proceed with these cells. In some experiments the cells were incubated for 2 h in starving medium and subsequently stimulated with 20 nM BMP2 for 30 min.

The cells were washed two times with ice-cold 1 x PBS, lysed with 650 μ l ice-cold TNE-CHAPS buffer per 15 cm plate and scraped into a 15 ml tube. Two plates of the same cell type were pooled resulting in 1,3 ml lysate, rotated for 30 min at 4°C and homogenized using a Potter (5 strokes at 1000 rpm, 4°C). As a control 100 μ l of the lysate were transferred to an eppendorf-tube and centrifuged for 20 min at 13000 rpm and 4°C. The cleared control-lysate was denatured by adding 20 μ l 6 x SDS-sample buffer and boiled for 5 min at 95°C. In the remaining homogenized lysate an OptiPrep™ concentration of 40% was adjusted by adding 2,7 ml 60% OptiPrep™ solution. The mixture was vortexed vigorously, transferred to an 12,5 ml ultracentrifuge tube (Beckman) and a discontinuous OptiPrep™ gradient (30%, 5%) was formed above the lysate by adding 4,5 ml 30% OptiPrep™ and subsequently 4,5 ml 5% OptiPrep™. The gradient was ultracentrifuged for 20 h at 39000 rpm and 4°C using the SW40Ti rotor (Beckman). Fractionation was performed in the cold room at 4°C from the top of the gradient by pipetting 12 x 1 ml fractions in eppendorf-tubes. Fractions were analyzed using SDS-PAGE and subsequent western blotting. To verify the separation method, a specific cav-1 antibody was applied. Potentially DRM-associated receptor constructs were detected by an antibody recognizing the HA-tag of the overexpressed receptors.

TNE-CHAPS buffer	20 mM CHAPS 25 mM TRIS/HCl pH 7,4 150 mM NaCl 3 mM EDTA 1x PMSF 1x Proteaseinhibitor Cocktail (Roche)
5%, 30% OptiPrep™	dilute 60% OptiPrep™ (original solution) with TNE

3.4.3 Protein precipitation by chloroform-methanol-extraction

To concentrate protein solutions, cell lysates or fractions after OptiPrep™ gradient centrifugation, proteins could be precipitated and resolved in a defined volume of solvent.

All the steps of this method should be carried out on ice or in the cold room as well as in the flue, because of the toxicity of chloroform.

800 µl of a 1 ml fraction were transferred to a 15 ml tube and 4 volumes methanol, 1 volume chloroform and 3 volumes dH₂O were added. After vortexing the mixture, it was centrifuged for 20 min at 3000 rpm and 4°C (without centrifuge brake). Two phases become visible. The intermediate phase contains proteins. The upper aqueous phase was discarded and 6 volumes methanol were added to the lower organic phase. This mixture was vortexed and centrifuged for 20 min at 3000 rpm and 4°C. Protein-pellets were air-dried and resolved in 50 – 100 µl 6 x SDS-sample buffer, boiled for 5 min at 95°C and subjected to SDS-PAGE and western blotting.

3.4.4 Protein quantification using the BCA assay (Redinbaugh-method)

For quantitative analysis of cell lysates it was necessary to determine the protein concentration of the lysate and to apply subsequently a defined protein amount in each lane of a SDS-gel. The protein concentration was determined by using the bicinchoninic acid (BCA) method (Redinbaugh and Turley, 1986).

The cell lysates were diluted in dH₂O (C2C12 cells: 1:10, 293T cells: 1:20) and 20 µl of each lysate added in doublets to a 96-well plate. For creating a calibration curve BSA standards - also in doublets - were added to the plate:

25 µg/ml – 50 µg/ml – 75 µg/ml – 100 µg/ml – 150 µg/ml – 200 µg/ml - 250 µg/ml

Solution A and B were mixed in a ratio of 49:1 and 200 µl of this mixture was added to the lysate dilutions. After incubation of 30 – 45 min at 60°C, a purple coloring is visible. The purple reaction product emerges from the chelate formation between two molecules of BCA and one Cu²⁺ -ion. Measurement of the coloring was accomplished via a microplate reader with the reference filter at 630 nm and testfilter at 550 nm. The protein concentration was calculated referring to the calibration curve.

Solution A	1,35% NaHCO ₃
	0,58% NaOH
	1% BCA (Pierce)
	0,57% K-Na tartrate
	dissolve in dH ₂ O, store in aliquots at -20°C

Solution B 2,3% CuSO₄ x 5 H₂O

3.4.5 Immunoprecipitation

Immunoprecipitations were performed to investigate potential interactions between two proteins. Therefore a particular protein was precipitated by incubating the cell lysate with an antibody which is specific for the respective protein. Afterwards Protein A-Sepharose was added which in turn specifically recognizes and binds the F_c part of the antibody. The immune-complex containing the protein-of-interest, the antibody and the heavy Sepharose beads are precipitated by centrifugation, washed and subjected to SDS-PAGE and western blotting.

In practice, cell lysates for co-immunoprecipitating cav-1 with BMP receptors were obtained by using special lysis conditions. Because caveolae are insoluble in detergents like Triton X-100 or CHAPS, n-octyl- β -D-glucosid was added to get cav-1 solved out from the membrane. The lysate was prepared like described in chapter 3.4.1. 1 μ g of cav-1 α antibody (Santa Cruz) was added and incubated under rotation over night (at least 4 h) at 4°C. The next day the mixture was incubated under rotation together with 50 μ l of a 1:1 Protein A-Sepharose/1 x PBS solution for 1 h at 4°C. The complex was precipitated by short centrifugation and washed three times with lysis buffer followed by two times washing with 1 x PBS. These steps were carried out in the cold room at 4°C. Finally 30 μ l of 2 x SDS-sample buffer were added to the dried Sepharose beads, boiled for 5 min at 95°C and the supernatant was subjected to SDS-PAGE and western blot analysis.

Lysis buffer for cav-1-IP	25 mM TRIS, pH 7,5 150 mM NaCl 3 mM EDTA 1% Triton X-100 60 mM n-Octyl- β -D-glucosid
2 x SDS-sample buffer	0,125 M TRIS/HCl, pH 6,8 4% SDS 10% β -Mercaptoethanol 0,02% Bromphenolblue

3.4.6 SDS-polyacrylamid gel electrophoresis (SDS-PAGE)

SDS-PAGE was performed according to Laemmli (Laemmli, 1970). Using this method, proteins are electrophoretically separated in the presence of SDS according to their

Methods

molecular weights in a discontinuous gel system. The denatured probes are concentrated in a stacking gel, followed by separation in the resolving gel.

7,5 – 12,5% polyacrylamid gels were prepared following the pipetting scheme below.

Reagent	stacking gel	resolving gel	resolving gel	resolving gel
		7,5%	10%	12,5%
AA/BAA	0,5 ml	3 ml	4 ml	5 ml
4 x Lower TRIS	-	3 ml	3 ml	3 ml
4 x Upper TRIS	1 ml	-	-	-
dH ₂ O	2,5 ml	6 ml	5 ml	4 ml
40% APS	8 µl	20 µl	20 µl	20 µl
TEMED	8 µl	20 µl	20 µl	20 µl

Table 3.3 Pipetting scheme for SDS-PAGE.

After polymerization of the gels, the probes were loaded on the gel together with a protein standard (see 2.12.2). The gel electrophoresis chamber was filled with SDS-running buffer and the gel electrophoresis was carried out at up to 220 V until the samples are separated enough. Finally the gels could be used for western blotting (see 3.4.7).

Acrylamid/Bis-acrylamid (AA/BAA)	30% Acrylamid 1% N,N'-Methylenbisacrylamid
4 x Lower TRIS	1,5 M TRIS 0,4% SDS dissolve in dH ₂ O, adjust pH 8,8
4 x Upper TRIS	0,5 M TRIS 0,4% SDS dissolve in dH ₂ O, adjust pH 6,8
40% APS	40% Ammoniumpersulfate in dH ₂ O
TEMED (Roth)	N,N,N',N'-Tetramethylethyldiamine
5 x SDS-running buffer	25 mM TRIS 190 mM glycin 0,1% SDS dissolve in dH ₂ O

3.4.7 Western blot and detection of immobilized proteins

After separating proteins by SDS-PAGE, they were subsequently transferred to and fixed on a nitrocellulose membrane, where they can be detected by specific antibodies followed by visualization by the enhanced chemoluminescence (ECL) reaction.

For the transfer of the proteins to the nitrocellulose membrane the “wetblot” method was applied by using the *Mini-V 8.10* system from BIO-RAD. The transfer was carried out for 75 min at 100 V using transfer buffer.

Subsequently the blot was stained reversibly with Ponceau S to verify successful transfer and discolored by dH₂O or TBS. To saturate unspecific binding sites for the primary antibody on the membrane, the membrane was blocked for 1 h at RT on the shaker. Next the membrane was incubated with primary antibody solution at 4°C over night or for 1 h at RT on the shaker. Following three wash steps with TBS-T (0,1 – 0,5%) each for 10 min, the membrane was incubated with secondary antibody for 1 h at RT on the shaker (blocking solutions and primary and secondary antibody solutions, see Table 2.1). After another three rounds of washing, proteins on the membrane could be visualized by ECL detection. Therefore 1 ml of solution 1 and 1 ml of solution 2 per blot were mixed immediately before use and distributed on the membrane. After 1 min incubation, the solution was removed and the emitted light could be detected via an X-ray film which was exposed on the membrane for various times and developed in the dark room by means of a developing machine.

To use the same membrane for a new incubation with a primary antibody, the bound antibodies could be removed by 20 - 30 min incubation at 56°C in stripping buffer. Afterwards the membrane needed to be washed extensively with wash buffer, before it could be blocked again.

Transfer buffer	25 mM TRIS 190 mM glycin 20% methanol
Ponceau S	0,5% Ponceau S 3% Trichlor acetic acid (TCA)
ECL-solution 1	1 ml Luminol solution 4,4 µl para-coumaric acid
ECL-solution 2	1 ml 0,1 M TRIS/HCl pH 8,5 1 µl 30% H ₂ O ₂

Luminol	2,5 mM 3-Aminophthalhydrazide 1% DMSO dissolve in 0,1 M TRIS/HCl pH 8,5 store at 4°C in the dark
stripping buffer	5 mM NaH ₂ PO ₄ 1% SDS dissolve in dH ₂ O add 1,35 µl β-Mercaptoethanol to 10 ml stripping buffer directly before use

3.4.8 Immunofluorescence

By applying immunofluorescence (IF) experiments it is possible to study expression and distribution of proteins directly in the cell or in the cell membrane. Furthermore, colocalization studies between two proteins can be accomplished by that method.

Principally, there are two different procedures to label proteins with fluorescently-marked antibodies. On the one hand, proteins exhibiting an extracellular epitope, e.g. transmembrane receptors carrying an N-terminal tag, were labeled at the living cell by incubation with primary and secondary antibodies before fixation and permeabilization. A side effect of this alternative is that the primary antibody can concentrate the proteins of interest in "patches". On the other hand, for proteins exhibiting an intracellular epitope, e.g. cav-1, it is necessary to fix and penetrate the cells before primary and secondary reagents were applied, so that the antibodies can reach their epitopes inside of the cell.

2 x 10⁴ C2C12 cells per chamber were seeded in a 4-chamberslide and incubated at 37°C over night. The next day cells were washed with DMEM without FCS and incubated in the same medium for 1 h at 37°C to get rid of the serum. Subsequently cells were washed with icecold HHB-buffer and incubated in the same buffer for 2 h at 4°C to block unspecific binding sites. Following a 1 h incubation at 4°C with primary antibody diluted in HHB-buffer (see Table 2.1) and three subsequent washing steps with HHB-buffer on ice, cells were incubated for 1 h at 4°C with appropriate secondary fluorescently-coupled reagents diluted in HHB-buffer (see Table 2.1). After cells were washed three times with HHB-buffer, they were fixed using the methanol/acetone method. For that cells were incubated for 5 min at -20°C in ice-cold methanol and subsequently for additional 2 min in ice-cold acetone. Depending on the antibodies used, cells were alternatively fixed by incubation in paraformaldehyde (PFA) solution for 10 min at RT, followed by membrane penetration with 0,2% Triton X-100 for 2 min at RT. Fixed cells were washed with HHB-buffer and embedded with Kaisers Glycerin

Gelatine (Merck). Optional cell nuclei could be stained before embedding procedure as control by using Hoechst solution or propidiumiodide.

For colocalization studies with an intracellular protein, fixed, non-embedded cells were additionally incubated for 1 h at RT with primary antibody dilution in HHB-buffer (see Table 2.1) directed against the cytoplasmic epitope of the target protein. Following three wash steps with HHB-buffers, cells were incubated again for 1 h at RT in secondary antibody dilution in HHB-buffer (see Table 2.1) and finally washed three times with HHB-buffer, before they were embedded in Kaisers Glycerin Gelatine.

HHB-buffer	HANKS balanced salt solution (Biochrom) 20 mM HEPES 1% BSA
PFA solution	4% PFA dissolved in 1 x PBS
Hoechst	Hoechst 33258 1:1000 in 1 x PBS
Propidiumiodide	100 ng/ml in 1 x PBS

3.4.9 Immuno-electron microscopy

To visualize target proteins, e.g. BMP receptors (and cav-1), directly in caveolae or CCPs, two different approaches of immuno-electron microscopy (I-EM) were applied. For the post-embedding I-EM, cells were plated directly in the 6-well plate, grown over night in the incubator and the medium was replaced by 4% formaldehyde to fix the cells. After 30 min incubation at RT, cells were scraped carefully into an eppendorf-tube with a cell scraper, centrifuged for 2 min at 5000 rpm and the supernatant was discarded. The pelleted cells were covered with 4% formaldehyde and incubated over night at 4°C. The next day they were washed five times each for 3 min with 1 x PBS at 4°C and the free aldehyde groups were saturated by adding 50 mM NH₄Cl in 1 x PBS for 15 min at RT. After five wash steps with dH₂O each for 3 min at 4°C, cells were dehydrated by incubating the cells in gradually increasing alcohol concentrations at -20°C, ending with an incubation in an 1:1 ethanol-LR-White (Science Services GmbH)-mixture over night at 4°C. Following subsequent LR-White incubation steps at 4°C (1 h, 3-4 h, over night) and RT (3-4h), cells were airproof embedded in gelatine capsules and polymerization was carried out at 40°C for at least 3 days. Ultrathin sections were incubated subsequently in PBS and washing buffer, each for 5 min. First and

Methods

gold-conjugated secondary antibodies were diluted in washing buffer and applied for 1 h at RT (for concentrations see Table 2.1) with two washing steps in between each for 10 min in washing buffer. After a fixation step for 2 min in 1,25% glutaraldehyde in PBS and three washing steps with dH₂O, sections were contrasted using 2% uranylacetate (in dH₂O) and Reynolds leadcitrate (diluted 1:1 with dH₂O) each for 5 min and with two washing steps with dH₂O in between.

To better display the structures of caveolae and CCPs, additionally the pre-embedding I-EM method was applied. Therefore the cells were plated on coverslips (diameter: 12 mm), which were put in a well of a 6-well plate. 5×10^4 C2C12 cells per well were seeded and grown over night in the incubator. If an intracellular epitope should be recognized, cells were permeabilized partially by incubation for 10 min in 4% paraformaldehyde and subsequently for 10 min in 0,2% Triton X-100 at RT. After washing the cells with PBS/BSA, first antibodies diluted in PBS/BSA were applied for 1 h at 4°C and afterwards non-bound antibodies were washed away with PBS/BSA. Then the coverslips were incubated with gold-conjugated secondary antibodies diluted in PBS/BSA for 2 h or over night at 4°C, followed by another wash step with PBS/BSA. Control cells were incubated only in secondary reagents to check for cross reactions due to the antibodies. Beginning with fixation of the cells with 2,5% glutaraldehyde and subsequently 2% OsO₄-solution, with the normal electron microscopy procedure was continued (see 3.3.8). Sections were analyzed with a *Zeiss EM10* electronmicroscope (Zeiss). These experiments were mainly carried out in the lab and under supervision of Prof. G. Krohne (Department of Electron Microscopy, University of Würzburg) by Daniela Bunsen and Elisabeth Meyer-Natus.

PBS/BSA	1% BSA dissolved in 1 x PBS
Washing buffer	PBS + 1% BSA + 0,1% Tween20

4 RESULTS

4.1 CAVEOLIN-1 EXPRESSION AND CAVEOLAE FORMATION IN DIVERSE CELL TYPES

The marker protein of caveolae, caveolin-1 (cav-1), plays a central role in the characterization of these plasma membrane invaginations (see 1.5.4). Because lipid rafts and caveolae share the same lipid composition and phase, the best possibility to distinguish between raft- and caveolae-contribution is the use of specific cell types, concerning their endogenous cav-1 expression. Cav-1 negative cells can be used to study lipid rafts specifically, because no caveolae are formed at their plasma membrane. Lipid rafts are thought to be present in every cell type, although a visual confirmation of this is still missing. Therefore it is very useful to investigate the endogenous properties of different cell types in terms of cav-1 expression and caveolae formation.

4.1.1 Caveolin-1 expression

In the following experiments mainly two different cell types were used: C2C12 and 293T cells (see 2.9). Cav-1 expression was investigated in these cells using RT-PCR and western blot. Successful conditions for cav-1-specific primers (see A 2 and Kogo and Fujimoto, 2000) and cav-1-specific antibodies (see Table 2.1) were established.

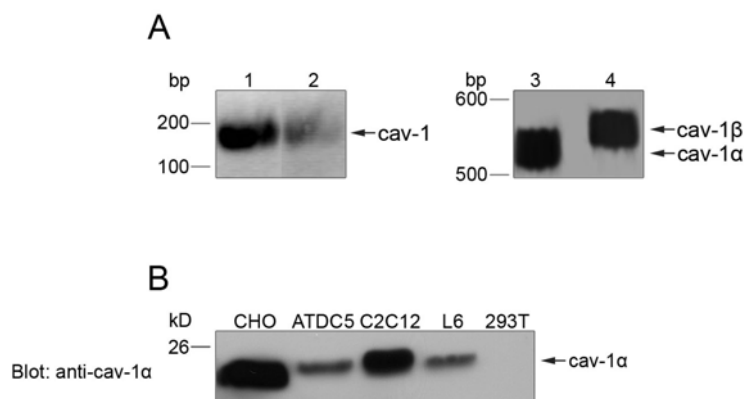


Fig. 4.1 Investigation of cav-1 expression in different cell types by RT-PCR and western blot. (A) RT-PCR analysis of HeLa, 293T and C2C12 cells. lane 1: HeLa RNA; human specific cav-1 primers, lane 2: 293T RNA; human specific cav-1 primers, lane 3 and 4: C2C12 RNA; mouse specific cav-1 α (lane 3) or cav-1 β (lane 4) primers (Kogo and Fujimoto, 2000). Primer sequences are listed in the appendix (A 2). (B) Cav-1 α -specific antibody (Santa Cruz) recognizes endogenous cav-1 α -protein in all tested cell types except for 293T cells.

Fig. 4.1 A shows the results obtained by RT-PCR. Using human, cav-1-specific primers (see A 2) a product of 164 bp size was expected. In lane 1 HeLa RNA was used as a control and

it was verified that cav-1 is expressed in these cells, whereas cav-1 expression in 293T cells is very low or even absent (lane 2).

For the mouse cell line C2C12, cav-1 isoform- and mouse-specific primers were applied and should result in gene products of the following sizes: for the α -isoform 551 bp and for the β -isoform 574 bp. It was published that the two isoforms of cav-1, α and β , are the products of differential translational start sites at a single cDNA, resulting in a 32 amino acid truncated β -isoform (Scherer et al., 1995). Kogo and Fujimoto demonstrated that the cav-1 isoforms in the mouse are produced by two distinct mRNAs, named FL (full length = α -isoform) and 5' V (5'-end variant = β -isoform). Because of this finding, they were able to generate specific primers for both isoforms (Kogo and Fujimoto, 2000) which were used in this experiment. The right panel demonstrates that both cav-1 isoforms are strongly expressed in C2C12 cells (lane 3 = α -specific primers, lane 4 = β -specific primers).

The annealing temperatures for the PCR reactions were established as follows: for human-specific primers 58°C (30 s) and for mouse-specific primers 55°C (30 s).

Fig. 4.1 B shows the result of a western blot analysis of different cell types (experiment by Dr. M. Sammar). All cell types, except for 293T cells, express cav-1 α . In pretests it could be verified that the cav-1-specific antibody from Santa Cruz only recognizes the α -isoform (see Fig. 4.2).

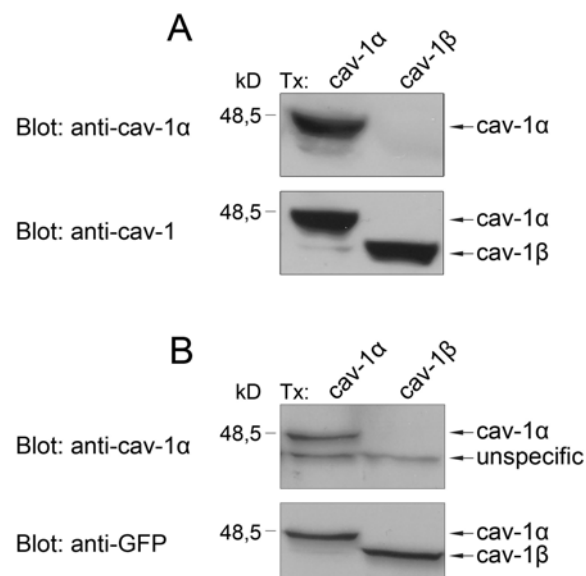


Fig. 4.2 Detection of cav-1-isoforms using different antibodies.

(A) 293T cells were transfected with EGFP-tagged cav-1 α or cav-1 β . Western blot analysis using Santa Cruz cav-1 antibody (polyclonal, sc-894, N-terminal epitope) detected only the cav-1 α -isoform, whereas the BD Transduction Laboratories antibody (monoclonal, clone 2297) recognized both isoforms. (B) The same experiment was repeated while detecting both isoforms via their EGFP-tag using a monoclonal GFP-specific antibody (Santa Cruz). Tx = transfection

By transfecting 293T cells with EGFP-tagged cav-1 α or cav-1 β respectively and subsequent western blotting, only the cav-1 α -isoform could be detected with this antibody. As control a GFP-recognizing (Fig. 4.2 B) or another cav-1-specified antibody from BD Transduction Laboratories (Fig. 4.2 A) were applied on the same blots.

4.1.2 Caveolae formation

To visualize the differences concerning caveolae-occurrence between 293T and C2C12 cells, electron microscopy studies were applied (see 3.3.8). The analyzed sections revealed only clathrin-coated pits (CCPs) in plasma membranes of 293T cells (Fig. 4.3 A), whereas C2C12 cell membranes exhibit additionally smaller, uncoated invaginations and vesicles in great quantities, which were identified as caveolae and caveosomes (Fig. 4.3 B).

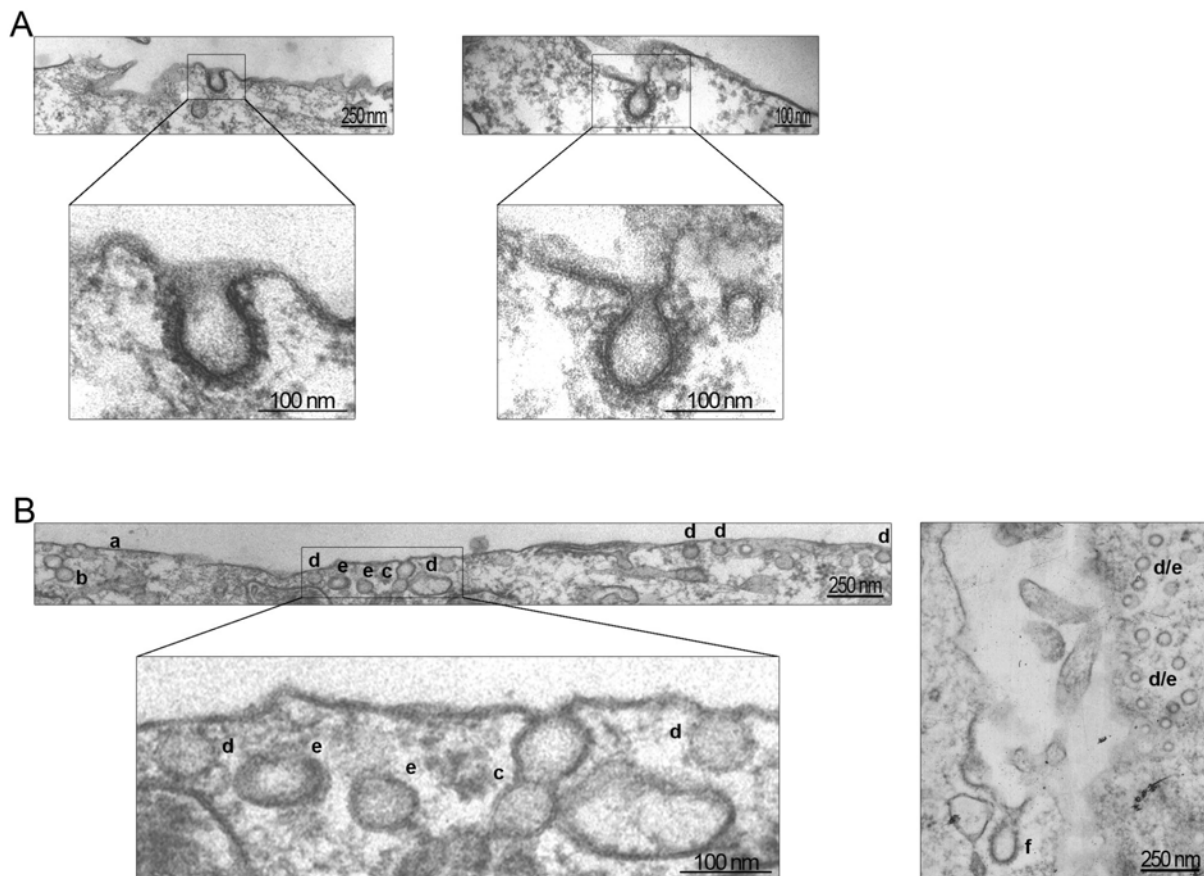


Fig. 4.3 Electron microscopy on 293T (A) and C2C12 (B) cells.

(A) Two examples of CCP identified in the plasma membrane of 293T cells. The pictures are shown in more detail in the lower panels. No caveolar structures were found. (B) In the plasma membrane of C2C12 cells caveolae are abundant; but also CCPs were identified (right panel, f). Additionally, “double-caveolae” (c) and “double-caveosomes” (b) are exhibited. a plasma membrane; b “double-caveosome”; c “double-caveola”; d caveolae; e caveosomes; f CCP

CCPs were recognized by their ciliated border and size which were found to be mostly around 100 nm in C2C12 cells and somewhat smaller, around 80 nm, in 293T cells (see Fig.

4.3 A and B, right panel). This is in accordance with published coated-vesicle sizes ranging from ~70 nm (Bomsel et al., 1986) to 350 nm (Perry and Gilbert, 1979) in diameter.

Caveolae are described in the literature to be flask-shaped, uncoated invaginations of 50 – 100 nm in size. But in different cell types and tissues, different sizes and morphologies were observed, e.g. grape-like clusters, rosettes or fused forms like elongated tubules or channels (reviewed in Razani et al., 2002c).

The above shown results demonstrate that the small amount of cav-1-RNA detected in 293T cells (Fig. 4.1 A, lane 2) does not contribute to caveolae formation in these cells. C2C12 cells which express cav-1 (Fig. 4.1 A, right panel and B) also exhibit caveolae in different morphologies at their cell surface. Therefore 293T cells were used in the following to study specifically lipid rafts as well as all effects described in these cells are attributed to lipid rafts alone.

4.2 LOCALIZATION OF BMP RECEPTORS IN PLASMA MEMBRANE REGIONS

BMPs transmit their signals through two kinds of transmembrane serine/threonine kinase receptors, BRI and BRII (1.3.1). The localization of these signaling proteins in distinct plasma membrane regions may contribute to their ability to transduce different signals inside the cell and initiate diverse signaling cascades and transcription of target genes.

Several methods for detecting raft/caveolae-associated proteins exist, among them biochemical studies as well as diverse optical and microscopical methods (Lagerholm et al., 2005; Simons and Toomre, 2000).

The following results were obtained by using separation and characterization of detergent-resistant membranes (DRMs) from C2C12 and 293T cell membranes (4.2.1), co-immunoprecipitation studies with the caveolae marker protein cav-1 (4.2.2) as well as immunomicroscopical techniques (4.2.3).

4.2.1 Isolation and analyses of caveolin-1-enriched membrane fractions

Lipid rafts and caveolae exhibit a special lipid composition which contributes to their unique biochemical properties. To separate rafts and caveolae from other cell- and membrane contents, it is possible to avail oneself of a specific property of these membrane regions – their detergent-insolubility in the cold. DRMs float – because of their high lipid content – to a low density during sucrose gradient centrifugation (Brown and Rose, 1992; Fra et al., 1994; Sargiacomo et al., 1993). After collecting fractions from the gradient, it is possible to detect proteins by western blotting and to compare whether these proteins are present in the same fractions with marker proteins of caveolae and rafts or not. Does a protein cofractionate with cav-1, one can assume that it is located in caveolae (or rafts). It should be mentioned that

rafts and caveolae are not distinguishable by this method. Other methods like antibody patching and immunofluorescence microscopy, electronmicroscopy and immunoprecipitation should be used to verify the possible association of the target protein with caveolae or rafts (Simons and Toomre, 2000).

4.2.1.1 Establishing the method

To establish stable conditions for this separation method in C2C12 cells, several steps of the procedure were subject of modifications, i.e. the extraction detergent Triton X-100. Triton X-100 is the most commonly used detergent to cause insolubility of raft-microdomains, but also a detergent-free method using Na_2CO_3 (Song et al., 1996) as well as the use of other detergents like CHAPS were reported (Kurzchalia et al., 1992; Monier et al., 1995). Because first experiments with C2C12 cells using Triton X-100 did not result in a sharp but instead a wide distributed cav-1 signal, Na_2CO_3 (data not shown) and CHAPS (Fig. 4.4) were tested on C2C12 cells.



Fig. 4.4 Comparison of Triton X-100 and CHAPS extracts.

C2C12 cells stably overexpressing BRIL-TC7 (Hassel et al., 2003; Nohe et al., 2002) were extracted using 1% Triton X-100 in TNE (upper panel) or 20 mM CHAPS in TNE (lower panel). Cav-1 α western blots show a shift of this protein to fractions with a lower density when CHAPS was used. The soluble fractions 10-12 are here almost empty of cav-1 α in contrast to Triton X-100 extraction where most of the cav-1 α signal is found in there.

It was reported that DRMs float to a density of about 15-20% sucrose in linear density gradients. By comparing the refraction indices of calibrated sucrose solutions and fractions, fractions 5-7 were identified as possible DRM fractions (data not shown). Because the cav-1 signal shifted more to these lower density fractions in the CHAPS extracts, this detergent was used in all further experiments to separate DRMs.

As Fig. 4.5 demonstrates, many other steps of the procedure were modified to get even better separation (results as shown by the cav-1 α western blot controls in Fig. 4.6, Fig. 4.7, Fig. 4.8 and Fig. 4.9). For example the use of a discontinuous OptiPrep™ gradient as well as an inverted direction of fractionation gave sharper signals.

One very important point was to use a higher number of cells with a higher expression rate of the respective overexpressed BMP receptor type. These cell lines were generated by viral

infection (Hassel et al., 2003) and were further improved by means of the selection antibiotic G418 (0,6 µg/ml).

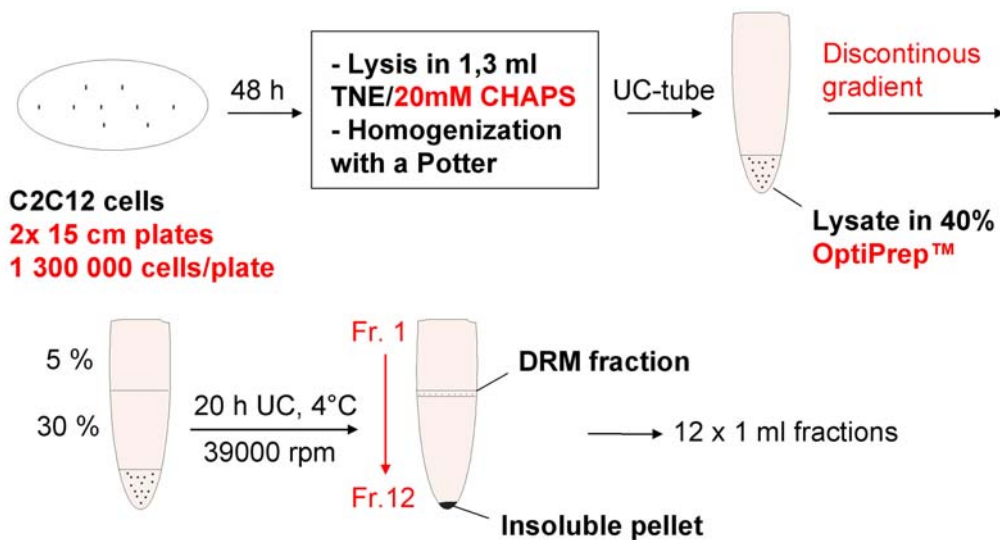


Fig. 4.5 Summary of the improvements on the separation of DRMs from C2C12 cells.

Red marked steps were modified during the establishment of the method. The final experimental workflow shown here is described in more detail in chapter 3.4.2.

4.2.1.2 Analyses of BMP receptor localization in C2C12 cells

To investigate the localization of BMP receptors in DRMs, C2C12 cells stably overexpressing HA-tagged BRII-LF, BRII-SF, BRII-TC1 or BRIIb were used. Unfortunately, it was not possible to get a stable expression of BRIIa in C2C12 cells. That is why this receptor type needed to be investigated after transient transfection in 293T cells (see 4.2.1.3).

BRII exists in two different splice variants, BRII-LF („long form“) and BRII-SF („short form“). While BRII-SF ends shortly after the kinase domain at amino acid 530, BRII-LF has an additional 508 residue-long cytoplasmic tail (Rosenzweig et al., 1995). The truncation mutant BRII-TC1 features no kinase domain and showed a dominant negative effect on the p38 pathway and ALP production, but no effect on the Smad pathway, because it is unable to form preformed receptor complexes (PFCs) (Nohe et al., 2002).

Fig. 4.6 shows the western blot analyses obtained after separation of DRMs from C2C12-BRII-LF cells. The cav-1 α control western blot shows a sharp separation of DRMs to fraction 6 and 7 (lower panel). The HA-western blot demonstrates that BRII-LF appeared widely distributed over the gradient, but was also present in DRM fractions (upper panel). In an additional experiment, cells were stimulated with BMP2 before lysates were collected, because of a possible influence of the ligand on the localization of BRII-LF. Fig. 4.6 B shows that the distribution of BRII-LF in the gradient was not altered by BMP2.

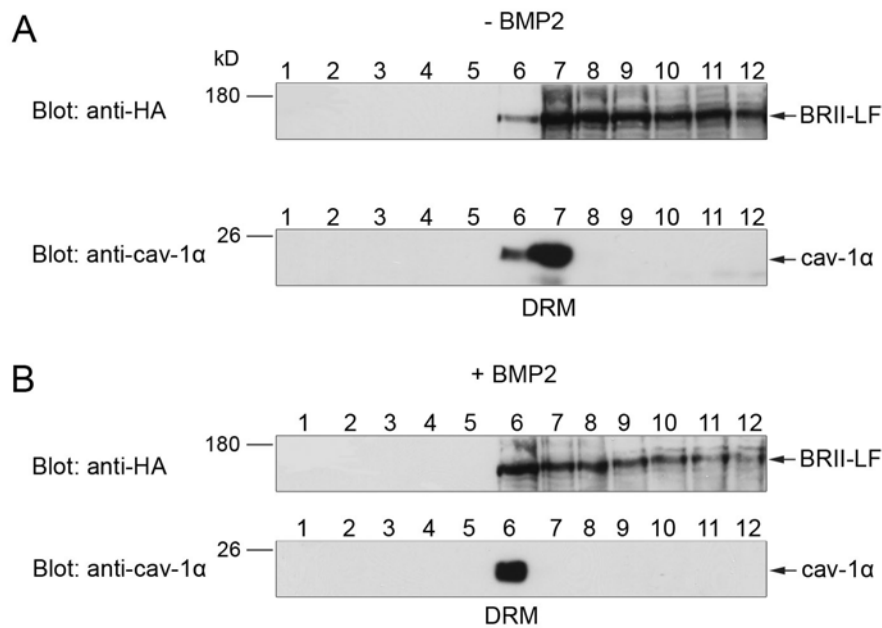


Fig. 4.6 Separation of DRMs from C2C12 cells stably overexpressing BRIL-LF.

C2C12 cells stably overexpressing HA-tagged BRIL-LF were cultivated and lysed in TNE/CHAPS as described (3.4.2). (A) Cells were incubated for 2.5 h in starving medium before lysates were collected. The cav-1 α control western blot (lower panel) and the HA-western blot (upper panel) are shown. (B) Cells were starved for 2 h followed by stimulation with 20 nM BMP2 for 30 min.

The same experiments were repeated using C2C12-BRIL-SF (Fig. 4.7) and C2C12-BRIL-TC1 cells (Fig. 4.8).

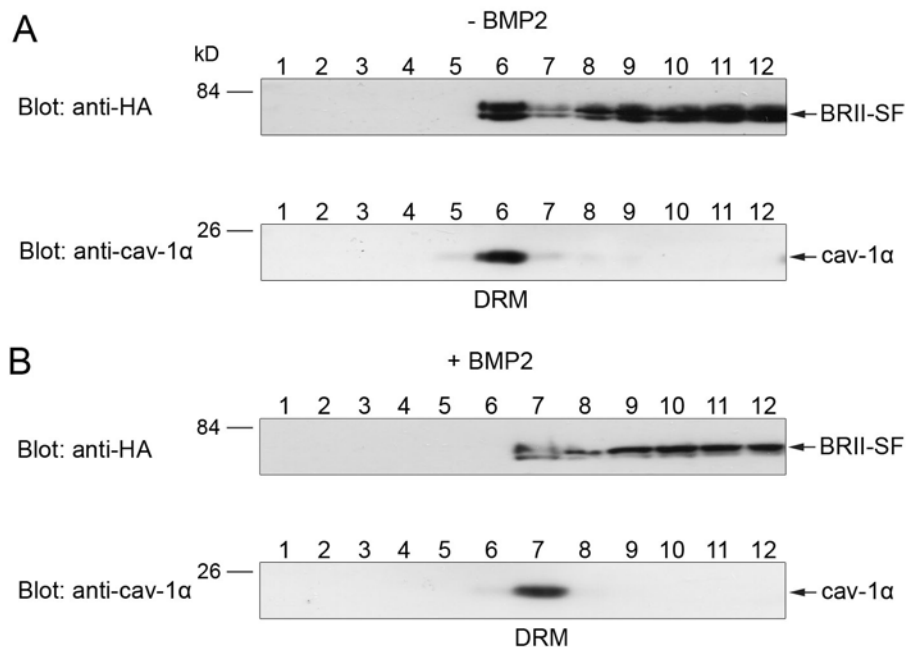


Fig. 4.7 Separation of DRMs from C2C12 cells stably overexpressing BRIL-SF.

C2C12 cells stably overexpressing HA-tagged BRIL-SF were cultivated and lysed in TNE/CHAPS as described in 3.4.2. Unstimulated (A) and stimulated (B) cell lysates were analyzed (as described in figure legend of Fig. 4.6)

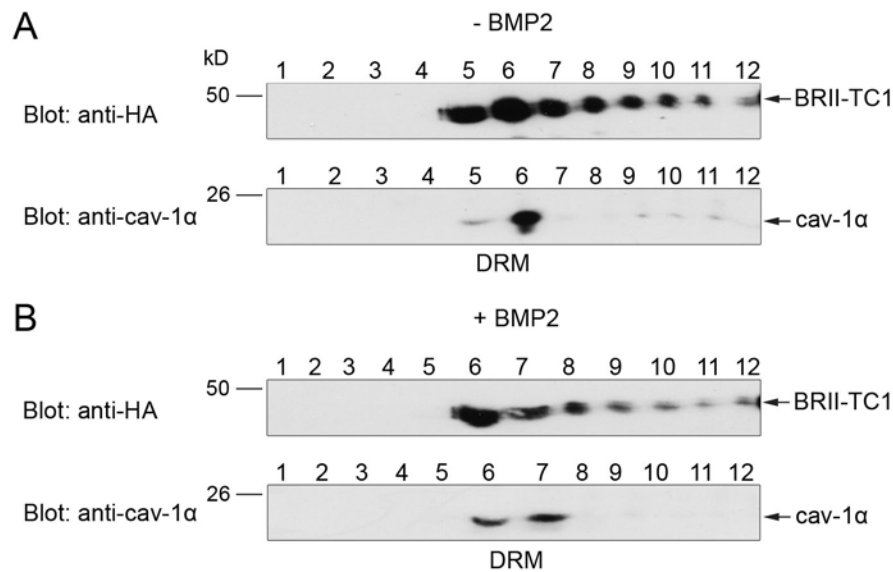


Fig. 4.8 Separation of DRMs from C2C12 cells stably overexpressing BRII-TC1.

C2C12 cells stably overexpressing HA-tagged BRII-TC1 were cultivated and lysed in TNE/CHAPS as described in 3.4.2. Unstimulated (A) and stimulated (B) cell lysates were analyzed (as described in figure legend of Fig. 4.6)

The analyses show that BRII-SF is distributed almost in the same manner like BRII-LF. However, BRII-TC1 seems to be more concentrated in DRM fractions than the longer BRII forms. Stimulation with the ligand BMP2 was not influencing these distributions significantly, as better seen after quantification of the western blots (Table 4.1).

To investigate the localization of BRI, C2C12-BRIb cells were used (Fig. 4.9).

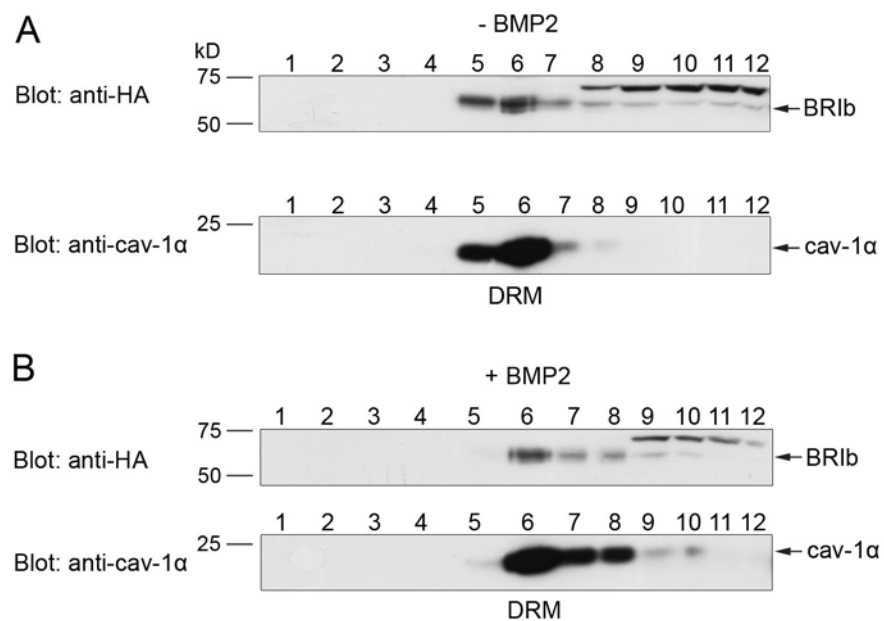


Fig. 4.9 Separation of DRMs from C2C12 cells stably overexpressing BRIb.

C2C12 cells stably overexpressing HA-tagged BRIb were cultivated and lysed in TNE/CHAPS as described in 3.4.2. Unstimulated (A) and stimulated (B) cell lysates were analyzed (as described in figure legend of Fig. 4.6)

In contrast to the BMP type II receptor and its derivatives, BR1b showed a different allocation. This receptor type is concentrated mainly in DRM fractions 5-7 which is not altered by stimulation with BMP2 (Fig. 4.9).

The signals were quantified to better display the differences between BR1I and BR1. For this the Scion Image software (Scion Corporation) was used and each measured lane was divided by the sum of all lanes (Table 4.1).

	- BMP2		+ BMP2		
	DRM	non-DRM	DRM	non-DRM	
BR1I-LF	19	49	20	28	partitioning of BR1I-LF [%]
	100	0	100	0	partitioning of cav-1 [%]
BR1I-SF	17	49	12	59	partitioning of BR1I-SF [%]
	84	0	89	0	partitioning of cav-1 [%]
BR1I-TC1	46	15	58	16	partitioning of BR1I-TC1 [%]
	91	4	100	0	partitioning of cav-1 [%]
BR1b	77	11	88	5	partitioning of BR1b [%]
	98	0	92	4	partitioning of cav-1 [%]

Table 4.1 Quantitative summary of flotation assays in C2C12 cells.

The western blots from Fig. 4.6, Fig. 4.7, Fig. 4.8 and Fig. 4.9 were quantified using the Scion Image software (Scion Corporation) and each individual fraction was divided by the sum of all fractions. The fraction with the highest cav-1 content was declared as "DRM" fraction. The sum of fractions 10-12 was taken as "non-DRM" partition.

Table 4.1 shows clearly that:

- BR1b is around four times (and BR1I-TC1 about two times) more concentrated in DRM fractions compared to BR1I-LF and BR1I-SF
- BMP2 has no or only a minor, negligible influence on the DRM occurrence of BMP receptors

4.2.1.3 Analyses of BMP receptor localization in 293T cells

As mentioned before, BR1a, the high affinity receptor for BMP2, could not be stably overexpressed in C2C12 cells with sufficient expression levels. To investigate whether this receptor – like BR1b – mainly cofractionates with DRMs, 293T cells were transiently transfected with HA-tagged BR1a and HA-tagged cav-1 α (because 293T cells are cav-1 negative cells; as shown in 4.1). Furthermore, it was possible, to examine the distribution of BR1a in non-caveolae DRMs by transfecting BR1a alone.

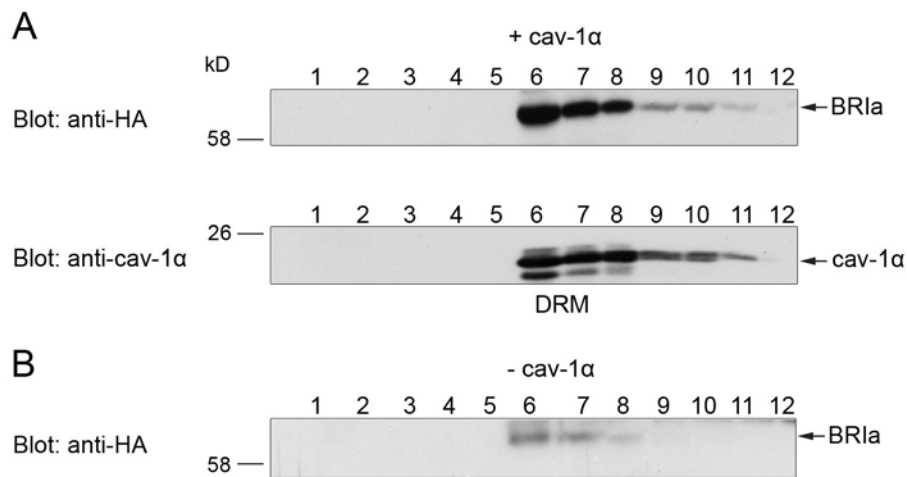


Fig. 4.10 Separation of DRMs from 293T cells transfected with BR1a together with or without cav-1α.

(A) 293T cells were transiently transfected with BR1a and cav-1α (both HA-tagged) and DRMs were separated like for C2C12 cells (described in 3.4.2). (B) 293T cells were transfected only with HA-tagged BR1a. Because 293T cells are cav-1 negative (4.1), investigation of BR1a distribution in non-caveolar DRMs is possible.

Fig. 4.10 aggregates several results and conclusions.

At first, overexpressed cav-1α appeared more blurred than endogenous cav-1α in C2C12 cells in which it usually was recognized only in 1-2 fractions. It is possible that the high expression rate in 293T cells (90% transfection efficiency) was responsible for that. Furthermore, a special establishment of the method for 293T cells could be required. Nevertheless, cav-1α was identified mainly in lighter fractions 6-8 and to a lesser extent in soluble non-DRM fractions 10-12 (Fig. 4.10 A, lower panel).

Secondly, the hypothesis that BR1a is similarly distributed to BR1b, was corroborated. BR1a appeared mainly in the same fractions as cav-1α (Fig. 4.10 A). Quantitation shows that 86% of BR1a were located in DRM fractions (Table 4.2).

Finally, BR1a was found in the same extent in non-caveolar DRM fractions (Fig. 4.10 B). This result suggests that BMP type I receptors may be associated with caveolae **and** lipid raft regions.

As control, also BR1I-LF was transiently transfected into 293T cells and its distribution in these cells was studied with or without additional cav-1α overexpression. Fig. 4.11 shows the same blurred cav-1α allocation like in the experiment before, an evenly distribution of BR1I-LF between DRM and non-DRM fractions (like in C2C12 cells; compare Fig. 4.6) and the same distribution in non-caveolar DRMs (Fig. 4.11 B).

Because of the blurred cav-1α signal, additionally the distribution of endogenous Interleukin 2 receptor β (IL2Rβ) was detected to verify more accurate DRM fractions. IL2Rβ was reported to be concentrated in DRM fractions and can be used as a marker for DRMs

(Goebel et al., 2002). IL2R β was mainly found in fraction 6 which confirmed the assumed DRM distribution.

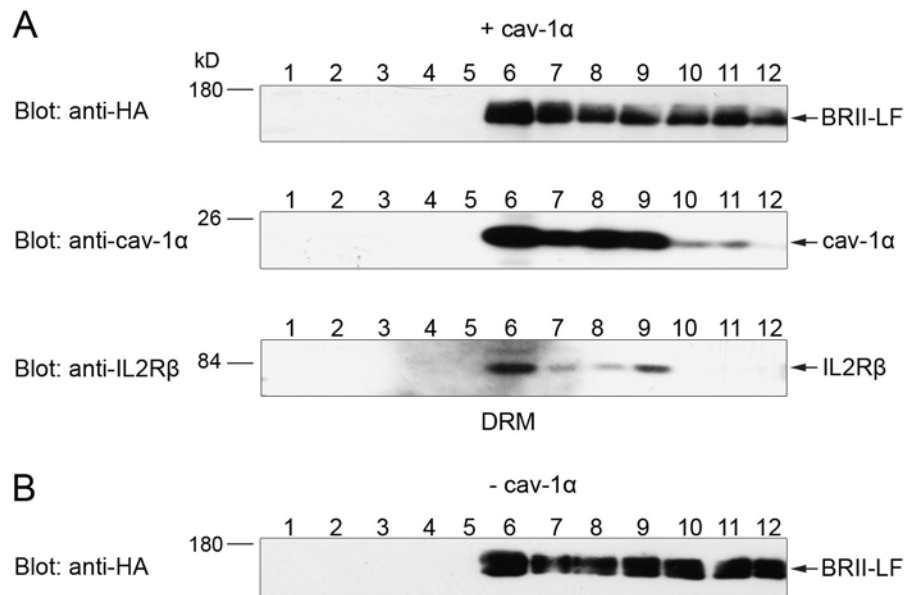


Fig. 4.11 Separation of DRMs from 293T cells transfected with BRIA-LF together with or without cav-1 α .

(A) 293T cells were transiently transfected with BRIA-LF and cav-1 α (both HA-tagged) and DRMs were separated like for C2C12 cells (described in 3.4.2). Additionally IL2R β distribution was investigated to confirm the major DRM fraction to be fraction 6. (B) 293T cells were transfected only with HA-tagged BRIA-LF. Because 293T cells are cav-1 negative (4.1), investigation of BRIA-LF distribution in non-caveolar DRMs is possible.

The same quantitation method like for C2C12 cells was applied and showed the following results:

	DRM	non-DRM	
BRIA	86	8	partitioning of BRIA [%]
	71	16	partitioning of cav-1 [%]
BRIA-LF	42	43	partitioning of BRIA-LF [%]
	69	9	partitioning of cav-1 [%]

Table 4.2 Quantitative summary of flotation assays in 293T cells.

The western blots from Fig. 4.10 and Fig. 4.11 were quantified using the Scion Image software (Scion Corporation) and each individual fraction was divided by the sum of all fractions. Because of the blurred distribution of the DRM marker cav-1 α , fractions 6-8 were declared as combined “DRM” fraction. The sum of fractions 10-12 was taken as “non-DRM” partition.

Table 4.2 demonstrates that BRIA was two times more concentrated in DRM fractions than BRIA-LF and that BRIA-LF is evenly distributed between DRM and non-DRM fractions.

Stimulation with BMP2 was also accomplished and resulted in the same pattern like without stimulation (data not shown), suggesting that the ligand is not influencing BMP receptor localization in DRM regions.

In summary, using the method of separation of DRMs it was discovered that all investigated BMP receptors were found in DRM regions - but to different extents. BMP type I receptors were mainly concentrated in these regions (around 80% occurrence) whereas BMP type II receptors were evenly distributed in DRM and non-DRM fractions. Activation of the receptor complex by adding BMP2 did not influence this localization. Furthermore, BRIa and BRII-LF were found in non-caveolar DRM regions, investigated by the use of the cav-1 negative cell line 293T.

4.2.2 Co-Immunoprecipitation studies to detect cav-1/BMP receptor interaction

Another criterion for localization of proteins in caveolae besides their occurrence in DRM fractions is the proof of interaction of the protein with cav-1 α . Here, the method of immunoprecipitation (IP) is commonly used (3.4.5). C2C12 cells stably overexpressing HA-tagged BRII-LF, BRII-SF, BRII-TC1 or BRIb were cultivated, endogenous cav-1 α immunoprecipitated by using the specific cav-1 α antibody (Santa Cruz; see Fig. 4.2) and the precipitates investigated for the occurrence of respective receptor constructs via their HA-tag.

Fig. 4.12 A shows the results obtained for C2C12-LF and C2C12-SF cells. The blots demonstrate that BRII-LF and BRII-SF were associated with cav-1 α in a ligand independent manner (Fig. 4.12 A, upper panel). Applying the IP-antibody (anti-cav-1 α) to the same blot verified that cav-1 α was in fact successfully immunoprecipitated from the lysate (Fig. 4.12 A, middle panel). As a general control direct cell lysates were probed with anti-HA antibody to confirm the proper expression of the receptor constructs in the cells (Fig. 4.12 A, lower panel).

BRII-TC1 is the shortest BRII truncation which was generated by recombinant PCR mutagenesis (sequence listed in A 2, Nohe et al., 2002). It ends 27 amino acids after the transmembrane domain in the cytoplasm, exhibiting no kinase and tail domains. This truncation mutant of BRII was not able to bind cav-1 α -independent of BMP2 stimulation (Fig. 4.12 B, upper left and middle right panel).

BRIb – like BRII-LF and BRII-SF – could be co-immunoprecipitated with endogenous cav-1 α (Fig. 4.12 C, upper panel). But what looked like a ligand effect could not be reproduced in further experiments. Rather, BMP2 showed in the average of three independent experiments no influence on the interaction between BRIb and cav-1 α .

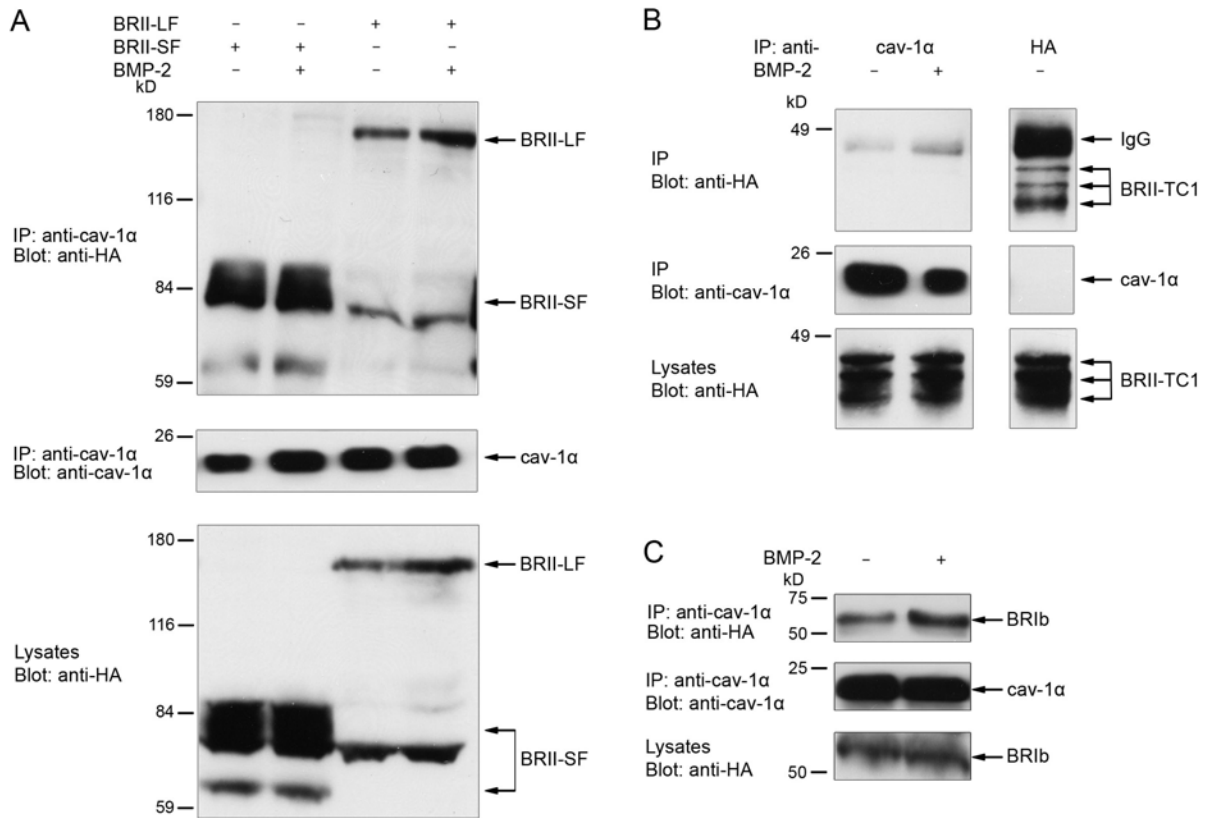


Fig. 4.12 Co-Immunoprecipitation studies between BMP receptors and cav-1α in C2C12 cells.

Endogenous cav-1α was immunoprecipitated from C2C12 cells stably overexpressing HA-tagged BR1I-LF, BR1I-SF, BR1I-TC1 or BR1b. After the cells were starved for 2 h and subsequently stimulated with 20 nM BMP2 for 30 min, the extracted lysates were precipitated with polyclonal rabbit antibodies directed against cav-1α followed by incubation with Protein A-Sepharose. The washed beads were subjected to SDS-PAGE and western blotting. Blotting with anti-HA antibody detected cav-1α bound BR1I-LF, BR1I-SF (A) and BR1b (C). BR1I-TC1 failed to bind cav-1α (B). Lysates from C2C12-BR1I-TC1 cells were additionally precipitated with anti-HA antibody, followed by western blotting with anti-cav-1α antibody (B, right panels). The successful IP was confirmed by probing the blots with the IP-antibody. As additional controls the direct lysates were tested for HA-signals.

BR1a and cav-1α were transiently transfected in 293T cells and cell lysates were precipitated with anti-cav-1α antibody. As controls BR1a and cav-1α were transfected together with the empty vector construct pcDNA3 respectively and treated alike.

Fig. 4.13 shows that BR1a interacted with cav-1α (left lane). The control transfections proved that BR1a could only be detected in the lane where both constructs together were transfected (middle and right lanes).

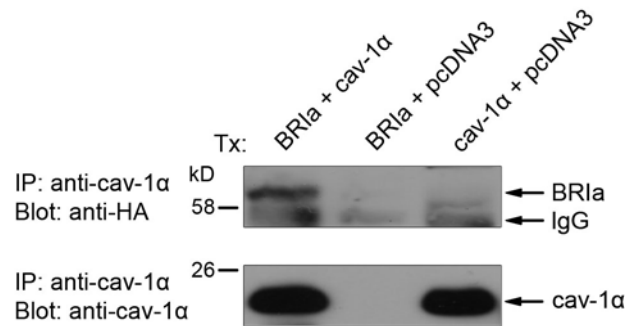


Fig. 4.13 Co-Immunoprecipitation of BR1a and cav-1α in 293T cells.

Respectively one 15 cm plate of 293T cells was transfected with the indicated DNA constructs (both HA-tagged) and the collected lysates were immunoprecipitated using cav-1α antibody, followed by incubation in Protein A-Sepharose, SDS-PAGE and western blotting with anti-HA as well as anti-cav-1α antibodies.

Taken together, all BMP receptor variants - except for BRII-TC1 - interacted with cav-1α. This association was not altered when the receptor complexes were activated by stimulation with BMP2.

4.2.3 Immuno-microscopical techniques to verify colocalization of cav-1 and BMP receptors

Immunofluorescence and immuno-electronmicroscopy are methods to visualize colocalization of two (or more) proteins at the cell surface, in vesicles or inside the cell. By labeling the proteins of interest with fluorescently-coupled or gold-conjugated antibodies directly on the living cell or after fixation, it is possible to gain important insight on the organization of the cell and cell membrane.

4.2.3.1 Immunofluorescence approach

Immunofluorescence (IF) experiments were applied to detect BMP receptors directly on the plasma membrane or in the cell by using a combination of a specific first antibody and a fluorescently labeled secondary antibody.

Classical IF is accomplished on living cells or after fixation of the cells at 4°C (mainly to prevent endocytic events), depending on the proposed localization and the accessibility of the protein to be labeled.

The BMP receptor constructs used in the following experiments were extracellularly HA-tagged and therefore accessible for an HA-specific antibody without permeabilization/fixation. Side effects of treating living cells with antibodies are that less background is obtained inside of the cell and that the receptors are concentrated in patches at the cell surface by the antibodies. Subsequently, the cells were incubated with the secondary, fluorescently

conjugated reagent, fixed and either instantly covered with gelatine or prior to that incubated with an antibody directed against the second protein of interest. In the latter case, a specific cav-1 α antibody was used to colocalize labeled BMP receptors with cav-1 α . Cav-1 is a protein with two transmembrane domains but no extracellular region. Because of that; the fixation prior to the antibody application is necessary to permeabilize the membrane, so the antibodies can reach their epitopes inside of the cell. Fig. 4.14 shows confocal images obtained for C2C12-LF and C2C12-BRIa cells. The unstable and low expression rate of BRIa in C2C12 cells was sufficient only for the IF approach (not for flotation or IP experiments, as mentioned above). It turned out that the low expression rates seemed not to result from an overall low expression but rather from some single cells with extremely high expression but a majority of cells without any expression (data not shown). Both types of BMP receptors were expressed uniformly at the plasma membrane; also antibody-induced patching is noticeable (Fig. 4.14, left panels). Cav-1 α antibodies were predominantly staining special regions of the plasma membrane (Fig. 4.14, middle panels) and colocalized with both receptor type labels at these sites (Fig. 4.14, right panels, yellow spots). The images were acquired with a Leica DRM confocal microscope (Leica) using x63 objective.

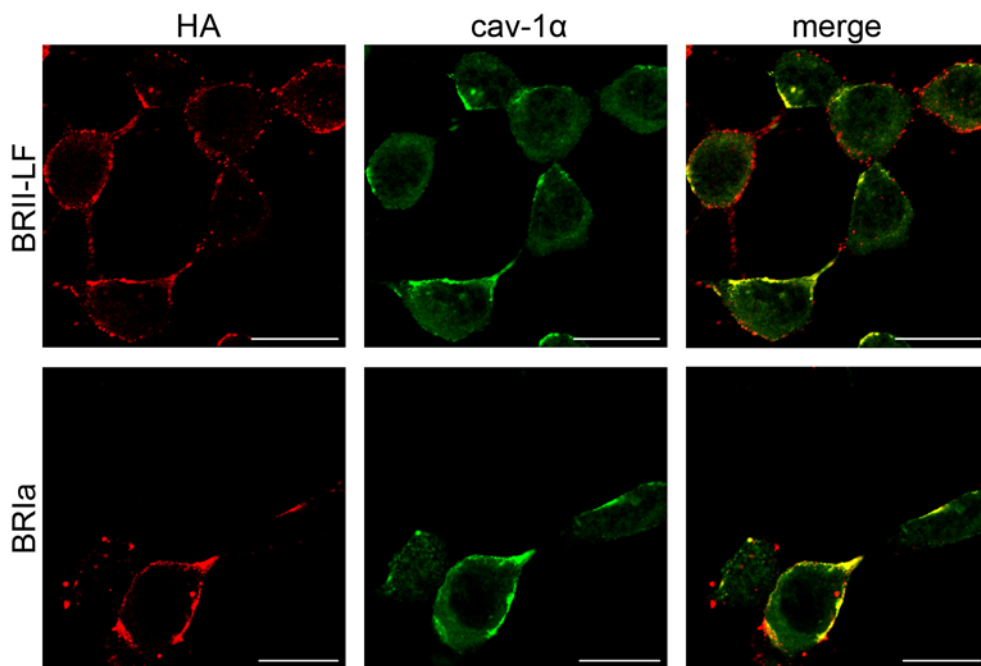


Fig. 4.14 Immunofluorescence approach in C2C12-LF and C2C12-BRIa cells.

C2C12 cells stably transfected with BRII-LF (upper panels) or BRIa (lower panels) were prepared as described (3.4.8). The left panels display the respective receptors labeled with monoclonal mouse antibody directed against the HA-tag, followed by incubation with Cy3-coupled goat anti mouse antibody. The middle panels show Cy2-labeled endogenous cav-1 α , whereas at the right panels both labels are overlapped. Images were exported to and processed with Adobe Photoshop. Bar: 20 μ m

The experiments were repeated after stimulation of the cells with BMP2, resulting in no significant change (data not shown). Unfortunately the resolution and sharpness of the

images could not be improved, to get single red, green and eventually yellow dots. Therefore C2C12-TC1 cells were labeled as negative control, because TC1 was not able to interact with cav-1 α , as seen by IP studies (Fig. 4.12) and the merging picture should not produce any yellow dots.

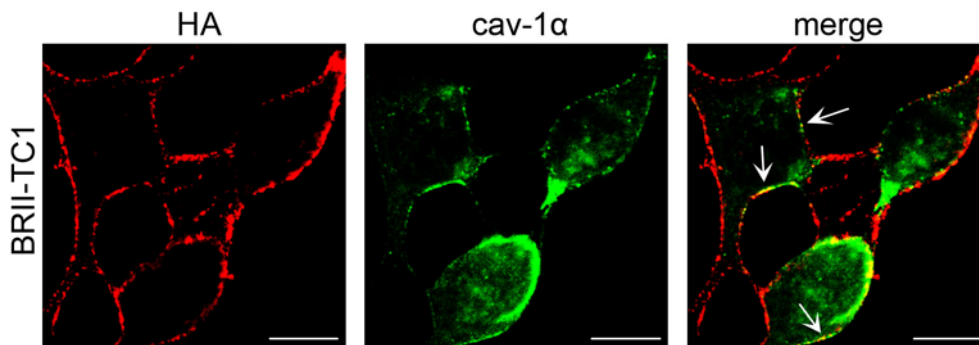


Fig. 4.15 Immunofluorescence approach in C2C12-TC1 cells.

C2C12 cells stably transfected with BII-TC1 were prepared as described (3.4.8). The left panel displays receptor labeling with monoclonal mouse antibody directed against the HA-tag, followed by incubation with Cy3-coupled goat anti mouse antibody. The middle panel shows Cy2-labeled endogenous cav-1 α , whereas at the right panels both labels are overlapped. Images were exported to and processed with Adobe Photoshop. Arrows indicate colocalization. Bar: 20 μ m

Fig. 4.15 shows that some merging patches could be observed (right panel, arrows). Because of that, it was tried to establish that method more appropriate by changing antibodies, antibody concentrations, incubation times, blocking and washing times and solutions, but without success. Thus the results displayed in Fig. 4.14 are maybe not reliable and should be proven by other techniques or an improved IF protocol.

4.2.3.2 Immuno-electronmicroscopy approach

To further investigate the localization pattern of BMP receptors, immuno-electronmicroscopy was accomplished. This method combines electronmicroscopy with labeling of target proteins via antibodies. Here, gold particle-coupled secondary antibodies were used and different proteins could be distinguished by the size of the gold particles.

BII-LF was immunogold-labeled in C2C12 cells stably expressing HA-tagged BII-LF at 4°C. Two kinds of labeling methods were applied: the pre-embedding method in which the labeling procedure was completed before the cells were fixed, embedded and sliced and the post-embedding method in which cells were fixed and embedded first and labeling occurs on ultrathin slices of the cells (see 3.4.9 for more details).

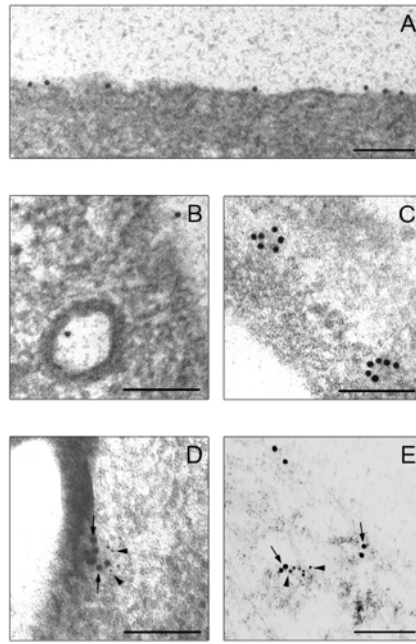


Fig. 4.16 Immunoelectronmicroscopy approach in C2C12-LF cells.

BR11-LF was labeled as described (3.4.9), using HA antibody followed by secondary antibodies conjugated to 12 nm colloidal gold. Cells were treated with antibodies before fixation and embedding (A, B) or cell pellets were fixed and embedded prior to antibody application (C, D, E). BR11-LF was observed at the cell surface (A) or in vesicles, identified as CCVs (B) as well as located in clusters of 50 – 75 nm in diameter (C). Sections were additionally incubated with cav-1 α antibody followed by secondary antibody conjugated to 6 nm colloidal gold (D, E). BR11-LF (arrows) was located in clusters together with cav-1 α (arrow heads). Bar: 100 nm

BR11-LF was detected predominantly at the cell surface (Fig. 4.16 A), but also in vesicles exhibiting a ciliated border and a size of around 100 nm in diameter (Fig. 4.16 B), when the pre-embedding labeling method was used.

On the other side, when the post-embedding labeling method was applied, cell membranes or vesicles were barely visible, because here cell pellets were sliced before labeling. BR11-LF accumulated in clusters of 50 – 75 nm in size (Fig. 4.16 C, D, E) and colocalized with cav-1 α in these clusters after double-label immuno-gold electron microscopy (Fig. 4.16 D, E).

Taken together, BR11-LF was found in both, CCVs and smaller, uncoated vesicles containing cav-1 α , most likely caveosomes.

4.3 FUNCTIONAL RELEVANCE OF ENDOCYTIC PATHWAYS ON BMP SIGNALING

Having established BMP receptor localization in DRM regions – lipid rafts and/or caveolae depending on the cell type – the next focus became the relevance of this on BMP signaling steps. To address DRMs, cholesterol depletion was combined with several read-out assays for BMP signaling. Furthermore, concentrating specifically on caveolae, cav-1 was overexpressed and knocked down and so the influence of caveolar localization of the receptors was measured.

In addition cav-1-containing and cav-1-deficient cells were used in some experiments to get more information about caveolae-specific influences on BMP signaling.

Moreover, there was evidence of BMP receptor occurrence in CCPs; that is why also these plasma membrane regions were under investigation in terms of influencing BMP signaling.

To investigate the effects of CCP-mediated endocytosis, a specific inhibitor of this internalization pathway was used in combination with BMP signaling assays.

Finally, application of dynamin2 dominant-negative mutant K44A blocks endocytosis in general and the influence of endocytosis on BMP signaling could be tested.

4.3.1 Influence of cholesterol-sensitive plasma membrane regions on BMP signaling

Cholesterol depletion is a common but not indisputable method to disrupt cholesterol-sensitive plasma membrane regions. Lipid rafts and caveolae are especially dependent on cholesterol (Hailstones et al., 1998; Rothberg et al., 1992; Schnitzer et al., 1994) mainly due to a higher cholesterol concentration compared to the surrounding lipid bilayer. Moreover, this sterol is involved in the formation of caveolae (Hailstones et al., 1998) and bound by cav-1 (Murata et al., 1995). Because of the occurrence of cholesterol all over the plasma membrane, it is possible that also other than DRM regions and related endocytic events can be affected by cholesterol depletion (Rodal et al., 1999). Therefore the effect of different cholesterol depleting reagents should be thoroughly investigated.

The phosphorylation of Smad1/5 is one of the initial steps in the BMP signaling cascade and can be analyzed by the use of an antibody raised specifically against the phosphorylated form of Smad1/5. This read-out assay in combination with cholesterol depletion gives evidence about the dependence of early steps of BMP signaling on DRM regions (4.3.1.2), whereas by the use of reporter genes transcriptional activities in response to BMP2 can be measured (4.3.1.3). Finally, the activity of the specific target gene ALP was determined in dependence on DRM regions and related endocytic events (4.3.1.4).

4.3.1.1 Cholesterol depletion decreases cholesterol levels

The determination of the cholesterol concentration gives information about the success of cholesterol depletion procedures and was accomplished by means of the *Amplex Red Cholesterol Assay Kit* (Molecular Probes) (3.3.5.4). At first, the effect of different media was analyzed and it was shown that – as expected - the cholesterol concentration was dependent on the serum addition in the medium (Fig. 4.17 A). Cholesterol concentration of cells incubated in growth medium containing 10% FCS was set to 100%. The use of 10% LPDS (lipoprotein-deficient serum), 10% Nu-serum and no serum addition resulted in a 20 – 40% decreased cholesterol concentration (Fig. 4.17 A).

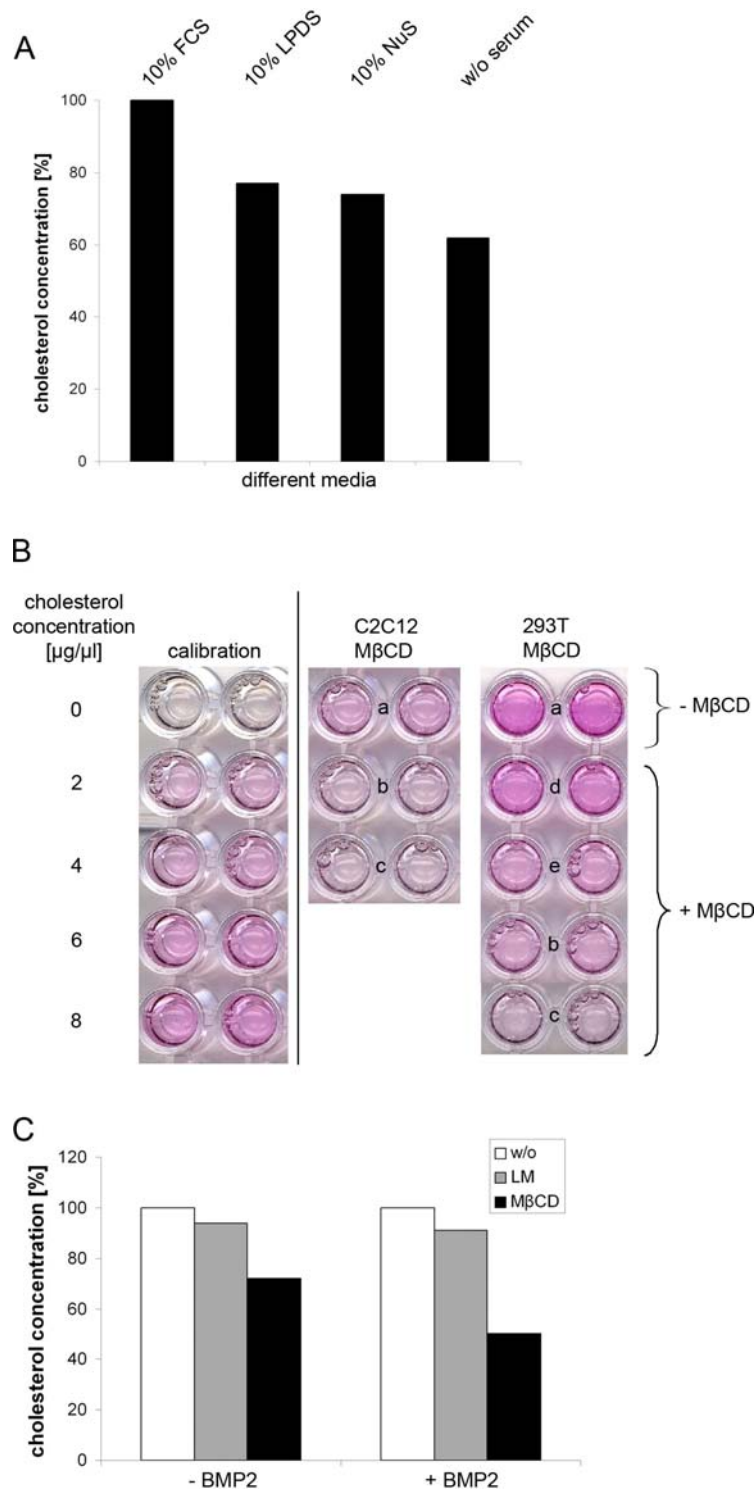


Fig. 4.17 Examples for cholesterol assays on C2C12 and 293T cells.

(A) C2C12 cells were incubated in the indicated media for 24 h, lysed and the cholesterol concentration was determined in duplicates. LPDS = lipoprotein-deficient serum; NuS = Nu-serum (B) The original 96-well plate containing the cholesterol assay was scanned and is displayed. Calibration was always done using cholesterol dilutions of known concentration (left side). C2C12 or 293T cells were incubated in DMEM without any additives over night and treated with MβCD or not. a = w/o MβCD; b = 10 mM MβCD, 30 min; c = 10 mM MβCD, 60 min; d = 1 mM MβCD, 30 min; e = 5 mM MβCD, 30 min (C) C2C12 cells were treated with DMEM + 0,5% LPDS for 24 h as control, the same buffer containing LM (3.3.5.2) or additionally incubated with 2,5 mM MβCD for 30 min (3.3.5.3). A P-Smad1/5 assay (3.3.7.1) was accomplished and part of the lysates was taken for testing the effect of cholesterol depletion (associated Smad assay, see Fig. 4.18).

Fig. 4.17 B displays a typical cholesterol assay. Calibration (left side) was accomplished using cholesterol dilutions with indicated concentrations. The gradually increasing pink color depicts that with each row the cholesterol concentration was amplified. On the right side of Fig. 4.17 B C2C12 or 293T cells were pretreated with different concentrations of M β CD for various times. The cholesterol concentration (respective the pink color) was decreased the longer M β CD was applied and the higher the M β CD concentration was in both kinds of cells. To check whether cholesterol depletion was efficient before a P-Smad1/5 assay was performed, part of the lysates was used for the cholesterol assay. Fig. 4.17 C shows as an example the reduction of cholesterol concentration from the experiment depicted in Fig. 4.18. Lovastatin treatment (LM) reduced cholesterol levels by around 10%, whereas M β CD treatment resulted in 30 – 50% decreased levels (Fig. 4.17 C). This effect was observed albeit of BMP2 stimulation.

4.3.1.2 Effect of cholesterol depletion on Smad1/5 phosphorylation

To investigate the influence of cholesterol-sensitive membrane regions and related endocytic events on BMP signaling, metabolic inhibition of cholesterol synthesis by Lovastatin as well as cholesterol sequestration by M β CD was used. C2C12 cells were incubated in starving medium containing 0,5% LPDS for 24 h and subsequently treated with 2,5 mM M β CD for 30 min. For Lovastatin treatment, LM (Lovastatin/Mevalonate mixture as described in 3.3.5.2) was added to the starving and stimulation medium. Cells were lysed and after protein determination 30 μ g protein were applied per lane and subjected to SDS-PAGE and western blotting with an antibody specific for the phosphorylated form of Smad1/5 and subsequently with a β -actin antibody as control for equal loading (additional to protein determination).

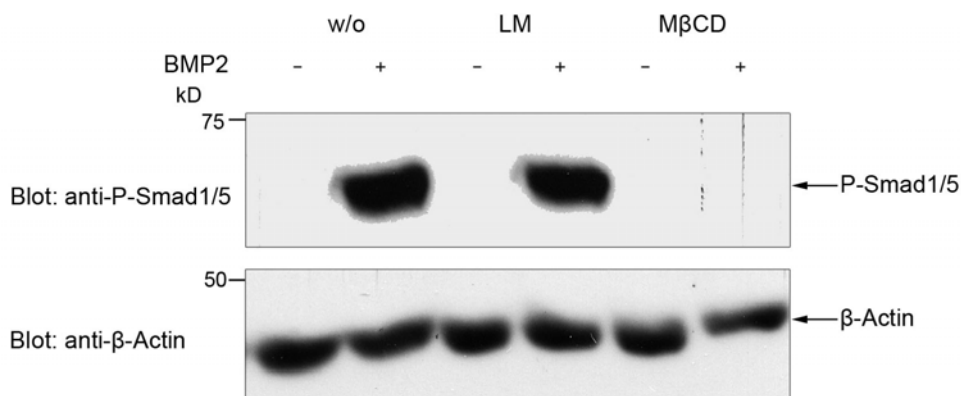


Fig. 4.18 Effect of cholesterol depletion on Smad1/5 phosphorylation in C2C12 cells.

C2C12 cells were treated with Lovastatin (LM) or M β CD to deplete cholesterol and affect cholesterol-sensitive membrane regions. Additionally part of the cells were stimulated with 20 nM BMP2 for 30 min to trigger Smad1/5 phosphorylation. 30 μ g protein were subjected to SDS-PAGE and western blotting using a Phospho-Smad1/5 specific antibody. The same blot was incubated with anti- β -Actin antibody for control.

Fig. 4.18 shows that LM decreased Smad1/5 phosphorylation only by around 10% (quantitation not shown), whereas M β CD abolishes the phosphorylation step. This result should be interpreted carefully, because the two methods applied should cause the same effect (cholesterol depletion); at first sight it is not understandable that the effects are so tremendous different or even opposite. With regard to the cholesterol assay accomplished with the same lysates (Fig. 4.17 C), it is possible that the around 50% decreased cholesterol depletion by M β CD caused severe membrane perturbation and therefore affected not only caveolae and lipid raft regions. In accordance with the literature, the more gentle Lovastatin treatment is more likely to fulfil the demands of cholesterol depletion experiments by decreasing the cholesterol concentration to affect specifically raft regions (and therefore disrupt raft association of specific proteins), but not the plasma membrane in general (Niv et al., 2002; Shvartsman et al., 2003) (see 5.2.1).

4.3.1.3 Effect of cholesterol depletion on transcriptional activity

Knowing that mild cholesterol depletion by Lovastatin only slightly influenced Smad1/5 phosphorylation, the next step was to investigate whether the continuation of BMP signaling is dependent on cholesterol-sensitive plasma membrane regions. Therefore a BRE-luciferase assay was performed (3.3.7.3), while cells were depleted for cholesterol like in the previous experiment.

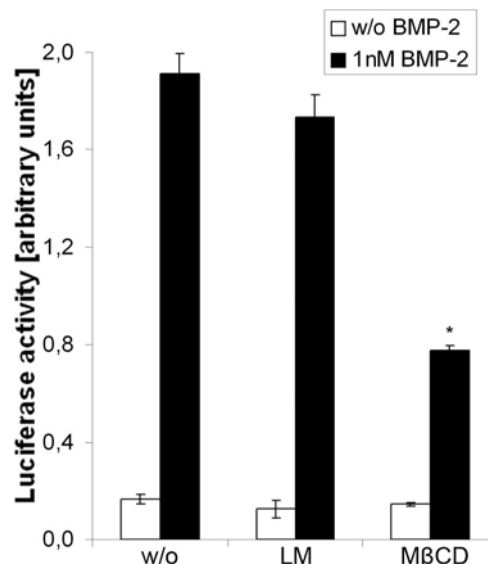


Fig. 4.19 Effect of cholesterol depletion on BMP2-dependent transcriptional activity in C2C12 cells.

C2C12 cells were transiently cotransfected with pBRE-luc and pRLTK before cholesterol depletion using Lovastatin (LM) or M β CD was accomplished (see 3.3.7.3, 3.3.5.2 and 3.3.5.3). Error bars represent standard deviation obtained by three independent experiments.

The diagram depicted in Fig. 4.19 shows that cholesterol depletion decreased BMP2-induced reportergene response, but the difference between the two treatments was also here obvious. While the Lovastatin effect is only around 10%, M β CD diminished the transcriptional activity by around 60%. Considering the before reported harshness of the M β CD treatment, it was concluded that Smad signaling, in terms of Smad1/5 phosphorylation and BMP2-induced reportergene response, is not significantly influenced by disruption of cholesterol-dependent plasma membrane regions.

4.3.1.4 Effect of cholesterol depletion on Alkaline phosphatase activity

To study the influence of cholesterol-sensitive membrane domains on ALP, a late response target gene of BMP2, an ALP assay was performed. ALP is a marker gene of osteoblast differentiation (Takuwa et al., 1991) and was shown to be induced by a Smad-independent pathway (Nohe et al., 2002). The ALP assay measures ALP activity by the use of pNPP as substrate (3.3.7.4) after 72 h of stimulation with at least 50 nM BMP2.

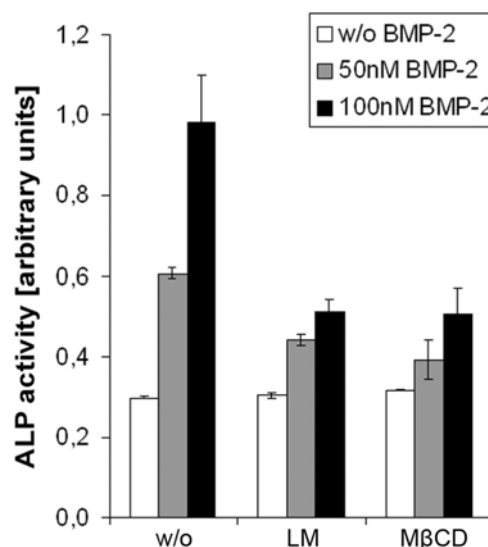


Fig. 4.20 Effect of cholesterol depletion on ALP activity in C2C12 cells.

C2C12 cells were grown in 96-well plates and treated for cholesterol depletion with Lovastatin or M β CD diluted in DMEM + 2% LPDS as described (3.3.5.2 and 3.3.5.3) along with stimulation with 50 or 100 nM BMP2 for 72 h. Cells were lysed and ALP activity was determined using pNPP as a substrate. Error bars represent standard deviation obtained by three independent experiments.

The experiment yielded in a 30 – 50% decreased ALP activity by both cholesterol depleting treatments (Fig. 4.20). This result suggests a clear influence of cholesterol-sensitive membrane regions on Smad-independent signaling. To confirm this data the level of phosphorylated p38-MAPK was determined using a specific antibody (3.3.7.2) after cholesterol was depleted. p38 was shown to play an important role in Smad-independent BMP2-mediated signal transduction and led to the production of ALP (Gallea et al., 2001;

Nohe et al., 2002). The experiment demonstrated that the level of Phospho-p38 was increased, independent of ligand as well as after stimulation with BMP2 (data not shown). It is possible that the rise of the signal was due to stress evoked by the cholesterol depleting reagents. Environmental stress activates MAPKs, including p38, resulting in hyperphosphorylation (Roux and Blenis, 2004).

4.3.2 Influence of caveolin-1 overexpression on BMP signaling

Cav-1 overexpression was shown to be able to induce caveolae formation in cells which lack cav-1 and caveolae (Fra et al., 1995). Moreover it was demonstrated that caveolae-mediated endocytosis was reduced by that (Sharma et al., 2004).

Furthermore, because cav-1 overexpression addresses specifically caveolae, it is possible to selectively study caveolae-related effects without interfering with lipid rafts-related impacts on BMP signaling.

4.3.2.1 Effect of caveolin-1 overexpression on Smad1/5 phosphorylation

To explore the influence of cav-1 overexpression on BMP signaling, C2C12 cells were transiently transfected with cav-1 α and a Phospho-Smad1/5 assay was performed (3.3.7.1).

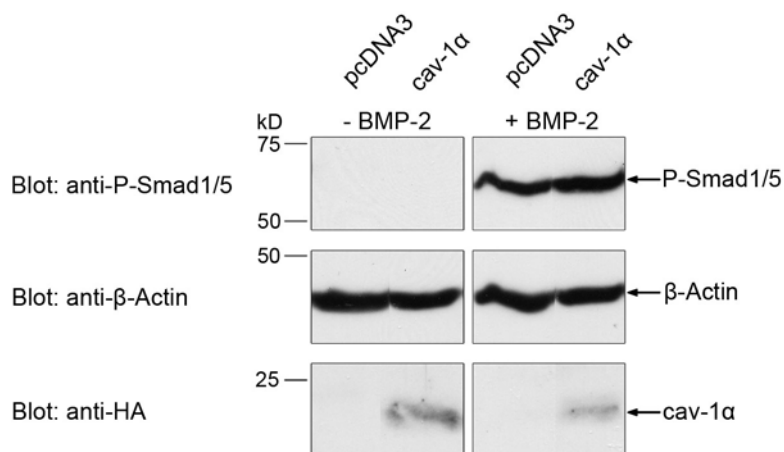


Fig. 4.21 Influence of cav-1 α overexpression on Smad1/5 phosphorylation in C2C12 cells.

C2C12 cells were transiently transfected with cav-1 α or an empty vector, the next day starved for 24 h and stimulated with 20 nM BMP2 for 30 min to induce phosphorylation of Smad1/5. Obtained cell lysates were subjected to SDS-PAGE and western blotting with a specific antibody against the phosphorylated form of Smad1/5. β -Actin and cav-1 α antibodies were applied as controls subsequently on the same membrane.

The experiment showed no differences in the phosphorylation level when cav-1 α was overexpressed in comparison to the empty vector transfection (Fig. 4.21). This result points

to an independence of Smad1/5 phosphorylation from cav-1 expression and caveolae formation.

293T cells are deficient of cav-1 and do not exhibit caveolae at their cell surface (see 4.1). Overexpression of cav-1 in these cells could yield in more tremendous effects.

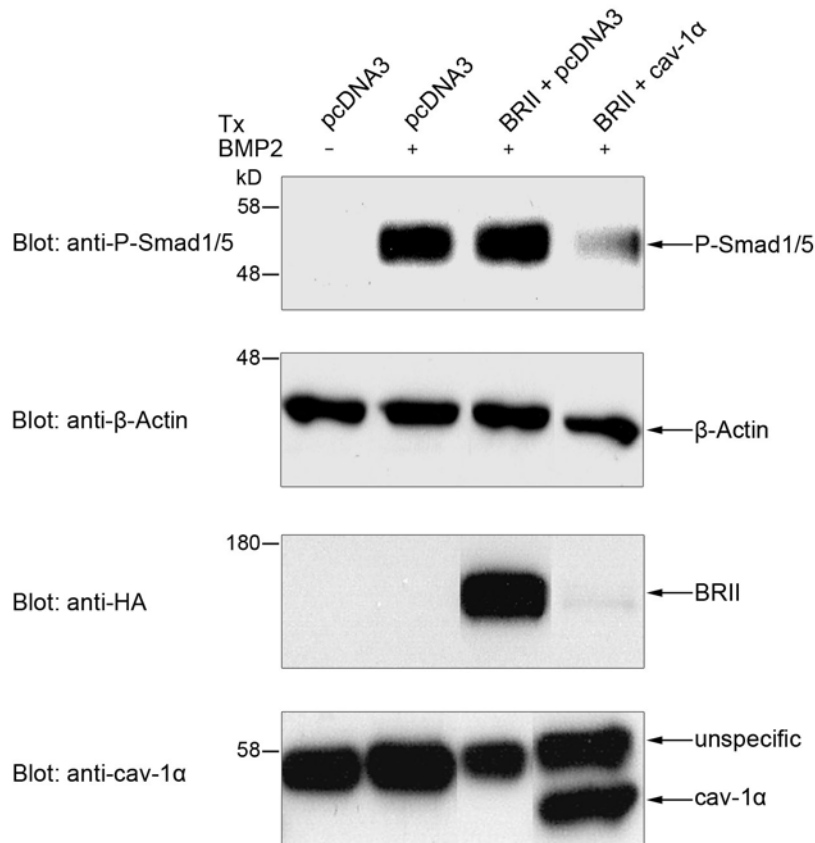


Fig. 4.22 Influence of cav-1 α overexpression on Smad1/5 phosphorylation in 293T cells.

293T cells were transiently transfected with the indicated DNA constructs (EGFP-tagged cav-1 α), the next day starved for 24 h and stimulated with 20 nM BMP2 for 30 min to induce phosphorylation of Smad1/5. Obtained cell lysates were subjected to SDS-PAGE and western blotting with a specific antibody against the phosphorylated form of Smad1/5. β -Actin, HA and cav-1 α antibodies were applied as controls subsequently on the same membrane. Tx = transfection

Fig. 4.22 shows that overexpression of HA-tagged BRII led to a slightly enhanced Smad1/5 phosphorylation, whereas additional expression of cav-1 α reduced this effect by around 60% (quantitation not shown). Furthermore, the anti-HA control western blot shows that although BRII was expressed in both eligible lanes, it was remarkably lower present in cav-1 α cotransfected cells (Fig. 4.22 third panel from the top). This phenomenon was observed several times and could be explained by interference of the cav-1 α DNA with the BRII DNA construct which leads to the downregulation. Because of the time span between transfection and lysis (around 48 h) it can not be ruled out that the protein products cav-1 and BRII are competing or that BRII may be degraded by cav-1 or caveolae. Thus, also the decreased Smad1/5 phosphorylation level would be more understandable.

In conclusion, it was discovered that cav-1 α overexpression reduced Smad1/5 phosphorylation in 293T cells which do not express cav-1 by themselves.

4.3.2.2 Effect of caveolin-1 overexpression on transcriptional activity

To explore the BMP signaling pathway downstream of Smad1/5 phosphorylation, reporter gene assays were performed after overexpressing cav-1 α and cav-1 β . Two different reporter gene constructs were used in this approach: SBE, the Smad binding element (Jonk et al., 1998), and BRE, the BMP-responsive element (Korchynskiy and ten Dijke, 2002; Kusanagi et al., 2000). SBE can be bound by all R-Smads, whereas BRE is bound by Smad1 and is therefore specific for BMP-mediated signals.

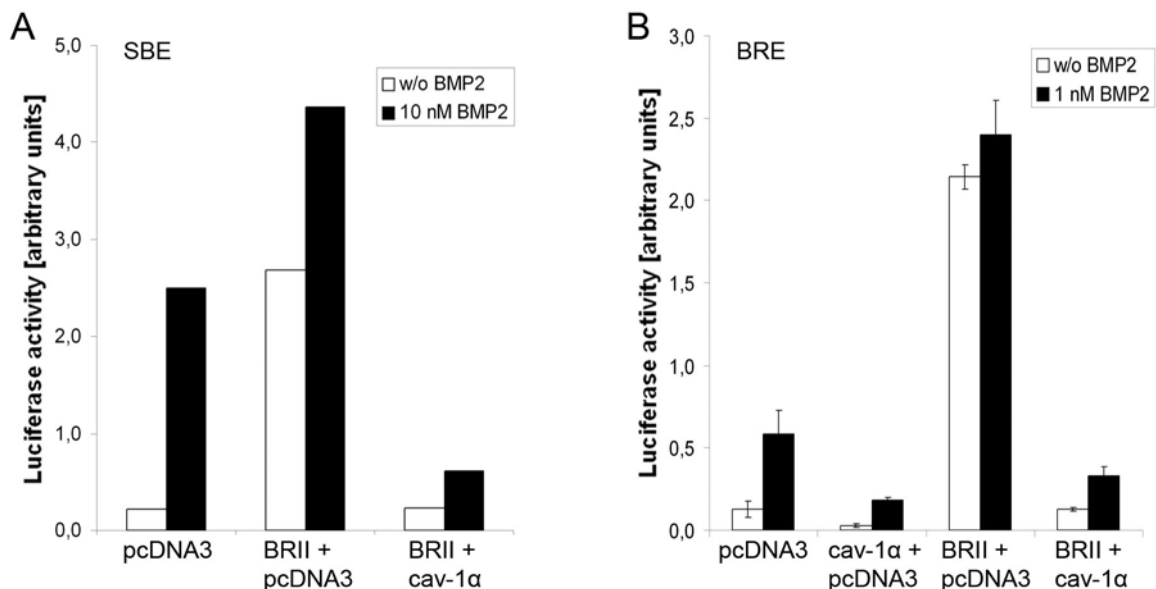


Fig. 4.23 Effect of EGFP-tagged cav-1 α overexpression on BMP2-induced transcriptional activity using SBE- or BRE-reporter gene constructs in C2C12 cells.

C2C12 cells were transiently cotransfected with the respective reporter gene construct, pRLTK and indicated DNA constructs. Subsequently, cells were starved for 5 h and stimulated with (A) 10 nM BMP2 (SBE) or (B) 1 nM BMP2 (BRE) for 16 – 24 h. Luciferase activity was measured as described (3.3.7.3). Error bars represent standard deviation obtained by three independent experiments (B).

Fig. 4.23 shows that in both cases overexpression of BRII induced transcriptional activity of these elements – already ligand independent. Cav-1 α , cav1 β or both isoforms of cav-1 reduced this induction when additionally overexpressed (Fig. 4.23 and β -isoform data not shown). Furthermore, the endogenous level of BMP signaling - without BRII overexpression - was reduced by cav-1 isoforms (right panel).

By checking the vector backbone of the cav-1 constructs used in the experiments above, it was realized that the pEGFP-C1 vector alone was able to reduce BMP2-induced transcriptional activity (Fig. 4.24).

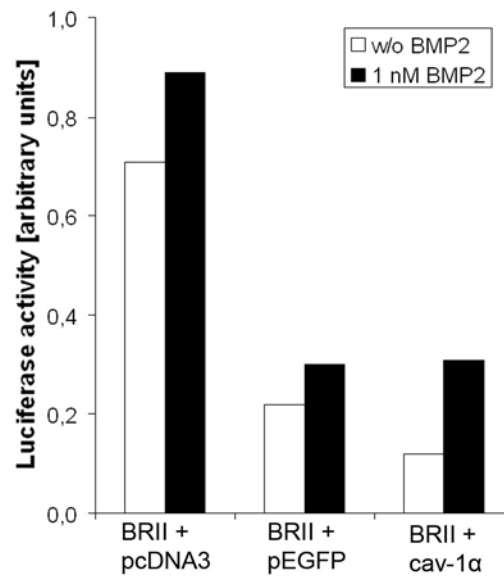


Fig. 4.24 Influence of the pEGFP-vector backbone on cav-1 effect on BMP signaling.

C2C12 cells were transiently transfected with pBRE-luc, pRLTK and indicated DNA constructs. Reportergene assay was performed as described (3.3.7.3).

To exclude effects from this vector backbone, HA-tagged cav-1 constructs in pcDNA3 as vector backbone were used (gift from Dr. C. Wunder, MPI for Infection Biology, Berlin). But also these constructs brought the same results, albeit the effect was not as tremendous as observed before (Fig. 4.25).

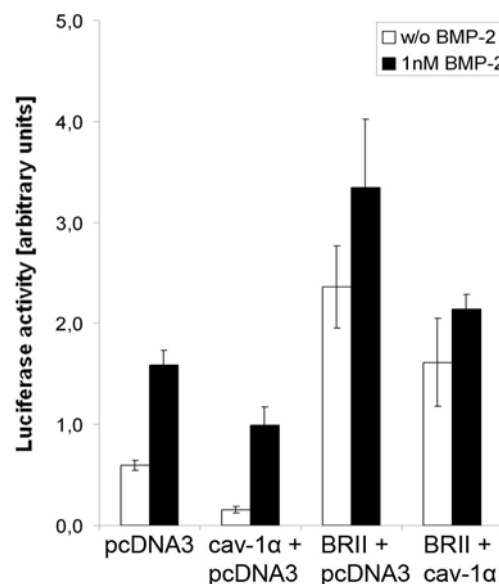


Fig. 4.25 Effect of HA-tagged cav-1 α overexpression on BMP2-induced transcriptional activity in C2C12 cells.

C2C12 cells were transiently transfected with pBRE-luc, pRLTK and indicated DNA constructs. Reportergene assay was performed as described (3.3.7.3). Error bars represent standard deviation obtained by three independent experiments.

Moreover, it could be shown that when BR1a or BR1I and BR1a together were expressed, luciferase activity rose and that this effect was abrogated by additional expression of cav-1 isoforms (data not shown).

These results indicate that BMP signal transduction via Smads is not promoted by caveolar structures at the cell surface. Smad signaling occurs more likely in different regions of the plasma membrane, although the receptors reside in DRM regions and are associated with cav-1 (4.2).

4.3.2.3 Effect of caveolin-1 overexpression on Alkaline phosphatase activity

Having established that ALP activity was dependent on cholesterol-sensitive membrane regions (4.3.1.4), the influence of cav-1 overexpression on this BMP2 target gene was examined.

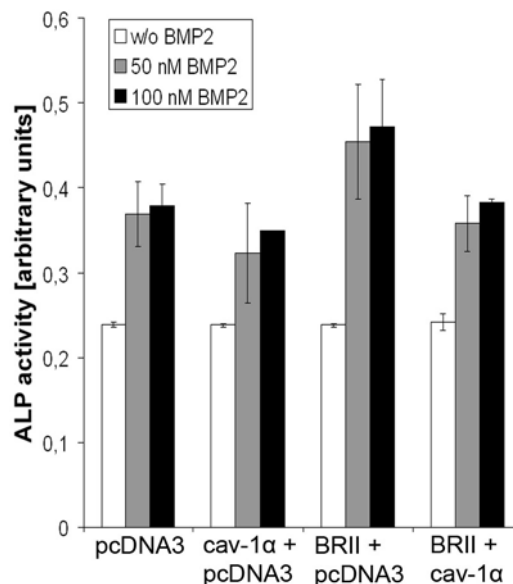


Fig. 4.26 Effect of cav-1 α overexpression on ALP activity in C2C12 cells.

C2C12 cells were transiently transfected with the indicated DNA constructs, subsequently starved for 5 h in DMEM + 2% FCS and stimulated for 72 h with 50 or 100 nM BMP2. ALP activity was measured as described (3.3.7.4). Error bars represent standard deviation obtained by three independent experiments.

ALP activity was reduced to a minor degree by cav-1 α overexpression as well as the slight induction by BR1I expression was compensated by additional cav-1 α expression (Fig. 4.26). In general, it was observed that any kind of transfection in 96-well plates resulted in an around 50% loss of ALP activity compared to the untransfected control - mainly due to cell death (data not shown). Because of that, it is not sure whether the results are reliable or not.

4.3.3 Influence of caveolin-1 knockdown by RNAi on BMP signaling

The opposite effect as in the chapter before – knockdown of cav-1 – was achieved by transfection of cav-1 specific siRNA (obtained and tested for efficiency in C2C12 cells by Santa Cruz). This treatment should result in the loss of caveolae at the cell surface and the consequences could be investigated using again the same read-out systems like before.

4.3.3.1 Effect of caveolin-1 knockdown on Smad1/5 phosphorylation

Establishment of the transfection of cav-1 specific siRNA resulted in the transfection protocol presented in chapter 3.2.8 and was verified using western blots (Fig. 4.27 lower panel). Transfection of a scrambled, fluorescently-marked oligonucleotide as control did not reduce endogenous cav-1 α expression in C2C12 cells, whereas application of the specific cav-1 siRNA almost abolished the expression of the target gene.

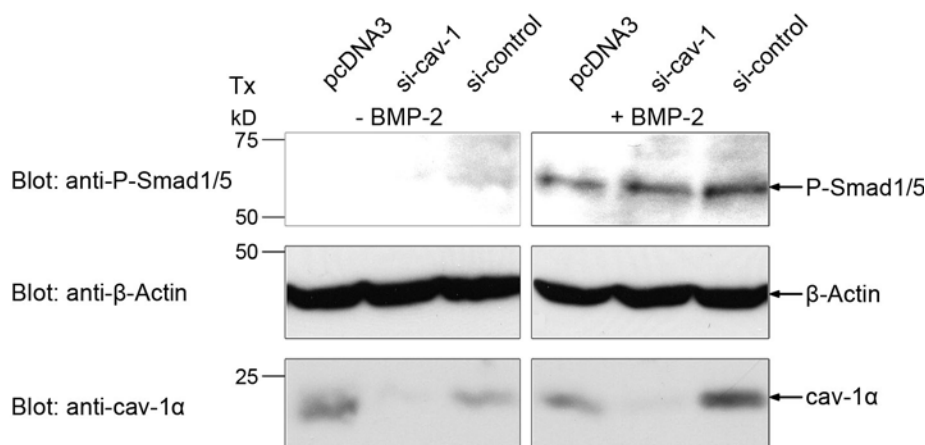


Fig. 4.27 Effect of cav-1 knockdown on Smad1/5 phosphorylation.

C2C12 cells were transfected with an empty vector, siRNA specific against cav-1 (Santa Cruz) or a scrambled, fluorescently-marked siRNA probe (= si-control) and a Phospho-Smad1/5 assay was performed as described (3.3.7.1). The same blot was incubated with anti- β -Actin and anti-cav-1 α antibodies for controls. The same results were obtained in three independent experiments.

Phosphorylation of Smad1/5 was unperturbed by cav-1 knockdown, confirming that this early step of BMP signaling occurs independently of cav-1 expression and caveolae.

4.3.3.2 Effect of caveolin-1 knockdown on transcriptional activity

As a consequential experiment, cav-1 was knocked down, followed by a reporter gene assay using pBRE-luc.

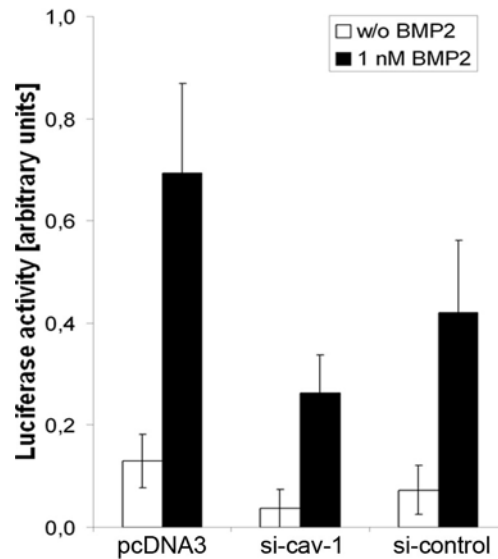


Fig. 4.28 Effect of cav-1 knockdown on BMP2-induced transcriptional activity.

C2C12 cells were transfected as detailed in the legend of Fig. 4.27 and additionally pBRE-luc and pRLTK. Subsequently, a reporter gene assay was performed as described (3.3.7.3). Error bars represent standard deviation obtained by three independent experiments.

Surprisingly, application of the si-control reduced BMP2-induced transcriptional activity already by around 40% compared to an empty vector transfection (Fig. 4.28), although it showed no effect on the cav-1 protein level (Fig. 4.27, lower panel). Recent findings suggest that off-target non-specific effects of RNAi can be encountered, e.g. induction of type 1 interferon which was shown to activate the JAK/STAT (Janus kinase/signal transducer and activator of transcription) pathway and other interferon-stimulated genes (Sledz et al., 2003; Sledz and Williams, 2004). Moreover, JAK/STAT signaling was demonstrated to induce Smad7 (Ulloa et al., 1999), which can result in attenuation of ligand-induced Smad-dependent gene expression.

However, transfection with specific cav-1 siRNA showed an additional reduction of BMP signal transduction (around 40% compared to si-control, Fig. 4.28), although Smad1/5 phosphorylation was unaffected (Fig. 4.27).

Taken together, these data assume that enhancing as well as reducing the cav-1 expression in C2C12 cells led to a decrease in BMP2-mediated transcriptional activity (compare Fig. 4.25 and Fig. 4.28). This conclusion points to the existence of a critical cav-1 concentration necessary for proper BMP signaling in general.

4.3.4 Influence of clathrin-coated pit-dependent endocytosis on BMP signaling

Having gained insight into the dependence of BMP signaling on cholesterol-sensitive plasma membrane regions and in particular on caveolae, CCPs were the next focus. By using chlorpromazine (CP), a specific inhibitor of CCP-mediated endocytosis, this endocytic

pathway was blocked and the impact on BMP signaling studied. Therefore the level of phosphorylated Smad1/5 (4.3.4.1), BMP2-induced transcriptional activity (4.3.4.2) as well as the activity of ALP (4.3.4.3) were investigated.

4.3.4.1 Effect of chlorpromazine on Smad1/5 phosphorylation

To explore whether Smad1/5 phosphorylation was altered by inhibition of CCP-mediated endocytosis, C2C12 cells were treated with CP. In pretests it turned out that CP concentrations of 20 μ M and more impaired the viability of the cells, particularly when used over longer time periods as needed for most of the signaling assays (data not shown). But in the literature concentrations of 50 – 100 μ M applied for 30 min were shown to affect CCP-mediated endocytosis (Wang et al., 1993). To solve that problem, FRAP (Fluorescence Recovery After Photobleaching) analysis were accomplished (by Maya Mouler Rechtman, Department of Neurobiochemistry, George S. Wise Faculty of Life Science, Tel Aviv University). These experiments demonstrated that application of 5 μ M CP for 16 h as well as 100 μ M for 30 min showed the same effect on BR11 endocytosis (Hartung et al., submitted, see 5.2 for details). Therefore the low CP-concentration was used in the following experiments.

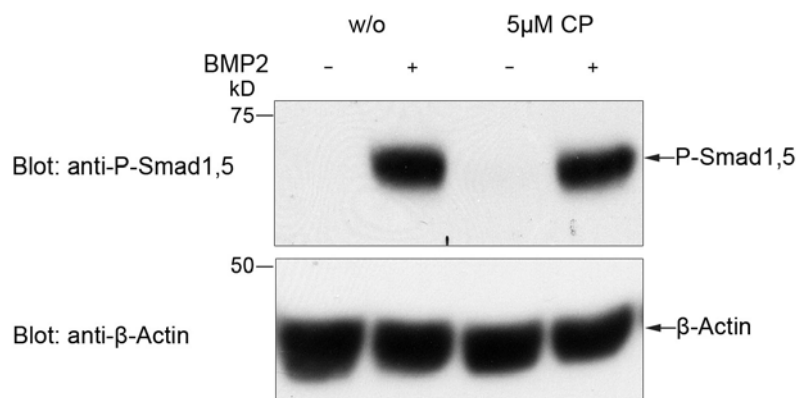


Fig. 4.29 Effect of chlorpromazine on Smad1/5 phosphorylation.

C2C12 cells were treated with 5 μ M CP in starving medium for 24 h and were subsequently stimulated with 20 nM BMP2 in the same medium for 30 min. 30 μ g of the lysates were subjected to SDS-PAGE and western blotting with an antibody specified against the phosphorylated form of Smad1/5, followed by β -Actin as control.

The Phospho-Smad1/5 western blot shows that the level of Smad1/5 phosphorylation was not altered by CP application, i.e. blocking of CCP-mediated endocytosis (Fig. 4.29). That means that this early step in BMP signaling does not depend on CCP-mediated endocytosis.

4.3.4.2 Effect of chlorpromazine on transcriptional activity

To follow up the effects of CP on BMP signaling, BRE-luciferase assays were performed while blocking CCP-mediated endocytic events.

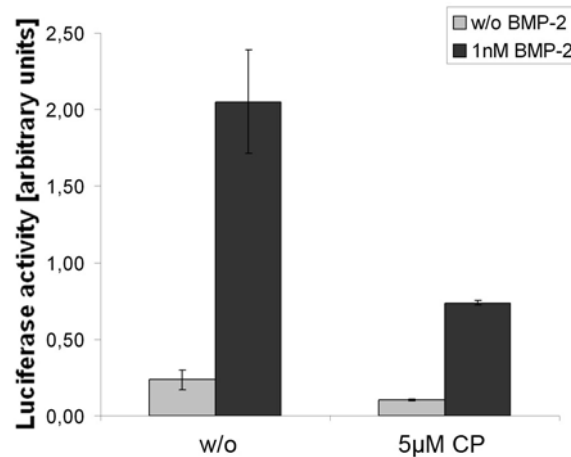


Fig. 4.30 Effect of chlorpromazine on BMP2-induced transcriptional activity.

C2C12 cells were transiently transfected with pBRE-luc and pRLTK, subsequently starved for 5 h and treated with 5 µM CP in starving medium for 16 h. The reporter gene assay was performed as described (3.3.7.3). Error bars represent standard deviation obtained by three independent experiments.

The reporter gene assay shows that BMP signaling was reduced by around 65% when CCP-mediated endocytosis was blocked (Fig. 4.30). From that it can be concluded that while Smad1/5 phosphorylation is unaffected, the continuation of BMP signaling seemed to be dependent on CCP endocytosis.

4.3.4.3 Effect of chlorpromazine on Alkaline phosphatase activity

In previous experiments it could be shown that ALP activity was inhibited by cholesterol depletion and therefore depended on DRM regions in the plasma membrane (Fig. 4.20). Because of that, it was interesting to follow up the question whether also CCPs are involved in signaling leading to ALP production.

Therefore C2C12 cells were treated with CP while stimulation with BMP2 and ALP activity was measured subsequently. Fig. 4.31 demonstrates that ALP activity was diminished by around 70 – 80% when CCP endocytosis was blocked by CP. That means that BMP signaling leading to ALP production, i.e. Smad-independent signaling, is not only dependent on DRM and caveolae regions, but also on a functional CCP-mediated endocytosis.

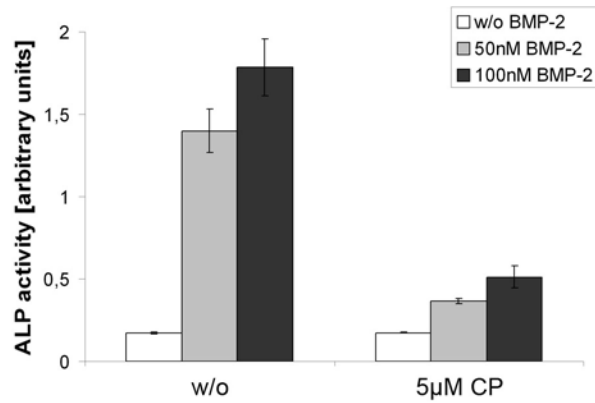


Fig. 4.31 Effect of chlorpromazine on ALP activity.

C2C12 cells were grown in 96-well plates and treated with 5 µM CP diluted in DMEM + 2% FCS as described (3.3.7.4) along with stimulation with 50 or 100 nM BMP2 for 72 h. Cells were lysed and ALP activity was determined using pNPP as a substrate. Error bars represent standard deviation obtained by three independent experiments.

Moreover, the level of phosphorylated p38 was determined using a specific antibody (3.3.7.2) while CCP-mediated endocytosis was blocked by CP. As it was shown for cholesterol depletion (4.3.1.4) this experiment demonstrated that the level of Phospho-p38 was increased, independent of ligand as well as after stimulation with BMP2 (data not shown), probably due to stress evoked by CP treatment.

4.3.5 Influence of the Dynamin2 mutant K44A on BMP signaling

Dynamin2 is a GTPase which plays an important role in clathrin-dependent endocytosis by being responsible mainly for vesicle fission (Song and Schmid, 2003). By transfecting the dominant-negative dynamin2 mutant K44A this process is blocked and therefore different kinds of endocytosis, i.e. CCP- or caveolae-mediated endocytosis, are inhibited (Henley et al., 1998; Takei et al., 1995; van der Blik et al., 1993). By investigating different parts of BMP signaling after transfecting dynamin2 wildtype or mutant, the dependence of BMP signal transduction on endocytosis was studied.

4.3.5.1 Effect of Dynamin 2 mutant K44A on Smad1/5 phosphorylation

Smad1/5 phosphorylation was measured after transfecting dynamin2 wildtype or dominant-negative mutant K44A as described (3.3.7.1).

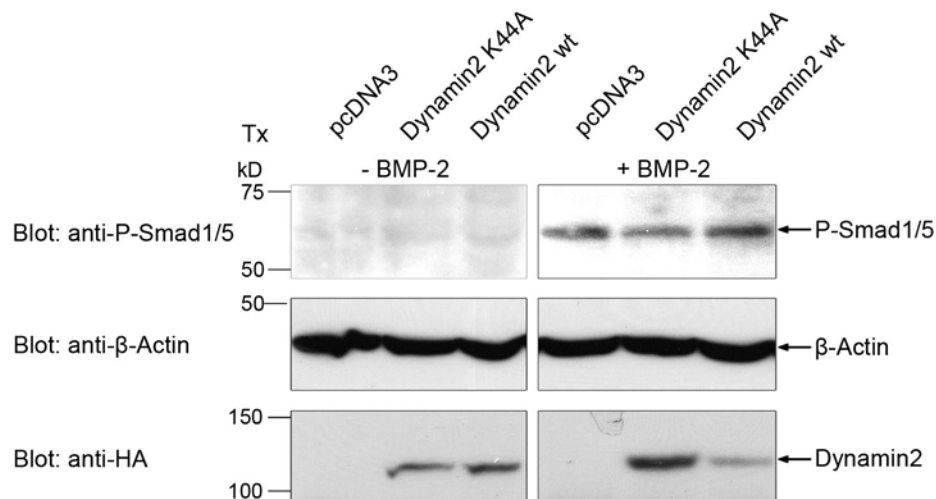


Fig. 4.32 Effect of dynamin 2 on Smad1/5 phosphorylation.

C2C12 cells were transiently transfected with an empty vector, HA-tagged dynamin2 K44A or dynamin2 wildtype (= wt) and cell lysates were subjected to SDS-PAGE and western blotting. The blot was incubated with anti-phospho-Smad1/5 antibody and as control with anti- β -Actin and anti-HA antibodies.

Fig. 4.32 shows that Smad1/5 was continuously phosphorylated although dynamin mutant K44A was expressed. From that it can be concluded that Smad1/5 phosphorylation is an event which does not depend on dynamin action, i.e. endocytic vesicle formation as long as it takes place dynamin-regulated.

4.3.5.2 Effect of Dynamin 2 mutant K44A on transcriptional activity

Next, the effect of dynamin2 K44A mutant on BMP2-induced transcriptional activity was investigated by means of BRE-reportergene assay.

Transfection of either wildtype or K44A mutant dynamin2 resulted in a decreased transcriptional response, ligand-independent as well as after stimulation with BMP2, in comparison to the empty vector transfection (Fig. 4.33). This result constitutes eventually a negative influence of the DNA constructs themselves on BMP signal transduction, although the vector backbone is pcDNA3 like for the control. Otherwise, there was no difference between dynamin2 wildtype and K44A mutant observed (Fig. 4.33) leading to the conclusion that endocytosis is not necessary for BMP2-dependent transcription of target genes. However, this result is in contrast to previous findings, which demonstrated clear dependence of BMP-Smad signal transduction on CCP-mediated endocytosis (4.3.4.2).

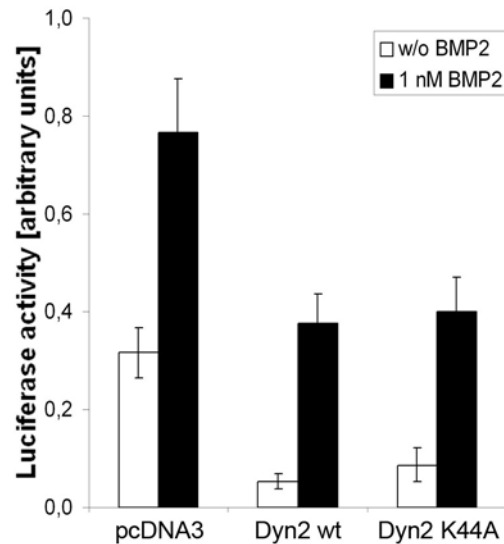


Fig. 4.33 Influence of dynamin 2 on BMP signaling.

C2C12 cells were transiently transfected with pBRE-luc and pRLTK as well as with an empty vector, HA-tagged dynamin2 K44A or dynamin2 wildtype (= wt). The reporter gene assay was performed as described (3.3.7.3). Error bars represent standard deviation obtained by three independent experiments.

4.3.5.3 Effect of Dynamin 2 mutant K44A on Alkaline phosphatase activity

ALP activity was presented to be dependent on DRM domains/caveolae as well as CCP-mediated endocytosis (4.3.1.4, 4.3.2.3 and 4.3.4.3). In the following experiment the influence of dynamin2 on ALP activity was investigated.

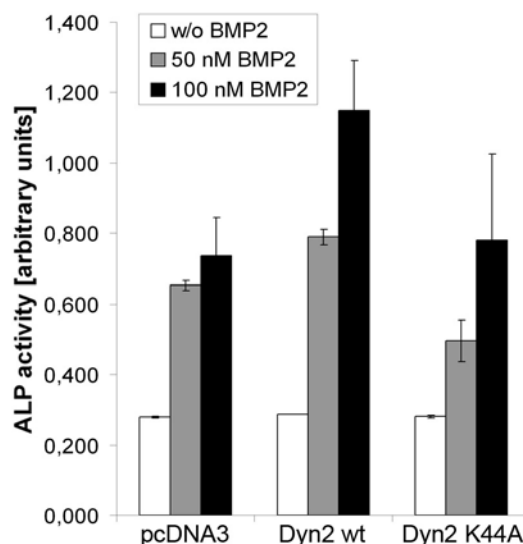


Fig. 4.34 Effect of dynamin 2 on ALP activity.

C2C12 cells were grown in 96-well plates and transiently transfected with indicated DNA constructs, starved for 5 h in DMEM + 2% FCS and stimulated with 50 or 100 nM BMP2 for 72 h. Cells were lysed and ALP activity was determined using pNPP as a substrate as described (3.3.7.4). Error bars represent standard deviation obtained by three independent experiments.

Results

Overexpression of dynamin2 wildtype resulted in an enhanced ALP activity, when cells were stimulated with 50 or 100 nM BMP2, whereas overexpression of dynamin2 K44A mutant yielded in a decreased ALP activity (Fig. 4.34). This suggests that ALP is produced in dependence on functional endocytic mechanisms, proving previous results that cholesterol-dependent plasma membrane regions, caveolae and CCP-mediated endocytosis influence ALP activity.

5 DISCUSSION

Endocytosis of growth factor receptors has an important regulatory influence on diverse signal transduction pathways. It controls mainly the number and activation state of cell surface receptors and is initiated at specific plasma membrane domains, e.g. clathrin-coated pits (CCPs), caveolae or lipid rafts. The effects of malfunctioning endocytic machinery can be tremendous and cause often severe pathologies, e.g. Alzheimers disease. Alzheimers disease is a devastating, neurodegenerative disease characterized by escalated levels of amyloid-beta ($A\beta$) which is known to form plaques causing the disease. It was found that $A\beta$ promotes endocytosis of NMDA (N-methyl-D-aspartate) receptors in cortical neurons and thereby reduce glutaminergic transmission and synaptic plasticity (Snyder et al., 2005). Furthermore, $A\beta$ is generated by proteolytic cleavage from the amyloid precursor protein (APP) which needs to be raft-associated to determine $A\beta$ production (Ehehalt et al., 2003; Simons and Ehehalt, 2002). The latter provides an additional link of this disease to special membrane regions. The example of Alzheimers disease demonstrates how important it is to investigate localization, endocytosis and trafficking of signaling molecules - which stand in the middle of the action of living cells.

Recently, it was shown that TGF- β and EGF signaling pathways depend on endocytic events and vesicles in different aspects (Di Fiore and De Camilli, 2001; Di Guglielmo et al., 2003; Hayes et al., 2002; Mitchell et al., 2004; Penheiter et al., 2002). Some groups described CCPs and early endosomes to promote signaling, otherwise caveolae and caveosomes seemed to represent sites where signaling is downregulated or attenuated. Others could not support at all caveolae contribution especially to TGF- β signaling (Mitchell et al., 2004). Lately, Sigismund et al. reported that the two ways of EGF receptor (EGFR) internalization are determined by critical EGF concentrations along with respective ubiquitination levels. Low ligand concentrations (non-ubiquitinated receptors) triggered nearly exclusively the clathrin-dependent pathway, whereas for high concentrations (correlating with ubiquitination of the receptors) this shifts to a clathrin-independent, lipid raft-regulated route. They showed further that Eps15, Eps15R and epsin play a role in coupling ubiquitinated cargo to clathrin-independent internalization of EGFR (Sigismund et al., 2005).

As demonstrated, there are a multitude of possibilities how growth factor receptor localization and endocytosis can influence signaling cascades. The presented study was set up to elucidate BMP receptor localization and its influence on BMP signaling.

5.1 LOCALIZATION OF BMP RECEPTORS

BMPs are members of the TGF- β superfamily and regulate proliferation, differentiation, chemotaxis and apoptosis (Hogan, 1996; Massague and Chen, 2000). BMP signaling involves two types of transmembrane serine/threonine kinases, BMP-type I and -type II receptors (BRI, BRII) (Canalis et al., 2003; Hoodless et al., 1996). BMP receptor activation occurs upon ligand binding to preformed receptor complexes (PFCs) or BMP2-induced signaling complexes (BISCs) composed of BRI and BRII (Nohe et al., 2002). Following ligand binding, the constitutive kinase of BRII activates BRI. The activated BRI phosphorylates downstream nuclear factors (e.g. R-Smads: Smad1/5/8) which then translocate to the nucleus together with the Co-Smad (Smad4) to regulate transcription of target genes. Binding of BMP2 to PFCs results in activation of the Smad pathway, whereas formation of heteromeric receptor complexes induced by BMP2 results in activation of the p38-MAPK pathway (Nohe et al., 2002).

BMP receptor localization has not been studied in detail in the past. News about this topic were just published lately (Nohe et al., 2005; Ramos et al., 2006). Nohe et al. suggested that cav-1 isoforms bind to BRII and that cav-1 α influences Smad signaling in A431 cells (Nohe et al., 2005). Ramos et al. implied a possible link between BRII localization in DRM/caveolae and pulmonary hypertension, a disease, which is characterized by reduced BRII and caveolin expression (Ramos et al., 2006).

The presented study investigated BMP receptor localization extensively, particularly with regard to DRM regions/caveolae and CCPs, to gain new insight into the events which initiates BMP signaling.

5.1.1 Evidences for BMP receptor localization in DRM regions and caveolae

Proteins associated with lipid rafts or caveolae are often identified by their insolubility in non-ionic detergents such as Triton X-100 or CHAPS at 4°C producing DRMs which float to a low density on sucrose or OptiPrep™ gradients after ultracentrifugation (Brown and London, 2000; Sargiacomo et al., 1993). To explore BMP receptor localization, DRMs were separated from cell lysates and analyzed concerning their BMP receptor content. It was demonstrated that BRI and BRII reside in DRMs and cofractionate with cav-1 α (Fig. 4.6, Fig. 4.7, Fig. 4.8, Fig. 4.9, Fig. 4.10, Fig. 4.11). Moreover, in cells which do not exhibit caveolae due to lack of cav-1 expression, BMP receptors are still included in DRM-fractions (Fig. 4.10, Fig. 4.11). These findings propose that BMP receptors are present in caveolae and/or non-caveolar DRMs. Furthermore, stimulation of cells with BMP2 for 30 min (sufficient for phosphorylation of Smad1/5) did not influence the distribution of the receptors, suggesting a general localization of BMP receptors in DRMs. Quantitation of the results showed that BRI was two

to four times more concentrated in DRMs compared to BR11 (Table 4.1, Table 4.2), concluding that the high affinity receptor for BMP2 is stronger associated with rafts or/and caveolae.

Although the method applied here is the most common approach for identifying putative raft/caveolae-associated proteins, it is not uncontroversial (Lagerholm et al., 2005; Simons and Toomre, 2000). On the one hand, it is possible that cytoskeleton-associated proteins are not able to float or the connection to rafts is too weak so that the protein is solubilized by the detergent (Hooper, 1999; Janes et al., 1999). On the other hand, it has to be considered that not only molecules from the plasma membrane but also from intracellular membranes can be isolated by this method. Moreover, the analysis is dependent on the detergent used as well as on temperature or cell type (Chamberlain, 2004; Schuck et al., 2003; Waugh et al., 1999). Furthermore, some publications see the danger of the formation of membrane domains by detergent extraction itself due to rearrangement of intermolecular associations (Heerklotz, 2002). However, studies on model membrane systems have shown that detergent extraction does not artefactually induce clustering (Hooper, 1999). Though, several diverse, complementary approaches, mainly microscopical techniques, should be undertaken to achieve a comprehensive analysis of the complexity of membrane compartmentalization.

Stronger association with DRMs could lead to a lower mobility of the respective receptor due to the biochemical properties of raft domains (see 1.5.1).

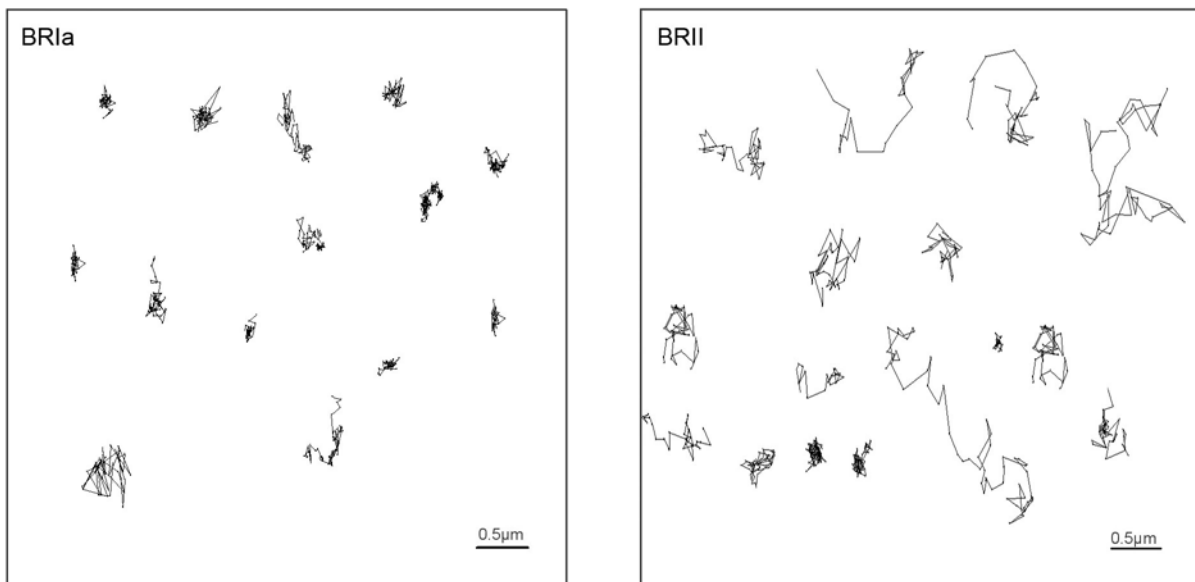


Fig. 5.1 Trajectories of BR1a and BR11 overexpressing C2C12 cells (Dr. A. Noskov, Prof. G. Harms, Virchow Center, University of Würzburg; unpublished data).

Single molecule microscopy was conducted on C2C12 cells stably overexpressing HA-tagged BR1a (left panel) or BR11 (right panel).

In collaboration with the group of Prof. G. Harms (experiments by Dr. A. Noskov, Virchow center, University of Würzburg) single molecule microscopy studies were conducted on C2C12 cells stably overexpressing BR_{II} or BR_{Ia}. Trajectories clarified that the mobility of BR_{Ia} is clearly decreased in comparison to BR_{II} (unpublished data, Fig. 5.1). This confirms the results from flotation assays discussed before. However, stimulation experiments found a decreased mobility of BR_{II} after BMP2 stimulation (unpublished data, data not shown) although a higher occurrence of BR_{II} in DRMs after BMP2 stimulation was not reflected in fractionation experiments (Table 4.1). One possible explanation for this discrepancy could be the different stimulation times used in the experiments. While single molecule microscopy was accomplished after very short stimulation (about 30 s to 1 min) with high concentrations of BMP2 (40 nM), flotation assays were performed after cells were stimulated with 20 nM BMP2 for 30 min. Probably the recruitment of BR_{II} in response to BMP2 is a faster process than other intracellular events.

To verify caveolae localization, co-immunoprecipitation, immunofluorescence and immunoelectronmicroscopy studies were the methods of choice. It could be shown that both receptor types interacted with endogenously expressed cav-1 α (Fig. 4.12, Fig. 4.13). Sequence analyses of BMP type I receptors revealed a cav-1 consensus motif (Couet et al., 1997a) in the kinase domain (YSFGLILW respective to amino acids 401 - 408 for BR_{Ib}, YSFGLIIW respective to amino acids 431 - 438 for BR_{Ia}) which confirms our finding of strong association between cav-1 α and type I receptors (Fig. 4.12 C, Fig. 4.13) as well as the high occurrence of BR_I in DRM-fractions (Fig. 4.9, Fig. 4.10). To prove the influence of these sites on BR_I-cav-1 interaction and in turn the impact of this physical interaction on BMP signaling, site directed mutagenesis of the putative caveolin-binding motif could bring new and consolidated cognitions and should be accomplished in future studies. Moreover, it would be interesting to analyze in this context whether binding of cav-1 α to the kinase domain of BR_{Ib} affects the kinase activity of this receptor, as it was discussed for EGFR which also binds cav-1 via its kinase domain (Couet et al., 1997b). Here, this interaction leads to the inhibition of the autophosphorylation of EGFR.

To map the potential binding site of cav-1 α on BR_{II}, BR_{II}-SF and BR_{II}-TC1 overexpressing cells were used in the same experiments. It turned out that the interaction of BR_{II} and cav-1 α required the kinase domain of BR_{II}, because BR_{II}-SF was able, whereas BR_{II}-TC1 failed to bind cav-1 α (Fig. 4.12 A, B). BR_{II}-TC1, the shortest BR_{II} truncation mutant, ends 27 amino acids after the transmembrane domain and therefore lacks the kinase- and tail-domains (sequence listed in A 2, Nohe et al., 2002). Since we could show previously that BR_{II}-TC1 is too short to form PFCs with BR_I (Nohe et al., 2002), it is possible that the observed co-immunoprecipitation of BR_{II} with cav-1 might be indirect via the associated BR_I. As a matter of fact, sequence analyses of BR_{II}-cytoplasmic region showed no correlation with the cav-1

binding site (Couet et al., 1997a), suggesting association via an alternative mechanism. In conclusion, these results point to the possibility that BRI might be associated directly with cav-1 α , whereas BRII could possibly be precipitated together with cav-1 α via its interaction with BRI.

Double-label immunofluorescence experiments showed a partial overlap between BMP receptor types (via their HA-tag) and endogenous cav-1 α (Fig. 4.14). But as the control labeling with BRII-TC1 overexpressing C2C12 cells demonstrated (Fig. 4.15), the method was not exact enough to make reliable statements.

Two different immuno-electronmicroscopy approaches were accomplished. Using the pre-embedding method (Fig. 4.16 A, B), cells were labeled prior to fixation. Here membranes remain intact and invaginations as well as vesicles still associated with the membrane can be observed. Unfortunately, cav-1 has no extracellular domain which is why permeabilization of the membrane was necessary, before the cells could be treated with an antibody against cav-1. This treatment penetrates and partially destroys the membrane. Because of that, the pre-embedding method was only applied in combination with single-labeling of BRII via its extracellularly HA-tag and not with double-labeling of BRII and cav-1 α . In this case, the receptor was predominantly observed at the cell surface (Fig. 4.16 A) as well as in CCPs or CCVs (Fig. 4.16 B, discussed in 5.1.2). Otherwise, the post-embedding method was used (Fig. 4.16 C, D, E) in which cell pellets were obtained, sliced and the ultrathin slices were incubated with different antibody solutions. Using this method, most of the membranes are destroyed and moreover the orientation of the cell in the pellet and slice is uncertain. Whether HA-antibody alone (Fig. 4.16 C) or additionally cav-1 α -antibody (Fig. 4.16 D, E) was applied, the receptor was predominantly found in clusters of about 50 - 75 nm in size. Application of cav-1 α -antibody proved that these clusters contain cav-1 α , the marker protein of caveolae. These results demonstrated again that BRII colocalized with cav-1 α in structures of the size of caveolae although the invagination itself could not be spotted due to limitations of the method applied.

In accordance with these findings, Nohe et al. published image cross-correlation spectroscopy studies which showed that BRIa and BRII colocalize with cav-1 at the cell surface of A431 cells. Moreover, they could demonstrate that the isoforms of cav-1 have different impacts on BMP receptor distribution in caveolae in response to BMP2 (Nohe et al., 2005).

Additional evidences for a localization of BMP receptors in DRMs/caveolae were obtained in collaboration with the group of Prof. Y. Henis (experiments by Keren Bitton-Worms and Maya Mouler Rechtman, Department of Neurobiochemistry, George S. Wise Faculty of Life Science, Tel Aviv University) using cholesterol depleting reagents (nystatin) or specific inhibitors of caveolae (genistein) in combination with FRAP analyses. It was found that while

BR1b was internalized regardless whether inhibitors were present or not, BR11 internalization was blocked efficiently (Hartung et al., submitted). This finding suggests a contribution of cholesterol- and caveolae-dependent endocytosis on the internalization of BR11, but not of BR1b. By that the localization of BR11 in DRMs and/or caveolae was indirectly confirmed. However, although all other studies on BR1b point to a DRM and/or caveolae localization, the results of the FRAP analyses showed no contribution of cholesterol- and caveolae-dependent endocytosis. This result points to a localization of BR1b in DRMs/caveolae without subsequent internalization of this receptor type via one of these pathways.

In summary, BR11 and BR1 could both be localized to DRM and/or caveolae domains in the plasma membrane by cofractionation, interaction and colocalization with cav-1, the caveolae marker protein. Furthermore, BR11 (but not BR1b) was shown to be internalized via this pathway (Fig. 5.2).

5.1.2 Evidences for BMP receptor localization in clathrin-coated pits

Lately, a proteomics-based screen was accomplished, discovering BR11 cytoplasmic domain-associated proteins (Hassel et al., 2004). Thereby Eps15R, a protein which constitutively resides in CCPs (Coda et al., 1998; Poupon et al., 2002), was found to interact with the cytoplasmic domain of BR11 (Hartung et al., submitted). This interaction was confirmed by co-immunoprecipitation studies and was also verified for BR11-SF and BR11-TC1 (Diplomarbeit of Dipl. Biol. V. Wenzel, 2005; Hartung et al., submitted). These results suggest an Eps15R-BR11 interaction site at the 27 amino acids-juxtamembrane domain of BR11 (amino acids 176 – 202). Since Eps15R was identified by GST-pulldown experiments using the 537 residues-cytoplasmic tail region of BR11 (amino acids 502 – 1038), a second binding site of Eps15R at BR11 is proposed. Eps15R is a related protein of Eps15 and epsin which play an important role in clathrin-mediated endocytosis of growth factor receptors (Klapisz et al., 2002). They function as adaptors between ubiquitinated membrane cargo and the clathrin-coat or other endocytic scaffolds (Polo et al., 2002). Therefore the interaction between BR11 and Eps15R represents a new link between the BMP signaling network and the CCP-mediated endocytic machinery and points to a localization of BR11 in CCPs. How the association between the two proteins influences BMP signaling need to be investigated in future studies.

The method of immuno-electronmicroscopy was primarily set up to identify colocalization of BR11 and cav-1 (5.1.1), but in addition BR11 was verified in CCPs or CCVs (Fig. 4.16 B). The vesicle was recognized by its size (around 100 nm in diameter) and ciliated border. Although this result needs to be re-examined and confirmed in the future, it provides an evidence for the localization of BR11 in CCPs/CCVs independent of BMP2 stimulation. That indeed BMP receptor endocytosis is dependent on CCPs could be shown in collaboration with the group of Prof. Y. Henis (experiments by Keren Bitton-Worms and Maya Mouléur Rechtman,

Department of Neurobiochemistry, George S. Wise Faculty of Life Science, Tel Aviv University). CCP-mediated endocytosis was blocked by diverse reagents (chlorpromazine, hypertonic treatment, cytosol acidification) and BMP receptor internalization was observed and evaluated by FRAP analysis (Hartung et al., submitted). Both BMP receptor types, BRII and BRIb, were not internalized anymore after inhibition of this endocytic pathway, proposing CCPs/CCVs as the major internalization route for BMP receptors.

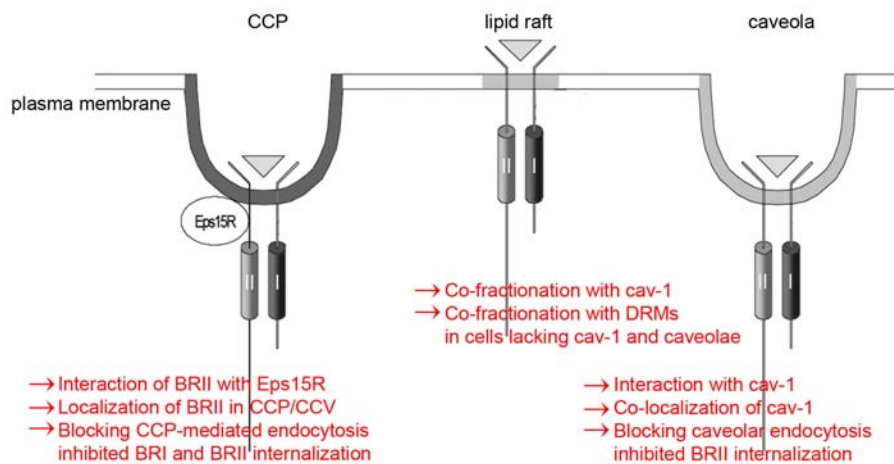


Fig. 5.2 Summary of main evidences for BMP receptor localization.

BRII and BRI co-fractionated, interacted and co-localized with cav-1, suggesting a potential localization in caveolae and/or lipid rafts. Additionally, an interaction between BRII and Eps15R was verified and BRII was spotted in CCPs/CCVs. Furthermore, both endocytic routes contributed to BMP receptor internalization. While only BRII seemed to be internalized via caveolae, both receptor types were found to be endocytosed via CCPs.

Taken together, BRII was shown to bind a key protein of the CCP-endocytic machinery, Eps15R, and could be localized to CCPs/CCVs using immuno-electronmicroscopy. Moreover, BRII and BRI were both shown to be internalized via CCPs/CCVs (Fig. 5.2).

5.2 IMPACT OF BMP RECEPTOR LOCALIZATION ON BMP SIGNAL TRANSDUCTION

The potential role of BMP receptor localization in different regions of the plasma membrane on determining the signaling pathways activated by PFCs and BISCs has not been explored so far. To investigate the contribution of BMP receptor localization in distinct regions of the plasma membrane and of receptor endocytosis on BMP signaling, we studied how Smad-dependent and Smad-independent BMP signaling pathways are altered, while intervening in endocytosis. Therefore mainly three different read-out assays were used: determination of phosphorylated Smad1/5 via western blotting with a specific antibody (5.2.1), measurement of the transcriptional activity in response to BMP2 via reporter gene assays (5.2.2) and determination of ALP production via an activity assay (5.2.3).

5.2.1 Effects on Smad1/5 phosphorylation

The R-Smads Smad1/5/8 are directly phosphorylated by the activated BMP type I receptor in response to BMP ligands (Kretzschmar et al., 1997; Macias-Silva et al., 1996). This event can be monitored by the use of a phosphorylation state-specific antibody, recognizing the dual serine phosphorylated Smad1 (Ser463/465). Previous studies revealed that increased Smad1 phosphorylation was first evident 2 min after addition of BMP2, peaked at 20 min and remained elevated for up to 2 h (Hoodless et al., 1996). Therefore, in the present experiments cells were stimulated with 20 nM BMP2 for 30 min after starving for 2 h and cell lysates were subjected to SDS-PAGE and western blotting (see 3.3.7.1).

To disrupt DRM regions, metabolic inhibition of cholesterol synthesis was employed by means of Lovastatin (3.3.5.2). As an alternative treatment, M β CD was used to sequester cholesterol from the plasma membrane (3.3.5.3). Both methods should result in disruption of lipid rafts and caveolae, because these membrane regions exhibit especially high cholesterol content and dependence. But as the literature shows, M β CD also affected CCP-mediated endocytosis (Rodal et al., 1999), whereas Lovastatin specifically impaired DRM regions (Niv et al., 2002; Shvartsman et al., 2003). By verifying the cholesterol concentration after cholesterol depletion with M β CD or Lovastatin, it could be shown that the effects were tremendously different (Fig. 4.17 C). While Lovastatin decreased the cholesterol concentration by around 10% (compare to literature: 30 – 35 %; Shvartsman et al., 2003), M β CD treatment resulted in depletion of the cholesterol level by around 30 – 50% (in other experiments up to 80%, data not shown). Therefore the effects of M β CD seemed to be not as reliable as the results obtained by the use of Lovastatin.

The latter treatment showed almost no influence on the level of phosphorylated Smad1/5 compared to an untreated control (around 10% reduction; Fig. 4.18). This result indicates that Smad1/5 might be phosphorylated independent of cholesterol and cholesterol-sensitive membrane domains which would be destroyed by Lovastatin. When the plasma membrane was more damaged by the use of M β CD, Smad1/5 phosphorylation was disrupted completely (Fig. 4.18). This reflects that the integrity of the plasma membrane in general was critical for the phosphorylation step.

To prove and more deepen the aspects discovered so far, the effect of manipulating the number of caveolae at the cell surface was investigated. Therefore cav-1 overexpression as well as cav-1 knockdown were accomplished and the phosphorylation level of Smad1/5 compared with controls. Both experiments produced the same result: that cav-1/caveolae did not influence the phospho-Smad1/5 level (Fig. 4.21, Fig. 4.27).

It was shown that cav-1 overexpression led to the induction of caveolae formation at the cell surface and that the uptake of caveolar markers was inhibited by that (Fra et al., 1995; Sharma et al., 2004). However, the internalization of some caveolar ligands was

demonstrated to be signal-mediated, requiring cav-1 expression (Minshall et al., 2000; Pelkmans et al., 2002). Otherwise, there are some ligands that are internalized independently of cav-1 expression, e.g. the autocrine motility factor or to some extent cholera toxin-B (CTB) (Balemans and Van Hul, 2002; Henley et al., 1998; Le and Nabi, 2003; Nichols, 2002; Parton et al., 1994; Puri et al., 2001; Wolf et al., 2002).

BRII was shown to be internalized constitutively via the caveolar pathway, whereas BRI seemed to be endocytosed independently of cholesterol-sensitive regions and caveolae (5.1.1; collaboration with the group of Prof. Y. Henis; Hartung et al., submitted). Consistent with that, phosphorylation of Smad1/5, which is triggered by activated BRI, seems to occur independently of caveolar invaginations and endocytosis.

Knowing that cholesterol-sensitive membrane regions are most likely not involved in Smad1/5 phosphorylation, the portion of CCP-mediated endocytosis on the phosphorylation step was investigated. To interfere specifically with clathrin-mediated internalization, chlorpromazine was applied on the cells. Chlorpromazine mediates the redistribution of AP-2 from the plasma membrane to endosomes (Wang et al., 1993; Yao et al., 2002) and was shown to inhibit CCP-mediated endocytosis without affecting caveolar-like internalization processes (Puri et al., 2001; Singh et al., 2003). Although chlorpromazine blocked endocytosis of both types of BMP receptors (5.1.2; collaboration with the group of Prof. Y. Henis; Hartung et al., submitted), it turned out that BMP2-induced Smad1/5 phosphorylation was unaffected by this treatment (Fig. 4.29). This suggests that activated BRI phosphorylates Smad1/5 independently of cholesterol-sensitive membrane regions, caveolae **and** clathrin-dependent endocytosis; the active BMP receptor complex is then most likely internalized through CCPs.

To complete the picture of endocytosis-independent Smad1/5 phosphorylation, endocytosis in general (caveolae- and CCP-mediated) was blocked by overexpression of a dominant-negative mutant of dynamin2 (K44A; Henley et al., 1998; Takei et al., 1995; van der Blik et al., 1993). It emerged that Smad1/5 was still phosphorylated, concluding endocytosis-independence of this event (Fig. 4.32).

For the related TGF- β signaling pathway some publications favor an impact of endocytic events on Smad2/3 phosphorylation (Di Guglielmo et al., 2003; Hayes et al., 2002; Penheiter et al., 2002), while others report endocytosis-independent phosphorylation of Smad2/3 (Lu et al., 2002; Runyan et al., 2005).

Taken together, the results of the present study propose that Smad1/5 is phosphorylated in response to BMP2 by BRI in a cholesterol-, cav-1-, CCP-mediated endocytosis- and dynamin2-independent manner, most likely at the cell surface (Fig. 5.3). However, it can not be ruled out that cholesterol-, cav-1-, clathrin- and dynamin-independent endocytosis

pathways exist which could be involved in Smad1/5 phosphorylation, although till now there is no evidence in the literature for that.

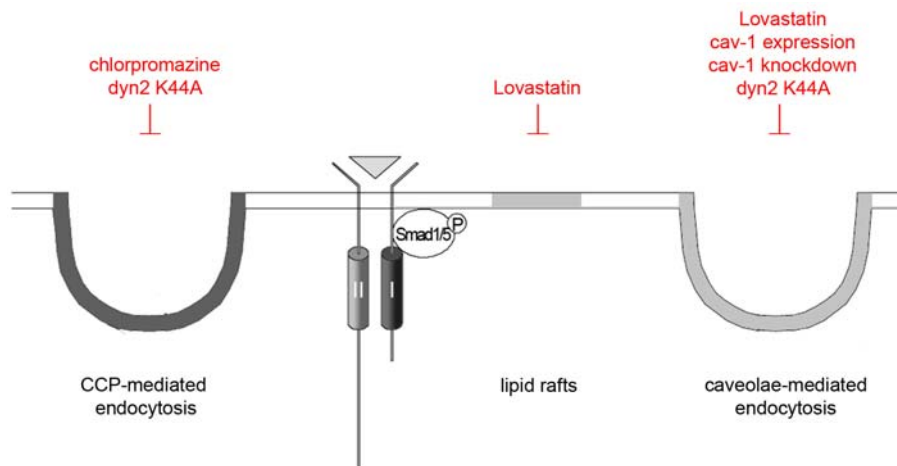


Fig. 5.3 Smad1/5 phosphorylation takes place at the cell surface.

Smad1/5 phosphorylation is not influenced upon inhibition of clathrin- or caveolae-mediated endocytosis or cholesterol-sensitive membrane regions, concluding that Smad1/5 is phosphorylated most likely independent of endocytic events at the cell surface.

5.2.2 Effects on BMP2-induced transcription of target genes

Reportergene studies are used to gain insight into the transcriptional activity of promoters or promoter elements after induction by growth factor ligands. BMP2 elicits its effects through transmembrane receptors which transduce the signal inside of the cell into the nucleus via effector molecules. These molecules enter the nucleus, recruit transcriptional coactivators or repressors and bind in complex with them to specific DNA sequences, e.g. the minimal Smad-binding element (SBE) (Jonk et al., 1998) or the BMP-responsive element (BRE) (Korchynskiy and ten Dijke, 2002; Kusanagi et al., 2000). These enhancer elements can be coupled to an easy analyzable reportergene, e.g. luciferase which in turn is activated as an “artificial target gene” of BMP2. By using this assay the effects of different inhibitors or overexpression of specific genes could be investigated.

Cholesterol depletion was accomplished again by the use of Lovastatin and M β CD. Inhibition of cholesterol biosynthesis by Lovastatin resulted in an only 10% reduced BMP2-dependent transcriptional activity compared to untreated cells (Fig. 4.19). Otherwise, M β CD led to much higher reductions (around 60%, Fig. 4.19), obviously due to extensive cholesterol sequestration from and disruption of the plasma membrane (compare 5.2.1). Relying on the Lovastatin results, cholesterol-sensitive membrane regions were shown to be not important for functional BMP signaling.

Following up this result, the influence of caveolae was investigated by overexpression or knockdown of cav-1. Both experiments resulted in reduced luciferase activities consistent

with a decreased transcription of target genes in response to BMP2 (Fig. 4.25, Fig. 4.28). Moreover, BRIA-mediated increase of luciferase activity was reduced by additional expression of cav-1. This negative effect of cav-1 expression was obtained ligand-independently **and** after stimulation with BMP2. Surprisingly, only the overall BMP signaling was reduced, whereas the inducibility by BMP2, calculated by the factor of induction, was not affected. This result indicates that cav-1 overexpression decreases BMP signaling not by disrupting the signaling cascade itself, but rather by affecting the number of signaling molecules which are available at the cell surface. Therefore it would be possible that caveolae constitute locations where BMP signaling is not transduced into the cell. Consequently, transcriptional activity will be reduced when caveolae formation is induced by cav-1 overexpression. Moreover, it could be possible that caveolae are the sites where BMP receptors are degraded and this process would be enhanced by cav-1 overexpression, as it was reported for the TGF- β receptors (Di Guglielmo et al., 2003). However, this possibility needs to be followed up in future experiments.

Cav-1 knockdown by specific siRNA resulted also in a reduction of transcriptional activity. This finding is only explainable by the existence of a critical cav-1 concentration which should be maintained in C2C12 cells for functional BMP signaling; formation of caveolae being only a minor point. This special concentration would be disrupted by overexpression or knockdown of cav-1 and could be recognized by BMP receptors because they were proven to interact with cav-1 (Fig. 4.12, Fig. 4.13) (Nohe et al., 2005). This explanation would also account for the discrepancy between cholesterol depletion- and cav-1 overexpression-experiments. Cholesterol depletion showed no influence on BMP signaling as mentioned above, whereas cav-1 seemed to influence the same read-out system for BMP signaling in both directions. Therefore an influence of the protein cav-1 itself and not the cholesterol-sensitive caveolae is most likely and need to be analyzed in more detail in the future.

Having established that both types of BMP receptors are mainly internalized via CCP-mediated endocytosis (see 5.1.2; collaboration with the group of Prof. Y. Henis; Hartung et al., submitted), a very important question was whether this endocytic pathway is also involved in BMP-Smad signaling. As shown before, Smad1/5 is phosphorylated independently of endocytosis at the cell surface (5.2.1). BRE-luciferase assays revealed that blocking CCP-mediated endocytosis by chlorpromazine reduced BMP2-induced transcriptional activity by 65% (Fig. 4.30). This experiment spatially separates Smad1/5 phosphorylation and the continuation of Smad signaling. Whereas the initial phosphorylation event occurs at the plasma membrane, the Smad signaling cascade, leading to transcription of BMP2-specific target genes, is promoted by CCP-mediated endocytosis. Further experiments should be planned to clarify the question whether CCVs contain other members of the signaling machinery, as it was shown for the TGF- β pathway (Di Guglielmo et al.,

2003). Here, SARA, Smad2 as well as the receptor complex could be localized to EEA1-positive vesicles and Smad2 phosphorylation and TGF- β -induced transcription of target genes were significantly reduced after interfering with CCP-mediated endocytosis (Di Guglielmo et al., 2003).

Finally, dynamin2 mutant K44A was expressed to block endocytosis via CCPs and caveolae. However, the results were inconsistent and not reliable as discussed in 4.3.5.2. These experiments should be repeated and improved in the future.

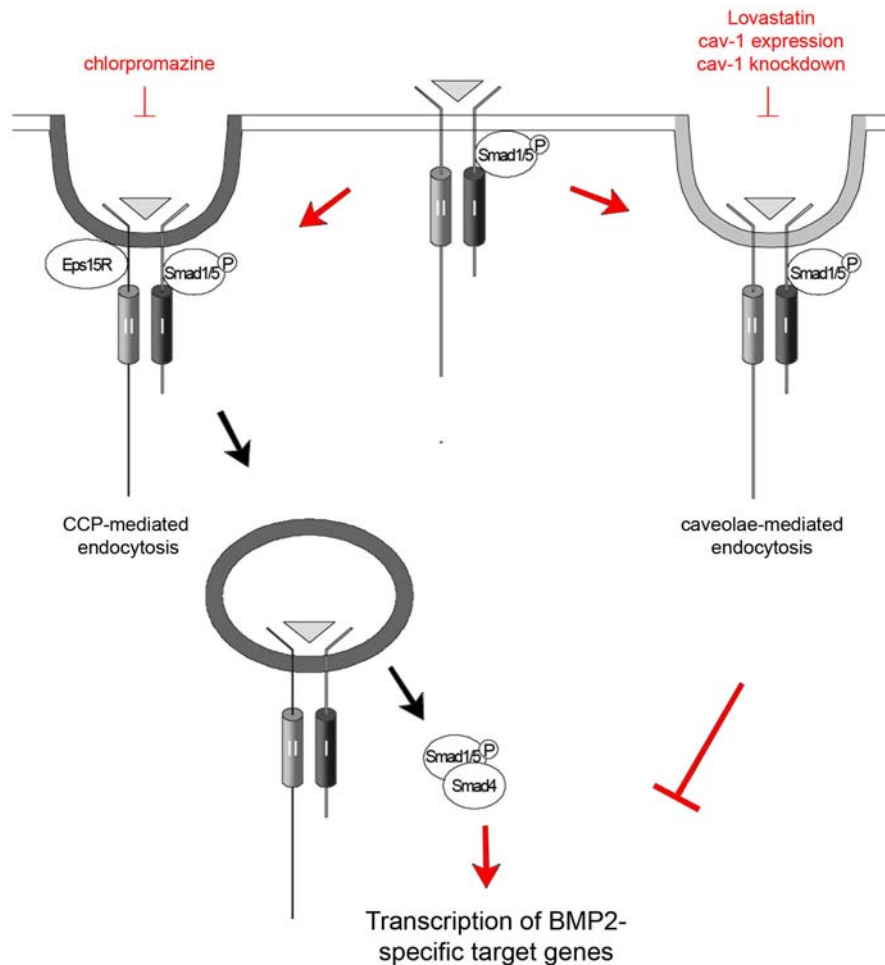


Fig. 5.4 Influence of endocytic events on BMP2 signal transduction.

Transcription of BMP2-specific target genes involves CCP-mediated endocytosis, because transcription was reduced while this internalization pathway was blocked. Moreover, it could be shown that both receptor types are mainly endocytosed through CCPs/CCVs (Hartung et al., submitted). Cholesterol-sensitive membrane domains seemed to be irrelevant for Smad signaling, but cav-1 influenced transcriptional activity in a manner that has to be determined in more detail in the future (result not illustrated above).

In summary, it was found that after phosphorylation of Smad1/5 at the cell surface (5.2.1), the activated receptor complex need to be internalized via CCPs for the induction of transcription of target genes (Fig. 5.4). Otherwise, a critical cav-1 concentration was observed, because enhancing as well as reducing of the cav-1 expression in C2C12 cells led

to reduced BMP signaling. Which kind of influence the interaction of BMP receptors and cav-1 exerts could not be clarified in this study and should be the subject of further experiments.

5.2.3 Effects on Alkaline phosphatase production

ALP is a hydrolase enzyme, dephosphorylating a multitude of substrates throughout the human body. Amongst others it is a marker gene of osteoblast differentiation and its production is induced upon BMP2 stimulation (Takuwa et al., 1991). Controversy remains whether ALP is induced Smad-dependently or Smad-independently. While some groups report that ALP production is regulated by the p38-MAPK pathway with or without influence of ERK signaling (Gallea et al., 2001; Lai and Cheng, 2002; Nohe et al., 2002; Suzuki et al., 2002; Suzuki et al., 1999), others demonstrate for example that infection of Smad1 and Smad5 induced (but Smad6 and Smad7 infection reduced) ALP activity, pointing to an involvement of these signal mediators on ALP production (Fujii et al., 1999). Therefore it would be possible that p38 and Smad1/5 pathways need to be activated by BMPs and induce transcription of another factor which in turn stimulates ALP production. Although this theory is not proven, it is supported by the long time stimulation which is necessary in the ALP assay (72 h, 3.3.7.4).

The ability of ALP to hydrolyze diverse substrates is used to measure its production and activity. Therefore pNPP (p-nitrophenyl-phosphate) acts as an artificial substrate and gets dephosphorylated by ALP to pNP (p-nitrophenol) which has a yellow color. The optical density (OD) can be measured and is proportional to the amount of pNP formed which in turn is proportional to the amount of active ALP present in the assay.

Cholesterol depletion was accomplished by means of Lovastatin and M β CD. The ALP assay showed that both treatments reduced ALP activity by 30 – 50% (Fig. 4.20). It was the only assay in which Lovastatin resulted in the same effect than M β CD, concluding that production of functional ALP depends on cholesterol-sensitive membrane domains.

Otherwise, cav-1 overexpression which should lead to the formation of more caveolae at the cell surface and reduced caveolar endocytosis of some ligands (Fra et al., 1995; Sharma et al., 2004) slightly reduced ALP activity (Fig. 4.26). Considering the relatively high standard deviations in this experiment (Fig. 4.26) as well as the fact that already the empty vector transfection resulted in an around 50% loss of ALP activity (due to cell death triggered by the transfection procedure; data not shown), it is questionable whether the results are reliable.

Having established that cholesterol-dependent plasma membrane regions influence ALP activity, the impact of CCP-mediated endocytosis was investigated. Chlorpromazine, which blocks clathrin-dependent endocytosis, tremendously reduced ALP activity (Fig. 4.31). This result suggests that the production of ALP is reliant on the same endocytic pathway which

promotes BMP-Smad signaling (see 5.2.2) - an interesting finding regarding the still open question of Smad-dependence of ALP production.

In agreement with the previous mentioned results, transfection of dynamin2 wt induced ALP activity, while dynamin2 K44A mutant was shown to reduce it (Fig. 4.34), concluding that ALP is produced in dependence of endocytic events in general.

Fig. 5.5 recapitulates the facts obtained by ALP assays. It can be concluded that ALP production is a process which depends on cholesterol-sensitive membrane domains, what distinguishes it from Smad1/5 phosphorylation and Smad signaling investigated before. Moreover, ALP production seems to be controlled by CCP- and dynamin2-mediated endocytosis which were shown to influence also Smad-dependent BMP signaling.

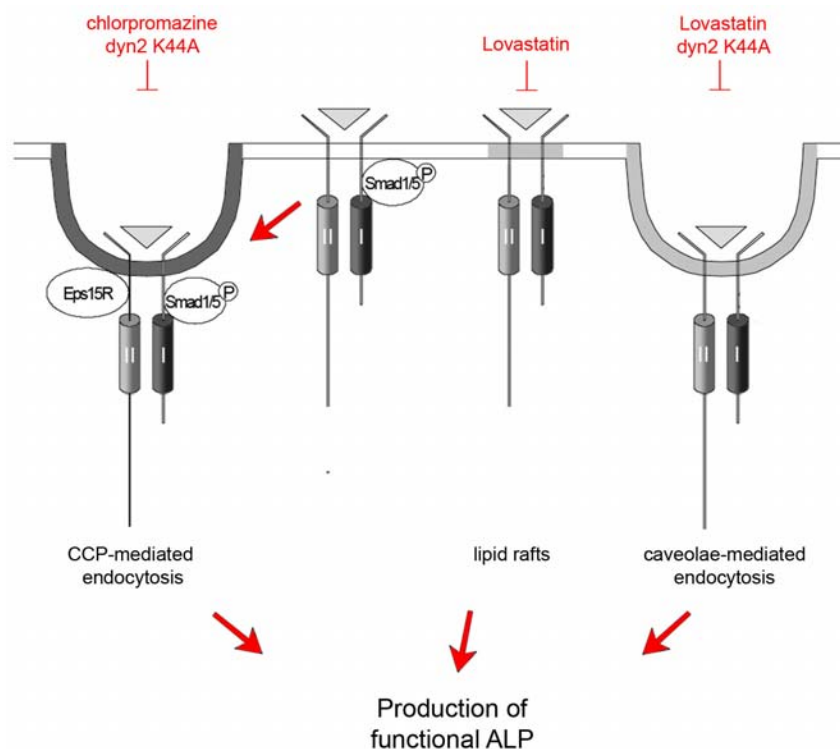


Fig. 5.5 ALP production is influenced by endocytic events.

ALP production is influenced upon inhibition of clathrin-mediated endocytosis and cholesterol-sensitive membrane regions, concluding that ALP is produced most likely in dependence of endocytic events in general.

5.3 THE CURRENT MODEL OF THE ENDOCYTIC IMPACT ON BMP SIGNALING

BMP2 signals are transmitted through distinct signaling cascades, either via Smad-dependent or Smad-independent pathways. Recently, it was shown that these signal transduction pathways are initiated by different oligomerization patterns of BMP receptor complexes. PFCs (preformed signaling complexes) trigger Smad-dependent signaling, whereas Smad-independent signaling via p38 is induced by BISCs (BMP2-induced signaling complexes) (Nohe et al., 2002). The current study demonstrates that also diverse endocytic

mechanisms as well as different discrete plasma membrane regions are involved in BMP signaling.

BMP2-induced signal transduction seems to be compartmentalized. The phosphorylation of Smad1/5 takes place at the cell surface - independent of endocytosis. Continuation of the signaling cascade is promoted by endocytosis demonstrated by the use of different specific inhibitors. Smad-dependent signaling is relying on CCP-mediated endocytosis, while Smad-independent pathways are additionally dependent on cholesterol-sensitive plasma membrane regions (Fig. 5.6).

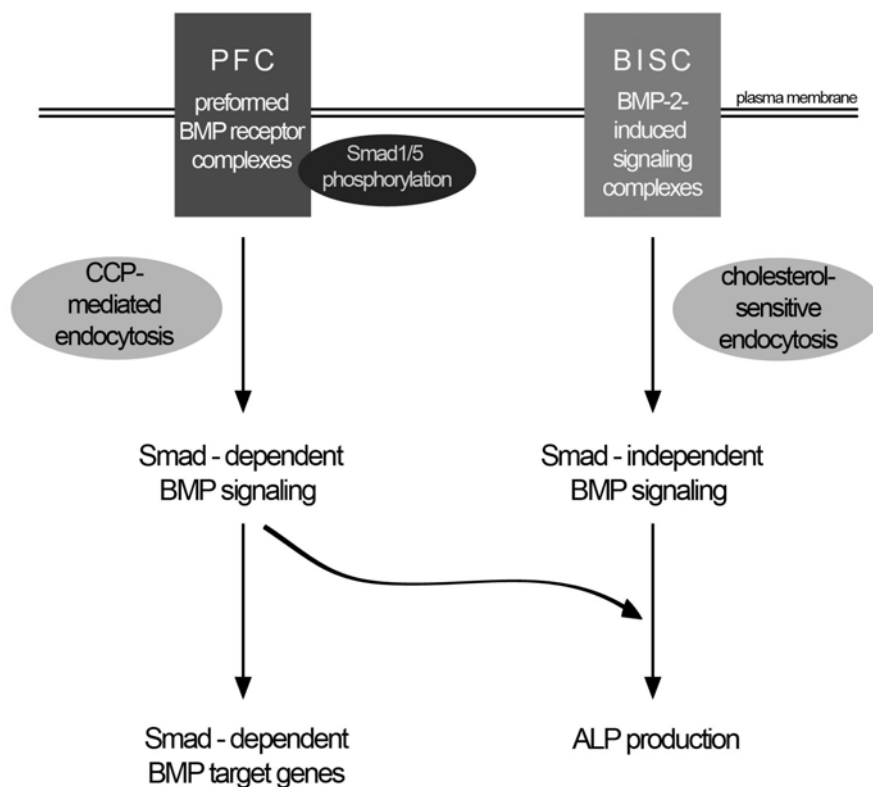


Fig. 5.6 Summary of the effects of BMP receptor localization on BMP signaling (Hartung et al., submitted).

BMP receptors are localized in CCPs and lipid rafts/caveolae and the signaling mode is influenced by their localization and internalization as illustrated. Whereas Smad1/5 is phosphorylated while present at the plasma membrane, Smad-dependent and Smad-independent continuations of BMP signaling rely on endocytic events.

6 SUMMARY – ZUSAMMENFASSUNG

SUMMARY

Endocytosis of growth factor receptors plays an important role in the activation and propagation as well as the attenuation of signaling pathways. Its malfunctioning can cause several pathologies, e.g. by controlling the level of receptors at the cell surface.

BMPs are members of the TGF- β superfamily and are involved in the regulation of proliferation, differentiation, chemotaxis and apoptosis. BMP signaling is initiated at two types of transmembrane serine/threonine kinases, BRI and BRII. BMP receptor activation occurs upon ligand binding to preformed complexes (PFCs) or BMP2-induced signaling complexes (BISCs) composed of BRI and BRII. Binding of BMP2 to PFCs results in activation of the Smad pathway, whereas BISCs initiate the activation of Smad-independent pathways via p38 resulting in the induction of Alkaline phosphatase (ALP).

BMP receptor endocytosis has not been extensively studied and the potential role of localization to different regions of the plasma membrane in determining the signaling pathways activated by PFCs and BISCs was not explored so far.

In the present work, the localization of BMP receptors in distinct membrane domains and the consequential impact on BMP signaling were investigated.

By separating detergent-resistant membranes (DRMs) from cell lysates and subsequent gradient ultracentrifugation, it could be demonstrated that BRI and BRII cofractionate with cav-1, the marker protein of caveolae. Moreover, both receptor types interacted with cav-1 and showed a partially colocalization with cav-1 at the plasma membrane. Although these results point to a caveolar localization, BMP receptors cofractionated also with DRMs in cells exhibiting no caveolae, suggesting an additional non-caveolar raft localization. Beyond that, BRII could also be localized to clathrin-coated pits (CCPs) by means of immuno-electronmicroscopy studies.

The second part of this thesis demonstrated that both membrane regions influence BMP signaling in distinct ways. Smad1/5 was shown to be phosphorylated independently of endocytic events at the cell surface. On the one hand, disruption of DRM regions by cholesterol depletion inhibited specifically BMP2-mediated ALP production, while Smad signaling was unaffected. On the other hand, inhibition of clathrin-mediated endocytosis by specific inhibitors affected BMP2-induced Smad signaling as well as the induction of ALP, suggesting that both Smad-dependent and Smad-independent signaling pathways are required for BMP2 induced ALP production.

These findings propose an important regulatory impact of different endocytic routes and membrane regions on BMP signaling as well as that a distinct membrane localization of BMP receptors account for specific signaling properties initiated at PFCs or BISCs.

ZUSAMMENFASSUNG

Endozytose von Wachstumsfaktor-Rezeptoren spielt eine entscheidende Rolle bei Aktivierung und Übertragung wie auch bei der Schwächung von Signalen. Störungen der Endozytose können schwere Krankheitsbilder hervorrufen, z.B. durch ihren Einfluss auf die Regulation der Rezeptormenge an der Zelloberfläche.

BMPs sind Mitglieder der TGF- β Superfamilie und sind involviert in die Regulation von Proliferation, Differenzierung, Chemotaxis und Apoptose. Zwei Arten von Transmembranproteinen, die Serin/Threonin-Kinase Aktivität besitzen, sind bedeutend für den BMP Signalweg – die BMP Rezeptoren BRI und BRII. Die Aktivierung von BRI und BRII erfolgt durch Ligandenbindung an präformierte Komplexe (PFCs) oder BMP2-induzierte Signalkomplexe (BISCs), die aus beiden Rezeptorarten bestehen. Wenn BMP2 an PFCs bindet, wird die Smad-Signalkaskade initiiert, wohingegen BISCs Smad-unabhängige Signale über p38 weiterleiten, was schließlich zur Produktion von alkalischer Phosphatase (ALP) führt.

Das Feld der BMP Rezeptor Endozytose wurde noch nicht sehr ausführlich untersucht, genauso wenig wie die potentielle Rolle, die unterschiedliche Rezeptorlokalisierungen in verschiedenen Plasmamembran-Regionen bei der Initiierung der Signalwege, die durch PFCs bzw. BISCs aktiviert werden, spielen könnten.

In der vorliegenden Arbeit wurden die Lokalisierung von BMP Rezeptoren in speziellen Membrandomänen sowie deren Einfluss auf die BMP Signalkaskade untersucht.

Mittels Reinigung von Detergenz-resistenten Membranen (DRMs) aus Zellysaten und anschließender Gradientenultrazentrifugation konnte gezeigt werden, dass BRI und BRII mit dem caveolären Markerprotein cav-1 kofraktionieren. Darüber hinaus interagieren beide Rezeptorarten mit cav-1 und koloalisieren auch teilweise mit cav-1 an der Plasmamembran. Obwohl diese Ergebnisse auf ein eindeutiges Vorkommen der Rezeptoren in Caveolae schließen lassen, kofraktionieren sie auch mit DRMs in Zellen, die von Natur aus keine Caveolae ausbilden, woraus man eine zusätzliche nicht-caveoläre Raft-Lokalisierung schlussfolgern kann. Des Weiteren konnte BRII mittels Immun-Elektronenmikroskopie in „clathrin-coated pits“ (CCPs) lokalisiert werden.

Im zweiten Teil der Arbeit wurde gezeigt, dass beide untersuchten Membranregionen die BMP Signalkaskade auf unterschiedliche Art und Weise beeinflussen. Es wurde bewiesen, dass Smad1/5 unabhängig von endozytotischen Vorgängen an der Plasmamembran phosphoryliert wird. Einerseits führte die Zerstörung von DRM-Regionen durch Cholesterindepletion zur spezifischen Inhibierung der BMP2-vermittelten ALP Produktion, ohne gleichzeitig die BMP Signalkaskade über Smads zu beeinflussen. Andererseits bewirkte eine spezifische Blockierung der Clathrin-vermittelten Endozytose eine Inhibition des BMP2-induzierten Smad-Signalwegs und auch der ALP Produktion, was auf ein Zusammenspiel von Smad-unabhängigen und Smad-abhängigen Signalwegen bei der ALP-Induzierung schließen lässt.

Die Ergebnisse der vorliegenden Studie lassen die Schlussfolgerung zu, dass verschiedene endozytotische Wege und Membranregionen einen bedeutenden, regulatorischen Einfluss auf die BMP Signalkaskade ausüben. Weiterhin wurde festgestellt, dass die Membranlokalisierung von BMP Rezeptoren für das Einschlagen verschiedener Signalwege ausgehend von PFCs und BISCs verantwortlich ist.

7 REFERENCES

www.ambion.com

<http://www.expasy.org/prosite/>

- Aderem, A., and D.M. Underhill. 1999. Mechanisms of phagocytosis in macrophages. *Annu Rev Immunol.* 17:593-623.
- Anderson, R.G. 1998. The caveolae membrane system. *Annu Rev Biochem.* 67:199-225.
- Anderson, R.G., and K. Jacobson. 2002. A role for lipid shells in targeting proteins to caveolae, rafts, and other lipid domains. *Science.* 296:1821-5.
- Arora, K., and R. Warrior. 2001. A new Smurf in the village. *Dev Cell.* 1:441-2.
- Atkinson, C., S. Stewart, P.D. Upton, R. Machado, J.R. Thomson, R.C. Trembath, and N.W. Morrell. 2002. Primary pulmonary hypertension is associated with reduced pulmonary vascular expression of type II bone morphogenetic protein receptor. *Circulation.* 105:1672-8.
- Avsian-Kretchmer, O., and A.J. Hsueh. 2004. Comparative genomic analysis of the eight-membered ring cystine knot-containing bone morphogenetic protein antagonists. *Mol Endocrinol.* 18:1-12.
- Babitt, J.L., Y. Zhang, T.A. Samad, Y. Xia, J. Tang, J.A. Campagna, A.L. Schneyer, C.J. Woolf, and H.Y. Lin. 2005. Repulsive guidance molecule (RGMa), a DRAGON homologue, is a bone morphogenetic protein co-receptor. *J Biol Chem.* 280:29820-7.
- Balemans, W., and W. Van Hul. 2002. Extracellular regulation of BMP signaling in vertebrates: a cocktail of modulators. *Dev Biol.* 250:231-50.
- Berk, M., S.Y. Desai, H.C. Heyman, and C. Colmenares. 1997. Mice lacking the ski proto-oncogene have defects in neurulation, craniofacial, patterning, and skeletal muscle development. *Genes Dev.* 11:2029-39.
- Bomsel, M., C. de Paillerets, H. Weintraub, and A. Alfsen. 1986. Lipid bilayer dynamics in plasma and coated vesicle membranes from bovine adrenal cortex. Evidence of two types of coated vesicle involved in the LDL receptor traffic. *Biochim. Biophys. Acta.* 859:15-25.
- Botchkarev, V.A. 2003. Bone morphogenetic proteins and their antagonists in skin and hair follicle biology. *J Invest Dermatol.* 120:36-47.
- Bottner, M., K. Krieglstein, and K. Unsicker. 2000. The transforming growth factor-beta: structure, signaling, and roles in nervous system development and functions. *J Neurochem.* 75:2227-40.
- Boussif, O., F. Lezoualc'h, M.A. Zanta, M.D. Mergny, D. Scherman, B. Demeneix, and J.P. Behr. 1995. A versatile vector for gene and oligonucleotide transfer into cells in culture and in vivo: polyethylenimine. *Proc Natl Acad Sci U S A.* 92:7297-301.
- Bouwmeester, T., S. Kim, Y. Sasai, B. Lu, and E.M. De Robertis. 1996. Cerberus is a head-inducing secreted factor expressed in the anterior endoderm of Spemann's organizer. *Nature.* 382:595-601.
- Brodsky, F.M., C.Y. Chen, C. Knuehl, M.C. Towler, and D.E. Wakeham. 2001. Biological basket weaving: formation and function of clathrin-coated vesicles. *Annu Rev Cell Dev Biol.* 17:517-68.
- Brown, D.A., and E. London. 1998. Structure and origin of ordered lipid domains in biological membranes. *J Membr Biol.* 164:103-14.
- Brown, D.A., and E. London. 2000. Structure and function of sphingolipid- and cholesterol-rich membrane rafts. *J. Biol. Chem.* 275:17221-4.
- Brown, D.A., and J.K. Rose. 1992. Sorting of GPI-anchored proteins to glycolipid-enriched membrane subdomains during transport to the apical cell surface. *Cell.* 68:533-44.
- Brown, J.D., M.R. DiChiara, K.R. Anderson, M.A. Gimbrone, Jr., and J.N. Topper. 1999. MEKK-1, a component of the stress (stress-activated protein kinase/c-Jun N-terminal kinase) pathway, can selectively activate Smad2-mediated transcriptional activation in endothelial cells. *J Biol Chem.* 274:8797-805.

- Brunet, L.J., J.A. McMahon, A.P. McMahon, and R.M. Harland. 1998. Noggin, cartilage morphogenesis, and joint formation in the mammalian skeleton. *Science*. 280:1455-7.
- Brunkow, M.E., J.C. Gardner, J. Van Ness, B.W. Paepers, B.R. Kovacevich, S. Proll, J.E. Skonier, L. Zhao, P.J. Sabo, Y. Fu, R.S. Alisch, L. Gillett, T. Colbert, P. Tacconi, D. Galas, H. Hamersma, P. Beighton, and J. Mulligan. 2001. Bone dysplasia sclerosteosis results from loss of the SOST gene product, a novel cystine knot-containing protein. *Am J Hum Genet*. 68:577-89.
- Cameron, P.L., J.W. Ruffin, R. Bollag, H. Rasmussen, and R.S. Cameron. 1997. Identification of caveolin and caveolin-related proteins in the brain. *J Neurosci*. 17:9520-35.
- Canalis, E., A.N. Economides, and E. Gazzerro. 2003. Bone morphogenetic proteins, their antagonists, and the skeleton. *Endocr. Rev.* 24:218-35.
- Cate, R.L., R.J. Mattaliano, C. Hession, R. Tizard, N.M. Farber, A. Cheung, E.G. Ninfa, A.Z. Frey, D.J. Gash, E.P. Chow, and et al. 1986. Isolation of the bovine and human genes for Mullerian inhibiting substance and expression of the human gene in animal cells. *Cell*. 45:685-98.
- Chamberlain, L.H. 2004. Detergents as tools for the purification and classification of lipid rafts. *FEBS Lett*. 559:1-5.
- Chang, C., D.A. Holtzman, S. Chau, T. Chickering, E.A. Woolf, L.M. Holmgren, J. Bodorova, D.P. Gearing, W.E. Holmes, and A.H. Brivanlou. 2001. Twisted gastrulation can function as a BMP antagonist. *Nature*. 410:483-7.
- Chang, H., D. Huylebroeck, K. Verschueren, Q. Guo, M.M. Matzuk, and A. Zwijsen. 1999. Smad5 knockout mice die at mid-gestation due to multiple embryonic and extraembryonic defects. *Development*. 126:1631-42.
- Chen, D., X. Ji, M.A. Harris, J.Q. Feng, G. Karsenty, A.J. Celeste, V. Rosen, G.R. Mundy, and S.E. Harris. 1998. Differential roles for bone morphogenetic protein (BMP) receptor type IB and IA in differentiation and specification of mesenchymal precursor cells to osteoblast and adipocyte lineages. *J Cell Biol*. 142:295-305.
- Chen, D., M. Zhao, and G.R. Mundy. 2004. Bone morphogenetic proteins. *Growth Factors*. 22:233-41.
- Chen, Y.G., A. Hata, R.S. Lo, D. Wotton, Y. Shi, N. Pavletich, and J. Massague. 1998. Determinants of specificity in TGF-beta signal transduction. *Genes Dev*. 12:2144-52.
- Chen, Y.G., and J. Massague. 1999. Smad1 recognition and activation by the ALK1 group of transforming growth factor-beta family receptors. *J Biol Chem*. 274:3672-7.
- Christiansen, J.H., E.G. Coles, and D.G. Wilkinson. 2000. Molecular control of neural crest formation, migration and differentiation. *Curr Opin Cell Biol*. 12:719-24.
- Coburn, M.C., V.E. Pricolo, F.G. DeLuca, and K.I. Bland. 1995. Malignant potential in intestinal juvenile polyposis syndromes. *Ann Surg Oncol*. 2:386-91.
- Coda, L., A.E. Salcini, S. Confalonieri, G. Pelicci, T. Sorkina, A. Sorkin, P.G. Pelicci, and P.P. Di Fiore. 1998. Eps15R is a tyrosine kinase substrate with characteristics of a docking protein possibly involved in coated pits-mediated internalization. *J Biol Chem*. 273:3003-12.
- Collins, B.M., A.J. McCoy, H.M. Kent, P.R. Evans, and D.J. Owen. 2002. Molecular architecture and functional model of the endocytic AP2 complex. *Cell*. 109:523-35.
- Conese, M., A. Nykjaer, C.M. Petersen, O. Cremona, R. Pardi, P.A. Andreasen, J. Gliemann, E.I. Christensen, and F. Blasi. 1995. alpha-2 Macroglobulin receptor/Ldl receptor-related protein(Lrp)-dependent internalization of the urokinase receptor. *J Cell Biol*. 131:1609-22.
- Conner, S.D., and S.L. Schmid. 2002. Identification of an adaptor-associated kinase, AAK1, as a regulator of clathrin-mediated endocytosis. *J Cell Biol*. 156:921-9.
- Conner, S.D., and S.L. Schmid. 2003. Regulated portals of entry into the cell. *Nature*. 422:37-44.
- Couet, J., S. Li, T. Okamoto, T. Ikezu, and M.P. Lisanti. 1997. Identification of peptide and protein ligands for the caveolin-scaffolding domain. Implications for the interaction of caveolin with caveolae-associated proteins. *J Biol Chem*. 272:6525-33.

- Couet, J., M. Sargiacomo, and M.P. Lisanti. 1997. Interaction of a receptor tyrosine kinase, EGF-R, with caveolins. Caveolin binding negatively regulates tyrosine and serine/threonine kinase activities. *J Biol Chem.* 272:30429-38.
- Dale, L., G. Howes, B.M. Price, and J.C. Smith. 1992. Bone morphogenetic protein 4: a ventralizing factor in early *Xenopus* development. *Development.* 115:573-85.
- Damm, E.M., L. Pelkmans, J. Kartenbeck, A. Mezzacasa, T. Kurzchalia, and A. Helenius. 2005. Clathrin- and caveolin-1-independent endocytosis: entry of simian virus 40 into cells devoid of caveolae. *J Cell Biol.* 168:477-88.
- Das, K., R.Y. Lewis, P.E. Scherer, and M.P. Lisanti. 1999. The membrane-spanning domains of caveolins-1 and -2 mediate the formation of caveolin hetero-oligomers. Implications for the assembly of caveolae membranes in vivo. *J Biol Chem.* 274:18721-8.
- Deng, Z., J.H. Morse, S.L. Slager, N. Cuervo, K.J. Moore, G. Venetos, S. Kalachikov, E. Cayanis, S.G. Fischer, R.J. Barst, S.E. Hodge, and J.A. Knowles. 2000. Familial primary pulmonary hypertension (gene PPH1) is caused by mutations in the bone morphogenetic protein receptor-II gene. *Am J Hum Genet.* 67:737-44.
- Derynck, R., and Y.E. Zhang. 2003. Smad-dependent and Smad-independent pathways in TGF-beta family signalling. *Nature.* 425:577-84.
- Di Fiore, P.P., and P. De Camilli. 2001. Endocytosis and signaling. an inseparable partnership. *Cell.* 106:1-4.
- Di Guglielmo, G.M., C. Le Roy, A.F. Goodfellow, and J.L. Wrana. 2003. Distinct endocytic pathways regulate TGF-beta receptor signalling and turnover. *Nat Cell Biol.* 5:410-21.
- Dietzen, D.J., W.R. Hastings, and D.M. Lublin. 1995. Caveolin is palmitoylated on multiple cysteine residues. Palmitoylation is not necessary for localization of caveolin to caveolae. *J Biol Chem.* 270:6838-42.
- Dong, C., Z. Li, R. Alvarez, Jr., X.H. Feng, and P.J. Goldschmidt-Clermont. 2000. Microtubule binding to Smads may regulate TGF beta activity. *Mol Cell.* 5:27-34.
- Drab, M., P. Verkade, M. Elger, M. Kasper, M. Lohn, B. Lauterbach, J. Menne, C. Lindschau, F. Mende, F.C. Luft, A. Schedl, H. Haller, and T.V. Kurzchalia. 2001. Loss of caveolae, vascular dysfunction, and pulmonary defects in caveolin-1 gene-disrupted mice. *Science.* 293:2449-52.
- DuBridge, R.B., P. Tang, H.C. Hsia, P.M. Leong, J.H. Miller, and M.P. Calos. 1987. Analysis of mutation in human cells by using an Epstein-Barr virus shuttle system. *Mol Cell Biol.* 7:379-87.
- Dupree, P., R.G. Parton, G. Raposo, T.V. Kurzchalia, and K. Simons. 1993. Caveolae and sorting in the trans-Golgi network of epithelial cells. *Embo J.* 12:1597-605.
- Ehehalt, R., P. Keller, C. Haass, C. Thiele, and K. Simons. 2003. Amyloidogenic processing of the Alzheimer beta-amyloid precursor protein depends on lipid rafts. *J Cell Biol.* 160:113-23.
- Ehrlich, M., A. Shmueli, and Y.I. Henis. 2001. A single internalization signal from the dileucine family is critical for constitutive endocytosis of the type II TGF-beta receptor. *J. Cell Sci.* 114:1777-86.
- Elbashir, S.M., J. Harborth, W. Lendeckel, A. Yalcin, K. Weber, and T. Tuschl. 2001. Duplexes of 21-nucleotide RNAs mediate RNA interference in cultured mammalian cells. *Nature.* 411:494-8.
- Engel, M.E., M.A. McDonnell, B.K. Law, and H.L. Moses. 1999. Interdependent SMAD and JNK signaling in transforming growth factor-beta-mediated transcription. *J Biol Chem.* 274:37413-20.
- Engelman, D.M. 2005. Membranes are more mosaic than fluid. *Nature.* 438:578-80.
- Engelman, J.A., X. Zhang, F. Galbiati, D. Volonte, F. Sotgia, R.G. Pestell, C. Minetti, P.E. Scherer, T. Okamoto, and M.P. Lisanti. 1998. Molecular genetics of the caveolin gene family: implications for human cancers, diabetes, Alzheimer disease, and muscular dystrophy. *Am J Hum Genet.* 63:1578-87.
- Enomoto, H., T. Ozaki, E. Takahashi, N. Nomura, S. Tabata, H. Takahashi, N. Ohnuma, M. Tanabe, J. Iwai, H. Yoshida, and et al. 1994. Identification of human DAN gene, mapping to the putative neuroblastoma tumor suppressor locus. *Oncogene.* 9:2785-91.

- Feng, X.H., and R. Derynck. 2005. Specificity and Versatility in TGF- Signaling Through Smads. *Annu Rev Cell Dev Biol.*
- Feron, O., L. Belhassen, L. Kobzik, T.W. Smith, R.A. Kelly, and T. Michel. 1996. Endothelial nitric oxide synthase targeting to caveolae. Specific interactions with caveolin isoforms in cardiac myocytes and endothelial cells. *J Biol Chem.* 271:22810-4.
- Finelli, A.L., C.A. Bossie, T. Xie, and R.W. Padgett. 1994. Mutational analysis of the Drosophila tolloid gene, a human BMP-1 homolog. *Development.* 120:861-70.
- Fingerhut, A., K. von Figura, and S. Honing. 2001. Binding of AP2 to sorting signals is modulated by AP2 phosphorylation. *J Biol Chem.* 276:5476-82.
- Florea, B.I., C. Meaney, H.E. Junginger, and G. Borchard. 2002. Transfection efficiency and toxicity of polyethylenimine in differentiated Calu-3 and nondifferentiated COS-1 cell cultures. *AAPS PharmSci.* 4:E12.
- Fra, A.M., M. Masserini, P. Palestini, S. Sonnino, and K. Simons. 1995. A photo-reactive derivative of ganglioside GM1 specifically cross-links VIP21-caveolin on the cell surface. *FEBS Lett.* 375:11-4.
- Fra, A.M., E. Williamson, K. Simons, and R.G. Parton. 1994. Detergent-insoluble glycolipid microdomains in lymphocytes in the absence of caveolae. *J Biol Chem.* 269:30745-8.
- Fujii, M., K. Takeda, T. Imamura, H. Aoki, T.K. Sampath, S. Enomoto, M. Kawabata, M. Kato, H. Ichijo, and K. Miyazono. 1999. Roles of bone morphogenetic protein type I receptors and Smad proteins in osteoblast and chondroblast differentiation. *Mol Biol Cell.* 10:3801-13.
- Fukuchi, M., T. Imamura, T. Chiba, T. Ebisawa, M. Kawabata, K. Tanaka, and K. Miyazono. 2001. Ligand-dependent degradation of Smad3 by a ubiquitin ligase complex of ROC1 and associated proteins. *Mol Biol Cell.* 12:1431-43.
- Funaba, M., C.M. Zimmerman, and L.S. Mathews. 2002. Modulation of Smad2-mediated signaling by extracellular signal-regulated kinase. *J Biol Chem.* 277:41361-8.
- Gabella, G. 1976. Quantitative morphological study of smooth muscle cells of the guinea-pig taenia coli. *Cell Tissue Res.* 170:161-86.
- Gaidarov, I., F. Santini, R.A. Warren, and J.H. Keen. 1999. Spatial control of coated-pit dynamics in living cells. *Nat Cell Biol.* 1:1-7.
- Galbiati, F., J.A. Engelman, D. Volonte, X.L. Zhang, C. Minetti, M. Li, H. Hou, Jr., B. Kneitz, W. Edelmann, and M.P. Lisanti. 2001. Caveolin-3 null mice show a loss of caveolae, changes in the microdomain distribution of the dystrophin-glycoprotein complex, and t-tubule abnormalities. *J Biol Chem.* 276:21425-33.
- Galbiati, F., D. Volonte, J.A. Engelman, G. Watanabe, R. Burk, R.G. Pestell, and M.P. Lisanti. 1998. Targeted downregulation of caveolin-1 is sufficient to drive cell transformation and hyperactivate the p42/44 MAP kinase cascade. *Embo J.* 17:6633-48.
- Gallea, S., F. Lallemand, A. Atfi, G. Rawadi, V. Ramez, S. Spinella-Jaegle, S. Kawai, C. Faucheu, L. Huet, R. Baron, and S. Roman-Roman. 2001. Activation of mitogen-activated protein kinase cascades is involved in regulation of bone morphogenetic protein-2-induced osteoblast differentiation in pluripotent C2C12 cells. *Bone.* 28:491-8.
- Gannon, F.H., F.S. Kaplan, E. Olmsted, G.C. Finkel, M.A. Zasloff, and E. Shore. 1997. Bone morphogenetic protein 2/4 in early fibromatous lesions of fibrodysplasia ossificans progressiva. *Hum Pathol.* 28:339-43.
- Garamszegi, N., J.J. Dore, Jr., S.G. Penheiter, M. Edens, D. Yao, and E.B. Leof. 2001. Transforming growth factor beta receptor signaling and endocytosis are linked through a COOH terminal activation motif in the type I receptor. *Mol Biol Cell.* 12:2881-93.
- Garcia-Cardena, G., P. Oh, J. Liu, J.E. Schnitzer, and W.C. Sessa. 1996. Targeting of nitric oxide synthase to endothelial cell caveolae via palmitoylation: implications for nitric oxide signaling. *Proc Natl Acad Sci U S A.* 93:6448-53.

- Geraci, M.W., M. Moore, T. Gesell, M.E. Yeager, L. Alger, H. Golpon, B. Gao, J.E. Loyd, R.M. Tuder, and N.F. Voelkel. 2001. Gene expression patterns in the lungs of patients with primary pulmonary hypertension: a gene microarray analysis. *Circ Res.* 88:555-62.
- Gil, J. 1983. Number and distribution of plasmalemmal vesicles in the lung. *Fed Proc.* 42:2414-8.
- Glaser, D.L., A.N. Economides, L. Wang, X. Liu, R.D. Kimble, J.P. Fandl, J.M. Wilson, N. Stahl, F.S. Kaplan, and E.M. Shore. 2003. In vivo somatic cell gene transfer of an engineered Noggin mutein prevents BMP4-induced heterotopic ossification. *J Bone Joint Surg Am.* 85-A:2332-42.
- Glinka, A., W. Wu, D. Onichtchouk, C. Blumenstock, and C. Niehrs. 1997. Head induction by simultaneous repression of Bmp and Wnt signalling in Xenopus. *Nature.* 389:517-9.
- Godbey, W.T., K.K. Wu, and A.G. Mikos. 2001. Poly(ethylenimine)-mediated gene delivery affects endothelial cell function and viability. *Biomaterials.* 22:471-80.
- Goebel, J., K. Forrest, L. Morford, and T.L. Roszman. 2002. Differential localization of IL-2- and -15 receptor chains in membrane rafts of human T cells. *J. Leukoc. Biol.* 72:199-206.
- Gong, Y., D. Krakow, J. Marcelino, D. Wilkin, D. Chitayat, R. Babul-Hirji, L. Hudgins, C.W. Cremers, F.P. Cremers, H.G. Brunner, K. Reinker, D.L. Rimo, D.H. Cohn, F.R. Goodman, W. Reardon, M. Patton, C.A. Francomano, and M.L. Warman. 1999. Heterozygous mutations in the gene encoding noggin affect human joint morphogenesis. *Nat Genet.* 21:302-4.
- Gronroos, E., U. Hellman, C.H. Heldin, and J. Ericsson. 2002. Control of Smad7 stability by competition between acetylation and ubiquitination. *Mol Cell.* 10:483-93.
- Gumbleton, M. 2001. Caveolae as potential macromolecule trafficking compartments within alveolar epithelium. *Adv Drug Deliv Rev.* 49:281-300.
- Hailstones, D., L.S. Sleer, R.G. Parton, and K.K. Stanley. 1998. Regulation of caveolin and caveolae by cholesterol in MDCK cells. *J Lipid Res.* 39:369-79.
- Hammond, S.M., A.A. Caudy, and G.J. Hannon. 2001. Post-transcriptional gene silencing by double-stranded RNA. *Nat Rev Genet.* 2:110-9.
- Hanahan, D. 1983. Studies on transformation of Escherichia coli with plasmids. *J Mol Biol.* 166:557-80.
- Hanyu, A., Y. Ishidou, T. Ebisawa, T. Shimanuki, T. Imamura, and K. Miyazono. 2001. The N domain of Smad7 is essential for specific inhibition of transforming growth factor-beta signaling. *J Cell Biol.* 155:1017-27.
- Harris, S.E., M.A. Harris, P. Mahy, J. Wozney, J.Q. Feng, and G.R. Mundy. 1994. Expression of bone morphogenetic protein messenger RNAs by normal rat and human prostate and prostate cancer cells. *Prostate.* 24:204-11.
- Hassel, S., A. Eichner, M. Yakymovych, U. Hellman, P. Knaus, and S. Souchelnytskyi. 2004. Proteins associated with type II bone morphogenetic protein receptor (BMPRII) and identified by two-dimensional gel electrophoresis and mass spectrometry. *Proteomics.* 4:1346-58.
- Hassel, S., S. Schmitt, A. Hartung, M. Roth, A. Nohe, N. Petersen, M. Ehrlich, Y.I. Henis, W. Sebald, and P. Knaus. 2003. Initiation of Smad-dependent and Smad-independent signaling via distinct BMP-receptor complexes. *J Bone Joint Surg Am.* 85-A Suppl 3:44-51.
- Hata, A., G. Lagna, J. Massague, and A. Hemmati-Brivanlou. 1998. Smad6 inhibits BMP/Smad1 signaling by specifically competing with the Smad4 tumor suppressor. *Genes Dev.* 12:186-97.
- Hay, E., J. Lemonnier, O. Fromigue, and P.J. Marie. 2001. Bone morphogenetic protein-2 promotes osteoblast apoptosis through a Smad-independent, protein kinase C-dependent signaling pathway. *J Biol Chem.* 276:29028-36.
- Hayes, S., A. Chawla, and S. Corvera. 2002. TGF beta receptor internalization into EEA1-enriched early endosomes: role in signaling to Smad2. *J Cell Biol.* 158:1239-49.
- Heerklotz, H. 2002. Triton promotes domain formation in lipid raft mixtures. *Biophys J.* 83:2693-701.

- Helms, J.B., and C. Zurzolo. 2004. Lipids as targeting signals: lipid rafts and intracellular trafficking. *Traffic*. 5:247-54.
- Henley, J.R., E.W. Krueger, B.J. Oswald, and M.A. McNiven. 1998. Dynamin-mediated internalization of caveolae. *J Cell Biol*. 141:85-99.
- Hicke, L. 2001. A new ticket for entry into budding vesicles-ubiquitin. *Cell*. 106:527-30.
- Hinshaw, J.E. 2000. Dynamin and its role in membrane fission. *Annu Rev Cell Dev Biol*. 16:483-519.
- Hocevar, B.A., A. Smine, X.X. Xu, and P.H. Howe. 2001. The adaptor molecule Disabled-2 links the transforming growth factor beta receptors to the Smad pathway. *Embo J*. 20:2789-801.
- Hogan, B.L. 1996. Bone morphogenetic proteins: multifunctional regulators of vertebrate development. *Genes Dev*. 10:1580-94.
- Holley, S.A., J.L. Neul, L. Attisano, J.L. Wrana, Y. Sasai, M.B. O'Connor, E.M. De Robertis, and E.L. Ferguson. 1996. The *Xenopus* dorsalizing factor noggin ventralizes *Drosophila* embryos by preventing DPP from activating its receptor. *Cell*. 86:607-17.
- Hoodless, P.A., T. Haerry, S. Abdollah, M. Stapleton, M.B. O'Connor, L. Attisano, and J.L. Wrana. 1996. MADR1, a MAD-related protein that functions in BMP2 signaling pathways. *Cell*. 85:489-500.
- Hooper, N.M. 1999. Detergent-insoluble glycosphingolipid/cholesterol-rich membrane domains, lipid rafts and caveolae (review). *Mol Membr Biol*. 16:145-56.
- Howe, J.R., J.L. Bair, M.G. Sayed, M.E. Anderson, F.A. Mitros, G.M. Petersen, V.E. Velculescu, G. Traverso, and B. Vogelstein. 2001. Germline mutations of the gene encoding bone morphogenetic protein receptor 1A in juvenile polyposis. *Nat Genet*. 28:184-7.
- Howe, J.R., F.A. Mitros, and R.W. Summers. 1998. The risk of gastrointestinal carcinoma in familial juvenile polyposis. *Ann Surg Oncol*. 5:751-6.
- Howe, J.R., S. Roth, J.C. Ringold, R.W. Summers, H.J. Jarvinen, P. Sistonen, I.P. Tomlinson, R.S. Houlston, S. Bevan, F.A. Mitros, E.M. Stone, and L.A. Aaltonen. 1998. Mutations in the SMAD4/DPC4 gene in juvenile polyposis. *Science*. 280:1086-8.
- Inman, G.J., F.J. Nicolas, and C.S. Hill. 2002. Nucleocytoplasmic shuttling of Smads 2, 3, and 4 permits sensing of TGF-beta receptor activity. *Mol Cell*. 10:283-94.
- Itoh, F., H. Asao, K. Sugamura, C.H. Heldin, P. ten Dijke, and S. Itoh. 2001. Promoting bone morphogenetic protein signaling through negative regulation of inhibitory Smads. *Embo J*. 20:4132-42.
- Itoh, S., F. Itoh, M.J. Goumans, and P. Ten Dijke. 2000. Signaling of transforming growth factor-beta family members through Smad proteins. *Eur J Biochem*. 267:6954-67.
- Janes, P.W., S.C. Ley, and A.I. Magee. 1999. Aggregation of lipid rafts accompanies signaling via the T cell antigen receptor. *J Cell Biol*. 147:447-61.
- Jarvinen, H., and K.O. Franssila. 1984. Familial juvenile polyposis coli; increased risk of colorectal cancer. *Gut*. 25:792-800.
- Jin, Y., G.L. Tipoe, E.C. Liong, T.Y. Lau, P.C. Fung, and K.M. Leung. 2001. Overexpression of BMP-2/4, -5 and BMPR-IA associated with malignancy of oral epithelium. *Oral Oncol*. 37:225-33.
- Jones, C.M., K.M. Lyons, P.M. Lapan, C.V. Wright, and B.L. Hogan. 1992. DVR-4 (bone morphogenetic protein-4) as a posterior-ventralizing factor in *Xenopus* mesoderm induction. *Development*. 115:639-47.
- Jonk, L.J., S. Itoh, C.H. Heldin, P. ten Dijke, and W. Kruijer. 1998. Identification and functional characterization of a Smad binding element (SBE) in the JunB promoter that acts as a transforming growth factor-beta, activin, and bone morphogenetic protein-inducible enhancer. *J Biol Chem*. 273:21145-52.
- Katagiri, T., A. Yamaguchi, M. Komaki, E. Abe, N. Takahashi, T. Ikeda, V. Rosen, J.M. Wozney, A. Fujisawa-Sehara, and T. Suda. 1994. Bone morphogenetic protein-2 converts the differentiation pathway of C2C12 myoblasts into the osteoblast lineage. *J Cell Biol*. 127:1755-66.

- Keller, P., and K. Simons. 1998. Cholesterol is required for surface transport of influenza virus hemagglutinin. *J Cell Biol.* 140:1357-67.
- Kirchhausen, T. 1999. Adaptors for clathrin-mediated traffic. *Annu Rev Cell Dev Biol.* 15:705-32.
- Kirchhausen, T. 2000. Clathrin. *Annu Rev Biochem.* 69:699-727.
- Kirkham, M., A. Fujita, R. Chadda, S.J. Nixon, T.V. Kurzchalia, D.K. Sharma, R.E. Pagano, J.F. Hancock, S. Mayor, and R.G. Parton. 2005. Ultrastructural identification of uncoated caveolin-independent early endocytic vehicles. *J Cell Biol.* 168:465-76.
- Kirsch, T., J. Nickel, and W. Sebald. 2000. BMP-2 antagonists emerge from alterations in the low-affinity binding epitope for receptor BMPR-II. *Embo J.* 19:3314-24.
- Klapisz, E., I. Sorokina, S. Lemeer, M. Pijnenburg, A.J. Verkleij, and P.M. van Bergen en Henegouwen. 2002. A ubiquitin-interacting motif (UIM) is essential for Eps15 and Eps15R ubiquitination. *J. Biol. Chem.* 277:30746-53.
- Knaus, P., and W. Sebald. 2001. Cooperativity of binding epitopes and receptor chains in the BMP/TGFbeta superfamily. *Biol Chem.* 382:1189-95.
- Kogo, H., and T. Fujimoto. 2000. Caveolin-1 isoforms are encoded by distinct mRNAs. Identification Of mouse caveolin-1 mRNA variants caused by alternative transcription initiation and splicing. *FEBS Lett.* 465:119-23.
- Korchynskiy, O., and P. ten Dijke. 2002. Identification and functional characterization of distinct critically important bone morphogenetic protein-specific response elements in the Id1 promoter. *J Biol Chem.* 277:4883-91.
- Kretzschmar, M., J. Doody, I. Timokhina, and J. Massague. 1999. A mechanism of repression of TGFbeta/ Smad signaling by oncogenic Ras. *Genes Dev.* 13:804-16.
- Kretzschmar, M., F. Liu, A. Hata, J. Doody, and J. Massague. 1997. The TGF-beta family mediator Smad1 is phosphorylated directly and activated functionally by the BMP receptor kinase. *Genes Dev.* 11:984-95.
- Kurisaki, A., S. Kose, Y. Yoneda, C.H. Heldin, and A. Moustakas. 2001. Transforming growth factor-beta induces nuclear import of Smad3 in an importin-beta1 and Ran-dependent manner. *Mol Biol Cell.* 12:1079-91.
- Kurzchalia, T.V., P. Dupree, R.G. Parton, R. Kellner, H. Virta, M. Lehnert, and K. Simons. 1992. VIP21, a 21-kD membrane protein is an integral component of trans-Golgi-network-derived transport vesicles. *J Cell Biol.* 118:1003-14.
- Kusanagi, K., H. Inoue, Y. Ishidou, H.K. Mishima, M. Kawabata, and K. Miyazono. 2000. Characterization of a bone morphogenetic protein-responsive Smad-binding element. *Mol Biol Cell.* 11:555-65.
- Kusanagi, K., M. Kawabata, H.K. Mishima, and K. Miyazono. 2001. Alpha-helix 2 in the amino-terminal mad homology 1 domain is responsible for specific DNA binding of Smad3. *J Biol Chem.* 276:28155-63.
- Kusu, N., J. Laurikkala, M. Imanishi, H. Usui, M. Konishi, A. Miyake, I. Thesleff, and N. Itoh. 2003. Sclerostin is a novel secreted osteoclast-derived bone morphogenetic protein antagonist with unique ligand specificity. *J Biol Chem.* 278:24113-7.
- Laemmli, U.K. 1970. Cleavage of structural proteins during the assembly of the head of bacteriophage T4. *Nature.* 227:680-5.
- Lagerholm, B.C., G.E. Weinreb, K. Jacobson, and N.L. Thompson. 2005. Detecting microdomains in intact cell membranes. *Annu Rev Phys Chem.* 56:309-36.
- Lai, C.F., and S.L. Cheng. 2002. Signal transductions induced by bone morphogenetic protein-2 and transforming growth factor-beta in normal human osteoblastic cells. *J Biol Chem.* 277:15514-22.
- Lamaze, C., A. Dujancourt, T. Baba, C.G. Lo, A. Benmerah, and A. Dautry-Varsat. 2001. Interleukin 2 receptors and detergent-resistant membrane domains define a clathrin-independent endocytic pathway. *Mol Cell.* 7:661-71.
- Lane, K.B., R.D. Machado, M.W. Pauculo, J.R. Thomson, J.A. Phillips, 3rd, J.E. Loyd, W.C. Nichols, and R.C. Trembath. 2000. Heterozygous germline mutations in BMPR2, encoding a TGF-beta receptor, cause familial primary pulmonary hypertension. The International PPH Consortium. *Nat Genet.* 26:81-4.

- Le, P.U., and I.R. Nabi. 2003. Distinct caveolae-mediated endocytic pathways target the Golgi apparatus and the endoplasmic reticulum. *J Cell Sci.* 116:1059-71.
- Lechleider, R.J., J.L. Ryan, L. Garrett, C. Eng, C. Deng, A. Wynshaw-Boris, and A.B. Roberts. 2001. Targeted mutagenesis of Smad1 reveals an essential role in chorioallantoic fusion. *Dev Biol.* 240:157-67.
- Lee, P.S., C. Chang, D. Liu, and R. Derynck. 2003. Sumoylation of Smad4, the common Smad mediator of transforming growth factor-beta family signaling. *J Biol Chem.* 278:27853-63.
- Lemonnier, J., C. Ghayor, J. Guicheux, and J. Caverzasio. 2004. Protein kinase C-independent activation of protein kinase D is involved in BMP-2-induced activation of stress mitogen-activated protein kinases JNK and p38 and osteoblastic cell differentiation. *J Biol Chem.* 279:259-64.
- Leong, G.M., N. Subramaniam, J. Figueroa, J.L. Flanagan, M.J. Hayman, J.A. Eisman, and A.P. Kouzmenko. 2001. Ski-interacting protein interacts with Smad proteins to augment transforming growth factor-beta-dependent transcription. *J Biol Chem.* 276:18243-8.
- Li, S., T. Okamoto, M. Chun, M. Sargiacomo, J.E. Casanova, S.H. Hansen, I. Nishimoto, and M.P. Lisanti. 1995. Evidence for a regulated interaction between heterotrimeric G proteins and caveolin. *J Biol Chem.* 270:15693-701.
- Li, S., K.S. Song, and M.P. Lisanti. 1996. Expression and characterization of recombinant caveolin. Purification by polyhistidine tagging and cholesterol-dependent incorporation into defined lipid membranes. *J Biol Chem.* 271:568-73.
- Lindner, R., and E. Ungewickell. 1992. Clathrin-associated proteins of bovine brain coated vesicles. An analysis of their number and assembly-promoting activity. *J Biol Chem.* 267:16567-73.
- Lisanti, M.P., P.E. Scherer, J. Vidugiriene, Z. Tang, A. Hermanowski-Vosatka, Y.H. Tu, R.F. Cook, and M. Sargiacomo. 1994. Characterization of caveolin-rich membrane domains isolated from an endothelial-rich source: implications for human disease. *J Cell Biol.* 126:111-26.
- Liu, J., P. Lee, F. Galbiati, R.N. Kitsis, and M.P. Lisanti. 2001. Caveolin-1 expression sensitizes fibroblastic and epithelial cells to apoptotic stimulation. *Am J Physiol Cell Physiol.* 280:C823-35.
- Lo, R.S., Y.G. Chen, Y. Shi, N.P. Pavletich, and J. Massague. 1998. The L3 loop: a structural motif determining specific interactions between SMAD proteins and TGF-beta receptors. *Embo J.* 17:996-1005.
- Lo, R.S., and J. Massague. 1999. Ubiquitin-dependent degradation of TGF-beta-activated smad2. *Nat Cell Biol.* 1:472-8.
- Lou, J., Y. Tu, S. Li, and P.R. Manske. 2000. Involvement of ERK in BMP-2 induced osteoblastic differentiation of mesenchymal progenitor cell line C3H10T1/2. *Biochem Biophys Res Commun.* 268:757-62.
- Lu, Z., J.T. Murray, W. Luo, H. Li, X. Wu, H. Xu, J.M. Backer, and Y.G. Chen. 2002. Transforming growth factor beta activates Smad2 in the absence of receptor endocytosis. *J. Biol. Chem.* 277:29363-8.
- Lunn, M.P., L.A. Johnson, S.E. Fromholt, S. Itonori, J. Huang, A.A. Vyas, J.E. Hildreth, J.W. Griffin, R.L. Schnaar, and K.A. Sheikh. 2000. High-affinity anti-ganglioside IgG antibodies raised in complex ganglioside knockout mice: reexamination of GD1a immunolocalization. *J Neurochem.* 75:404-12.
- Luo, K., S.L. Stroschein, W. Wang, D. Chen, E. Martens, S. Zhou, and Q. Zhou. 1999. The Ski oncoprotein interacts with the Smad proteins to repress TGFbeta signaling. *Genes Dev.* 13:2196-206.
- Macias-Silva, M., S. Abdollah, P.A. Hoodless, R. Pirone, L. Attisano, and J.L. Wrana. 1996. MADR2 is a substrate of the TGFbeta receptor and its phosphorylation is required for nuclear accumulation and signaling. *Cell.* 87:1215-24.
- Massague, J. 2000. How cells read TGF-beta signals. *Nat Rev Mol Cell Biol.* 1:169-78.
- Massague, J., and Y.G. Chen. 2000. Controlling TGF-beta signaling. *Genes Dev.* 14:627-44.

- McMahon, J.A., S. Takada, L.B. Zimmerman, C.M. Fan, R.M. Harland, and A.P. McMahon. 1998. Noggin-mediated antagonism of BMP signaling is required for growth and patterning of the neural tube and somite. *Genes Dev.* 12:1438-52.
- Merrifield, C.J., M.E. Feldman, L. Wan, and W. Almers. 2002. Imaging actin and dynamin recruitment during invagination of single clathrin-coated pits. *Nat Cell Biol.* 4:691-8.
- Miller, W.E., and R.J. Lefkowitz. 2001. Expanding roles for beta-arrestins as scaffolds and adapters in GPCR signaling and trafficking. *Curr Opin Cell Biol.* 13:139-45.
- Millet, C., P. Lemaire, B. Orsetti, P. Guglielmi, and V. Francois. 2001. The human chordin gene encodes several differentially expressed spliced variants with distinct BMP opposing activities. *Mech Dev.* 106:85-96.
- Minshall, R.D., C. Tiruppathi, S.M. Vogel, W.D. Niles, A. Gilchrist, H.E. Hamm, and A.B. Malik. 2000. Endothelial cell-surface gp60 activates vesicle formation and trafficking via G(i)-coupled Src kinase signaling pathway. *J Cell Biol.* 150:1057-70.
- Mishina, Y., A. Suzuki, N. Ueno, and R.R. Behringer. 1995. Bmpr encodes a type I bone morphogenetic protein receptor that is essential for gastrulation during mouse embryogenesis. *Genes Dev.* 9:3027-37.
- Mishra, S.K., P.A. Keyel, M.J. Hawryluk, N.R. Agostinelli, S.C. Watkins, and L.M. Traub. 2002. Disabled-2 exhibits the properties of a cargo-selective endocytic clathrin adaptor. *Embo J.* 21:4915-26.
- Mitchell, H., A. Choudhury, R.E. Pagano, and E.B. Leof. 2004. Ligand-dependent and -independent transforming growth factor-beta receptor recycling regulated by clathrin-mediated endocytosis and Rab11. *Mol Biol Cell.* 15:4166-78.
- Mobley, B.A., and B.R. Eisenberg. 1975. Sizes of components in frog skeletal muscle measured by methods of stereology. *J Gen Physiol.* 66:31-45.
- Monier, S., R.G. Parton, F. Vogel, J. Behlke, A. Henske, and T.V. Kurzchalia. 1995. VIP21-caveolin, a membrane protein constituent of the caveolar coat, oligomerizes in vivo and in vitro. *Mol Biol Cell.* 6:911-27.
- Morris, S.M., and J.A. Cooper. 2001. Disabled-2 colocalizes with the LDLR in clathrin-coated pits and interacts with AP-2. *Traffic.* 2:111-23.
- Mousavi, S.A., L. Malerod, T. Berg, and R. Kjekken. 2004. Clathrin-dependent endocytosis. *Biochem J.* 377:1-16.
- Moustakas, A., S. Souchelnytskyi, and C.H. Heldin. 2001. Smad regulation in TGF-beta signal transduction. *J Cell Sci.* 114:4359-69.
- Munoz-Sanjuan, I., and A.H. Brivanlou. 2002. Neural induction, the default model and embryonic stem cells. *Nat Rev Neurosci.* 3:271-80.
- Murata, M., J. Peranen, R. Schreiner, F. Wieland, T.V. Kurzchalia, and K. Simons. 1995. VIP21/caveolin is a cholesterol-binding protein. *Proc Natl Acad Sci U S A.* 92:10339-43.
- Napolitano, L. 1963. The Differentiation Of White Adipose Cells. An Electron Microscope Study. *J Cell Biol.* 18:663-79.
- Newman, J.H., L. Wheeler, K.B. Lane, E. Loyd, R. Gaddipati, J.A. Phillips, 3rd, and J.E. Loyd. 2001. Mutation in the gene for bone morphogenetic protein receptor II as a cause of primary pulmonary hypertension in a large kindred. *N Engl J Med.* 345:319-24.
- Nichols, B.J. 2002. A distinct class of endosome mediates clathrin-independent endocytosis to the Golgi complex. *Nat Cell Biol.* 4:374-8.
- Nickel, J., M.K. Dreyer, T. Kirsch, and W. Sebald. 2001. The crystal structure of the BMP-2:BMPR-IA complex and the generation of BMP-2 antagonists. *J Bone Joint Surg Am.* 83-A Suppl 1:S7-14.
- Nishimura, R., K. Hata, F. Ikeda, T. Matsubara, K. Yamashita, F. Ichida, and T. Yoneda. 2003. The role of Smads in BMP signaling. *Front Biosci.* 8:s275-84.
- Niv, H., O. Gutman, Y. Kloog, and Y.I. Henis. 2002. Activated K-Ras and H-Ras display different interactions with saturable nonraft sites at the surface of live cells. *J. Cell Biol.* 157:865-72.

- Nohe, A., S. Hassel, M. Ehrlich, F. Neubauer, W. Sebald, Y.I. Henis, and P. Knaus. 2002. The mode of bone morphogenetic protein (BMP) receptor oligomerization determines different BMP-2 signaling pathways. *J Biol Chem.* 277:5330-8.
- Nohe, A., E. Keating, T.M. Underhill, P. Knaus, and N.O. Petersen. 2005. Dynamics and interaction of caveolin-1 isoforms with BMP-receptors. *J Cell Sci.* 118:643-50.
- Okamoto, T., A. Schlegel, P.E. Scherer, and M.P. Lisanti. 1998. Caveolins, a family of scaffolding proteins for organizing "preassembled signaling complexes" at the plasma membrane. *J Biol Chem.* 273:5419-22.
- Olusanya, O., P.D. Andrews, J.R. Swedlow, and E. Smythe. 2001. Phosphorylation of threonine 156 of the mu2 subunit of the AP2 complex is essential for endocytosis in vitro and in vivo. *Curr Biol.* 11:896-900.
- Onichtchouk, D., Y.G. Chen, R. Dosch, V. Gawantka, H. Delius, J. Massague, and C. Niehrs. 1999. Silencing of TGF-beta signalling by the pseudoreceptor BAMBI. *Nature.* 401:480-5.
- Pagano, R.E. 2003. Endocytic trafficking of glycosphingolipids in sphingolipid storage diseases. *Philos Trans R Soc Lond B Biol Sci.* 358:885-91.
- Palcy, S., and D. Goltzman. 1999. Protein kinase signalling pathways involved in the up-regulation of the rat alpha1(I) collagen gene by transforming growth factor beta1 and bone morphogenetic protein 2 in osteoblastic cells. *Biochem J.* 343 Pt 1:21-7.
- Parton, R.G. 2001. Cell biology. Life without caveolae. *Science.* 293:2404-5.
- Parton, R.G., B. Joggerst, and K. Simons. 1994. Regulated internalization of caveolae. *J Cell Biol.* 127:1199-215.
- Parton, R.G., and A.A. Richards. 2003. Lipid rafts and caveolae as portals for endocytosis: new insights and common mechanisms. *Traffic.* 4:724-38.
- Pelkmans, L., E. Fava, H. Grabner, M. Hannus, B. Habermann, E. Krausz, and M. Zerial. 2005. Genome-wide analysis of human kinases in clathrin- and caveolae/raft-mediated endocytosis. *Nature.* 436:78-86.
- Pelkmans, L., D. Puntener, and A. Helenius. 2002. Local actin polymerization and dynamin recruitment in SV40-induced internalization of caveolae. *Science.* 296:535-9.
- Penheiter, S.G., H. Mitchell, N. Garamszegi, M. Edens, J.J. Dore, Jr., and E.B. Leof. 2002. Internalization-dependent and -independent requirements for transforming growth factor beta receptor signaling via the Smad pathway. *Mol. Cell Biol.* 22:4750-9.
- Peplowska, K., and C. Ungermann. 2005. Expanding dynamin: from fission to fusion. *Nat Cell Biol.* 7:103-4.
- Perry, M.M., and A.B. Gilbert. 1979. Yolk transport in the ovarian follicle of the hen (*Gallus domesticus*): lipoprotein-like particles at the periphery of the oocyte in the rapid growth phase. *J. Cell Sci.* 39:257-72.
- Persson, U., H. Izumi, S. Souchelnytskyi, S. Itoh, S. Grimsby, U. Engstrom, C.H. Heldin, K. Funahashi, and P. ten Dijke. 1998. The L45 loop in type I receptors for TGF-beta family members is a critical determinant in specifying Smad isoform activation. *FEBS Lett.* 434:83-7.
- Peterson, R.S., R.A. Andhare, K.T. Rousche, W. Knudson, W. Wang, J.B. Grossfield, R.O. Thomas, R.E. Hollingsworth, and C.B. Knudson. 2004. CD44 modulates Smad1 activation in the BMP-7 signaling pathway. *J Cell Biol.* 166:1081-91.
- Piccolo, S., E. Agius, L. Leyns, S. Bhattacharyya, H. Grunz, T. Bouwmeester, and E.M. De Robertis. 1999. The head inducer Cerberus is a multifunctional antagonist of Nodal, BMP and Wnt signals. *Nature.* 397:707-10.
- Piccolo, S., E. Agius, B. Lu, S. Goodman, L. Dale, and E.M. De Robertis. 1997. Cleavage of Chordin by Xolloid metalloprotease suggests a role for proteolytic processing in the regulation of Spemann organizer activity. *Cell.* 91:407-16.
- Piccolo, S., Y. Sasai, B. Lu, and E.M. De Robertis. 1996. Dorsoventral patterning in *Xenopus*: inhibition of ventral signals by direct binding of chordin to BMP-4. *Cell.* 86:589-98.
- Pierreux, C.E., F.J. Nicolas, and C.S. Hill. 2000. Transforming growth factor beta-independent shuttling of Smad4 between the cytoplasm and nucleus. *Mol Cell Biol.* 20:9041-54.

- Polo, S., S. Sigismund, M. Faretta, M. Guidi, M.R. Capua, G. Bossi, H. Chen, P. De Camilli, and P.P. Di Fiore. 2002. A single motif responsible for ubiquitin recognition and monoubiquitination in endocytic proteins. *Nature*. 416:451-5.
- Poupon, V., S. Polo, M. Vecchi, G. Martin, A. Dautry-Varsat, N. Cerf-Bensussan, P.P. Di Fiore, and A. Benmerah. 2002. Differential nucleocytoplasmic trafficking between the related endocytic proteins Eps15 and Eps15R. *J. Biol. Chem.* 277:8941-8.
- Pulaski, L., M. Landstrom, C.H. Heldin, and S. Souchelnytskyi. 2001. Phosphorylation of Smad7 at Ser-249 does not interfere with its inhibitory role in transforming growth factor-beta-dependent signaling but affects Smad7-dependent transcriptional activation. *J Biol Chem.* 276:14344-9.
- Puri, V., R. Watanabe, R.D. Singh, M. Dominguez, J.C. Brown, C.L. Wheatley, D.L. Marks, and R.E. Pagano. 2001. Clathrin-dependent and -independent internalization of plasma membrane sphingolipids initiates two Golgi targeting pathways. *J Cell Biol.* 154:535-47.
- Ramos, M., M.W. Lame, H.J. Segall, and D.W. Wilson. 2006. The BMP type II receptor is located in lipid rafts, including caveolae, of pulmonary endothelium in vivo and in vitro. *Vascul Pharmacol.* 44:50-9.
- Razani, B., T.P. Combs, X.B. Wang, P.G. Frank, D.S. Park, R.G. Russell, M. Li, B. Tang, L.A. Jelicks, P.E. Scherer, and M.P. Lisanti. 2002. Caveolin-1-deficient mice are lean, resistant to diet-induced obesity, and show hypertriglyceridemia with adipocyte abnormalities. *J Biol Chem.* 277:8635-47.
- Razani, B., J.A. Engelman, X.B. Wang, W. Schubert, X.L. Zhang, C.B. Marks, F. Macaluso, R.G. Russell, M. Li, R.G. Pestell, D. Di Vizio, H. Hou, Jr., B. Kneitz, G. Lagaud, G.J. Christ, W. Edelmann, and M.P. Lisanti. 2001. Caveolin-1 null mice are viable but show evidence of hyperproliferative and vascular abnormalities. *J Biol Chem.* 276:38121-38.
- Razani, B., X.B. Wang, J.A. Engelman, M. Battista, G. Lagaud, X.L. Zhang, B. Kneitz, H. Hou, Jr., G.J. Christ, W. Edelmann, and M.P. Lisanti. 2002. Caveolin-2-deficient mice show evidence of severe pulmonary dysfunction without disruption of caveolae. *Mol Cell Biol.* 22:2329-44.
- Razani, B., S.E. Woodman, and M.P. Lisanti. 2002. Caveolae: from cell biology to animal physiology. *Pharmacol Rev.* 54:431-67.
- Razani, B., X.L. Zhang, M. Bitzer, G. von Gersdorff, E.P. Bottinger, and M.P. Lisanti. 2001. Caveolin-1 regulates transforming growth factor (TGF)-beta/SMAD signaling through an interaction with the TGF-beta type I receptor. *J Biol Chem.* 276:6727-38.
- Redinbaugh, M.G., and R.B. Turley. 1986. Adaptation of the bicinchoninic acid protein assay for use with microtiter plates and sucrose gradient fractions. *Anal Biochem.* 153:267-71.
- Ridley, A.J. 2001. Rho proteins: linking signaling with membrane trafficking. *Traffic.* 2:303-10.
- Robinson, M.S., and J.S. Bonifacino. 2001. Adaptor-related proteins. *Curr Opin Cell Biol.* 13:444-53.
- Rodal, S.K., G. Skretting, O. Garred, F. Vilhardt, B. van Deurs, and K. Sandvig. 1999. Extraction of cholesterol with methyl-beta-cyclodextrin perturbs formation of clathrin-coated endocytic vesicles. *Mol Biol Cell.* 10:961-74.
- Rodriguez Esteban, C., J. Capdevila, A.N. Economides, J. Pascual, A. Ortiz, and J.C. Izpisua Belmonte. 1999. The novel Cer-like protein Caronte mediates the establishment of embryonic left-right asymmetry. *Nature.* 401:243-51.
- Rosenzweig, B.L., T. Imamura, T. Okadome, G.N. Cox, H. Yamashita, P. ten Dijke, C.H. Heldin, and K. Miyazono. 1995. Cloning and characterization of a human type II receptor for bone morphogenetic proteins. *Proc Natl Acad Sci U S A.* 92:7632-6.
- Ross, J.J., O. Shimmi, P. Vilmos, A. Petryk, H. Kim, K. Gaudenz, S. Hermanson, S.C. Ekker, M.B. O'Connor, and J.L. Marsh. 2001. Twisted gastrulation is a conserved extracellular BMP antagonist. *Nature.* 410:479-83.
- Rothberg, K.G., J.E. Heuser, W.C. Donzell, Y.S. Ying, J.R. Glenney, and R.G. Anderson. 1992. Caveolin, a protein component of caveolae membrane coats. *Cell.* 68:673-82.

- Roux, P.P., and J. Blenis. 2004. ERK and p38 MAPK-activated protein kinases: a family of protein kinases with diverse biological functions. *Microbiol Mol Biol Rev.* 68:320-44.
- Runyan, C.E., H.W. Schnaper, and A.C. Poncelet. 2005. The role of internalization in transforming growth factor beta1-induced Smad2 association with Smad anchor for receptor activation (SARA) and Smad2-dependent signaling in human mesangial cells. *J. Biol. Chem.* 280:8300-8.
- Sabharanjak, S., P. Sharma, R.G. Parton, and S. Mayor. 2002. GPI-anchored proteins are delivered to recycling endosomes via a distinct cdc42-regulated, clathrin-independent pinocytotic pathway. *Dev Cell.* 2:411-23.
- Samad, T.A., A. Rebbapragada, E. Bell, Y. Zhang, Y. Sidis, S.J. Jeong, J.A. Campagna, S. Perusini, D.A. Fabrizio, A.L. Schneyer, H.Y. Lin, A.H. Brivanlou, L. Attisano, and C.J. Woolf. 2005. DRAGON, a bone morphogenetic protein co-receptor. *J Biol Chem.* 280:14122-9.
- Sandvig, K., S. Olsnes, J.E. Brown, O.W. Petersen, and B. van Deurs. 1989. Endocytosis from coated pits of Shiga toxin: a glycolipid-binding protein from *Shigella dysenteriae* 1. *J Cell Biol.* 108:1331-43.
- Sanger, F., S. Nicklen, and A.R. Coulson. 1977. DNA sequencing with chain-terminating inhibitors. *Proc Natl Acad Sci U S A.* 74:5463-7.
- Sargiacomo, M., P.E. Scherer, Z. Tang, E. Kubler, K.S. Song, M.C. Sanders, and M.P. Lisanti. 1995. Oligomeric structure of caveolin: implications for caveolae membrane organization. *Proc Natl Acad Sci U S A.* 92:9407-11.
- Sargiacomo, M., M. Sudol, Z. Tang, and M.P. Lisanti. 1993. Signal transducing molecules and glycosyl-phosphatidylinositol-linked proteins form a caveolin-rich insoluble complex in MDCK cells. *J Cell Biol.* 122:789-807.
- Scherer, P.E., R.Y. Lewis, D. Volonte, J.A. Engelman, F. Galbiati, J. Couet, D.S. Kohtz, E. van Donselaar, P. Peters, and M.P. Lisanti. 1997. Cell-type and tissue-specific expression of caveolin-2. Caveolins 1 and 2 co-localize and form a stable hetero-oligomeric complex in vivo. *J Biol Chem.* 272:29337-46.
- Scherer, P.E., M.P. Lisanti, G. Baldini, M. Sargiacomo, C.C. Mastick, and H.F. Lodish. 1994. Induction of caveolin during adipogenesis and association of GLUT4 with caveolin-rich vesicles. *J Cell Biol.* 127:1233-43.
- Scherer, P.E., T. Okamoto, M. Chun, I. Nishimoto, H.F. Lodish, and M.P. Lisanti. 1996. Identification, sequence, and expression of caveolin-2 defines a caveolin gene family. *Proc Natl Acad Sci U S A.* 93:131-5.
- Scherer, P.E., Z. Tang, M. Chun, M. Sargiacomo, H.F. Lodish, and M.P. Lisanti. 1995. Caveolin isoforms differ in their N-terminal protein sequence and subcellular distribution. Identification and epitope mapping of an isoform-specific monoclonal antibody probe. *J Biol Chem.* 270:16395-401.
- Scheufler, C., W. Sebald, and M. Hulsmeyer. 1999. Crystal structure of human bone morphogenetic protein-2 at 2.7 Å resolution. *J Mol Biol.* 287:103-15.
- Schmid, S.L. 1997. Clathrin-coated vesicle formation and protein sorting: an integrated process. *Annu Rev Biochem.* 66:511-48.
- Schnitzer, J.E., P. Oh, E. Pinney, and J. Allard. 1994. Filipin-sensitive caveolae-mediated transport in endothelium: reduced transcytosis, scavenger endocytosis, and capillary permeability of select macromolecules. *J Cell Biol.* 127:1217-32.
- Schubert, W., P.G. Frank, B. Razani, D.S. Park, C.W. Chow, and M.P. Lisanti. 2001. Caveolae-deficient endothelial cells show defects in the uptake and transport of albumin in vivo. *J Biol Chem.* 276:48619-22.
- Schuck, S., M. Honsho, K. Ekroos, A. Shevchenko, and K. Simons. 2003. Resistance of cell membranes to different detergents. *Proc Natl Acad Sci U S A.* 100:5795-800.
- Schwartz, E.A., E. Reaven, J.N. Topper, and P.S. Tsao. 2005. Transforming growth factor-beta receptors localize to caveolae and regulate endothelial nitric oxide synthase in normal human endothelial cells. *Biochem J.* 390:199-206.
- Scott, I.C., I.L. Blitz, W.N. Pappano, S.A. Maas, K.W. Cho, and D.S. Greenspan. 2001. Homologues of Twisted gastrulation are extracellular cofactors in antagonism of BMP signalling. *Nature.* 410:475-8.

- Seto, E.S., H.J. Bellen, and T.E. Lloyd. 2002. When cell biology meets development: endocytic regulation of signaling pathways. *Genes Dev.* 16:1314-36.
- Sever, S., H. Damke, and S.L. Schmid. 2000. Garrotes, springs, ratchets, and whips: putting dynamin models to the test. *Traffic.* 1:385-92.
- Sharma, D.K., J.C. Brown, A. Choudhury, T.E. Peterson, E. Holicky, D.L. Marks, R. Simari, R.G. Parton, and R.E. Pagano. 2004. Selective stimulation of caveolar endocytosis by glycosphingolipids and cholesterol. *Mol Biol Cell.* 15:3114-22.
- Sharma, D.K., A. Choudhury, R.D. Singh, C.L. Wheatley, D.L. Marks, and R.E. Pagano. 2003. Glycosphingolipids internalized via caveolar-related endocytosis rapidly merge with the clathrin pathway in early endosomes and form microdomains for recycling. *J Biol Chem.* 278:7564-72.
- Shi, Y., A. Hata, R.S. Lo, J. Massague, and N.P. Pavletich. 1997. A structural basis for mutational inactivation of the tumour suppressor Smad4. *Nature.* 388:87-93.
- Shvartsman, D.E., M. Kotler, R.D. Tall, M.G. Roth, and Y.I. Henis. 2003. Differently anchored influenza hemagglutinin mutants display distinct interaction dynamics with mutual rafts. *J. Cell Biol.* 163:879-88.
- Sigismund, S., T. Woelk, C. Puri, E. Maspero, C. Tacchetti, P. Transidico, P.P. Di Fiore, and S. Polo. 2005. Clathrin-independent endocytosis of ubiquitinated cargos. *Proc Natl Acad Sci U S A.* 102:2760-5.
- Simons, K., and R. Ehehalt. 2002. Cholesterol, lipid rafts, and disease. *J Clin Invest.* 110:597-603.
- Simons, K., and E. Ikonen. 1997. Functional rafts in cell membranes. *Nature.* 387:569-72.
- Simons, K., and D. Toomre. 2000. Lipid rafts and signal transduction. *Nat Rev Mol Cell Biol.* 1:31-9.
- Singer, S.J., and G.L. Nicolson. 1972. The fluid mosaic model of the structure of cell membranes. *Science.* 175:720-31.
- Singh, R.D., V. Puri, J.T. Valiyaveetil, D.L. Marks, R. Bittman, and R.E. Pagano. 2003. Selective caveolin-1-dependent endocytosis of glycosphingolipids. *Mol. Biol. Cell.* 14:3254-65.
- Sirard, C., J.L. de la Pompa, A. Elia, A. Itie, C. Mirtsos, A. Cheung, S. Hahn, A. Wakeham, L. Schwartz, S.E. Kern, J. Rossant, and T.W. Mak. 1998. The tumor suppressor gene Smad4/Dpc4 is required for gastrulation and later for anterior development of the mouse embryo. *Genes Dev.* 12:107-19.
- Sledz, C.A., M. Holko, M.J. de Veer, R.H. Silverman, and B.R. Williams. 2003. Activation of the interferon system by short-interfering RNAs. *Nat Cell Biol.* 5:834-9.
- Sledz, C.A., and B.R. Williams. 2004. RNA interference and double-stranded-RNA-activated pathways. *Biochem Soc Trans.* 32:952-6.
- Slepnev, V.I., and P. De Camilli. 2000. Accessory factors in clathrin-dependent synaptic vesicle endocytosis. *Nat Rev Neurosci.* 1:161-72.
- Smart, E.J., G.A. Graf, M.A. McNiven, W.C. Sessa, J.A. Engelman, P.E. Scherer, T. Okamoto, and M.P. Lisanti. 1999. Caveolins, liquid-ordered domains, and signal transduction. *Mol Cell Biol.* 19:7289-304.
- Snyder, E.M., Y. Nong, C.G. Almeida, S. Paul, T. Moran, E.Y. Choi, A.C. Nairn, M.W. Salter, P.J. Lombroso, G.K. Gouras, and P. Greengard. 2005. Regulation of NMDA receptor trafficking by amyloid-beta. *Nat. Neurosci.* 8:1051-8.
- Song, B.D., and S.L. Schmid. 2003. A molecular motor or a regulator? Dynamin's in a class of its own. *Biochemistry.* 42:1369-76.
- Song, K.S., S. Li, T. Okamoto, L.A. Quilliam, M. Sargiacomo, and M.P. Lisanti. 1996. Co-purification and direct interaction of Ras with caveolin, an integral membrane protein of caveolae microdomains. Detergent-free purification of caveolae microdomains. *J Biol Chem.* 271:9690-7.
- Song, K.S., M. Sargiacomo, F. Galbiati, M. Parenti, and M.P. Lisanti. 1997. Targeting of a G alpha subunit (Gi1 alpha) and c-Src tyrosine kinase to caveolae membranes: clarifying the role of N-myristoylation. *Cell Mol Biol (Noisy-le-grand).* 43:293-303.

- Song, K.S., Z. Tang, S. Li, and M.P. Lisanti. 1997. Mutational analysis of the properties of caveolin-1. A novel role for the C-terminal domain in mediating homo-typic caveolin-caveolin interactions. *J Biol Chem.* 272:4398-403.
- Sunyach, C., A. Jen, J. Deng, K.T. Fitzgerald, Y. Frobert, J. Grassi, M.W. McCaffrey, and R. Morris. 2003. The mechanism of internalization of glycosylphosphatidylinositol-anchored prion protein. *Embo J.* 22:3591-601.
- Suzuki, A., J. Guicheux, G. Palmer, Y. Miura, Y. Oiso, J.P. Bonjour, and J. Caverzasio. 2002. Evidence for a role of p38 MAP kinase in expression of alkaline phosphatase during osteoblastic cell differentiation. *Bone.* 30:91-8.
- Suzuki, A., G. Palmer, J.P. Bonjour, and J. Caverzasio. 1999. Regulation of alkaline phosphatase activity by p38 MAP kinase in response to activation of Gi protein-coupled receptors by epinephrine in osteoblast-like cells. *Endocrinology.* 140:3177-82.
- Takahara, K., G.E. Lyons, and D.S. Greenspan. 1994. Bone morphogenetic protein-1 and a mammalian tolloid homologue (mTld) are encoded by alternatively spliced transcripts which are differentially expressed in some tissues. *J Biol Chem.* 269:32572-8.
- Takei, K., P.S. McPherson, S.L. Schmid, and P. De Camilli. 1995. Tubular membrane invaginations coated by dynamin rings are induced by GTP-gamma S in nerve terminals. *Nature.* 374:186-90.
- Takuwa, Y., C. Ohse, E.A. Wang, J.M. Wozney, and K. Yamashita. 1991. Bone morphogenetic protein-2 stimulates alkaline phosphatase activity and collagen synthesis in cultured osteoblastic cells, MC3T3-E1. *Biochem Biophys Res Commun.* 174:96-101.
- Tang, Z., P.E. Scherer, T. Okamoto, K. Song, C. Chu, D.S. Kohtz, I. Nishimoto, H.F. Lodish, and M.P. Lisanti. 1996. Molecular cloning of caveolin-3, a novel member of the caveolin gene family expressed predominantly in muscle. *J Biol Chem.* 271:2255-61.
- Tebar, F., S.K. Bohlander, and A. Sorkin. 1999. Clathrin assembly lymphoid myeloid leukemia (CALM) protein: localization in endocytic-coated pits, interactions with clathrin, and the impact of overexpression on clathrin-mediated traffic. *Mol Biol Cell.* 10:2687-702.
- Thiele, C., M.J. Hannah, F. Fahrenholz, and W.B. Huttner. 2000. Cholesterol binds to synaptophysin and is required for biogenesis of synaptic vesicles. *Nat Cell Biol.* 2:42-9.
- Thomsen, P., K. Roepstorff, M. Stahlhut, and B. van Deurs. 2002. Caveolae are highly immobile plasma membrane microdomains, which are not involved in constitutive endocytic trafficking. *Mol Biol Cell.* 13:238-50.
- Tremblay, K.D., N.R. Dunn, and E.J. Robertson. 2001. Mouse embryos lacking Smad1 signals display defects in extra-embryonic tissues and germ cell formation. *Development.* 128:3609-21.
- Triantafilou, K., M. Triantafilou, and R.L. Dedrick. 2001. A CD14-independent LPS receptor cluster. *Nat Immunol.* 2:338-45.
- Tsukazaki, T., T.A. Chiang, A.F. Davison, L. Attisano, and J.L. Wrana. 1998. SARA, a FYVE domain protein that recruits Smad2 to the TGFbeta receptor. *Cell.* 95:779-91.
- Ulloa, L., J. Doody, and J. Massague. 1999. Inhibition of transforming growth factor-beta/SMAD signalling by the interferon-gamma/STAT pathway. *Nature.* 397:710-3.
- Urist, M.R. 1965. Bone: formation by autoinduction. *Science.* 150:893-9.
- van der Blik, A.M., T.E. Redelmeier, H. Damke, E.J. Tisdale, E.M. Meyerowitz, and S.L. Schmid. 1993. Mutations in human dynamin block an intermediate stage in coated vesicle formation. *J. Cell Biol.* 122:553-63.
- Vinals, F., T. Lopez-Rovira, J.L. Rosa, and F. Ventura. 2002. Inhibition of PI3K/p70 S6K and p38 MAPK cascades increases osteoblastic differentiation induced by BMP-2. *FEBS Lett.* 510:99-104.
- Vukicevic, S., F.P. Luyten, and A.H. Reddi. 1989. Stimulation of the expression of osteogenic and chondrogenic phenotypes in vitro by osteogenin. *Proc Natl Acad Sci U S A.* 86:8793-7.

References

- Waite, K.A., and C. Eng. 2003. From developmental disorder to heritable cancer: it's all in the BMP/TGF-beta family. *Nat Rev Genet.* 4:763-73.
- Wang, L.H., K.G. Rothberg, and R.G. Anderson. 1993. Mis-assembly of clathrin lattices on endosomes reveals a regulatory switch for coated pit formation. *J Cell Biol.* 123:1107-17.
- Wang, W., F.V. Mariani, R.M. Harland, and K. Luo. 2000. Ski represses bone morphogenic protein signaling in *Xenopus* and mammalian cells. *Proc Natl Acad Sci U S A.* 97:14394-9.
- Watanabe, M., N. Masuyama, M. Fukuda, and E. Nishida. 2000. Regulation of intracellular dynamics of Smad4 by its leucine-rich nuclear export signal. *EMBO Rep.* 1:176-82.
- Waugh, M.G., D. Lawson, and J.J. Hsuan. 1999. Epidermal growth factor receptor activation is localized within low-buoyant density, non-caveolar membrane domains. *Biochem J.* 337 (Pt 3):591-7.
- Way, M., and R.G. Parton. 1995. M-caveolin, a muscle-specific caveolin-related protein. *FEBS Lett.* 376:108-12.
- Wicks, S.J., S. Lui, N. Abdel-Wahab, R.M. Mason, and A. Chantry. 2000. Inactivation of smad-transforming growth factor beta signaling by Ca(2+)-calmodulin-dependent protein kinase II. *Mol Cell Biol.* 20:8103-11.
- Wilde, A., and F.M. Brodsky. 1996. In vivo phosphorylation of adaptors regulates their interaction with clathrin. *J Cell Biol.* 135:635-45.
- Winnier, G., M. Blessing, P.A. Labosky, and B.L. Hogan. 1995. Bone morphogenetic protein-4 is required for mesoderm formation and patterning in the mouse. *Genes Dev.* 9:2105-16.
- Wolf, A.A., Y. Fujinaga, and W.I. Lencer. 2002. Uncoupling of the cholera toxin-G(M1) ganglioside receptor complex from endocytosis, retrograde Golgi trafficking, and downstream signal transduction by depletion of membrane cholesterol. *J Biol Chem.* 277:16249-56.
- Wrana, J.L., L. Attisano, R. Wieser, F. Ventura, and J. Massague. 1994. Mechanism of activation of the TGF-beta receptor. *Nature.* 370:341-7.
- Wu, J.W., M. Hu, J. Chai, J. Seoane, M. Huse, C. Li, D.J. Rigotti, S. Kyin, T.W. Muir, R. Fairman, J. Massague, and Y. Shi. 2001. Crystal structure of a phosphorylated Smad2. Recognition of phosphoserine by the MH2 domain and insights on Smad function in TGF-beta signaling. *Mol Cell.* 8:1277-89.
- Xia, Y., Y. Sidis, A. Mukherjee, T.A. Samad, G. Brenner, C.J. Woolf, H.Y. Lin, and A. Schneyer. 2005. Localization and action of Dragon (repulsive guidance molecule b), a novel bone morphogenetic protein coreceptor, throughout the reproductive axis. *Endocrinology.* 146:3614-21.
- Xiao, Z., N. Watson, C. Rodriguez, and H.F. Lodish. 2001. Nucleocytoplasmic shuttling of Smad1 conferred by its nuclear localization and nuclear export signals. *J Biol Chem.* 276:39404-10.
- Xu, L., Y.G. Chen, and J. Massague. 2000. The nuclear import function of Smad2 is masked by SARA and unmasked by TGFbeta-dependent phosphorylation. *Nat Cell Biol.* 2:559-62.
- Xu, L., Y. Kang, S. Col, and J. Massague. 2002. Smad2 nucleocytoplasmic shuttling by nucleoporins CAN/Nup214 and Nup153 feeds TGFbeta signaling complexes in the cytoplasm and nucleus. *Mol Cell.* 10:271-82.
- Xu, M.Q., G. Feldman, M. Le Merrer, Y.Y. Shugart, D.L. Glaser, J.A. Urtizberea, M. Fardeau, J.M. Connor, J. Triffitt, R. Smith, E.M. Shore, and F.S. Kaplan. 2000. Linkage exclusion and mutational analysis of the noggin gene in patients with fibrodysplasia ossificans progressiva (FOP). *Clin Genet.* 58:291-8.
- Yagi, K., D. Goto, T. Hamamoto, S. Takenoshita, M. Kato, and K. Miyazono. 1999. Alternatively spliced variant of Smad2 lacking exon 3. Comparison with wild-type Smad2 and Smad3. *J Biol Chem.* 274:703-9.
- Yakymovych, I., P. Ten Dijke, C.H. Heldin, and S. Souchelnytskyi. 2001. Regulation of Smad signaling by protein kinase C. *Faseb J.* 15:553-5.

- Yamada, E. 1955. The fine structure of the gall bladder epithelium of the mouse. *J Biophys Biochem Cytol.* 1:445-58.
- Yamaguchi, A., T. Katagiri, T. Ikeda, J.M. Wozney, V. Rosen, E.A. Wang, A.J. Kahn, T. Suda, and S. Yoshiki. 1991. Recombinant human bone morphogenetic protein-2 stimulates osteoblastic maturation and inhibits myogenic differentiation in vitro. *J Cell Biol.* 113:681-7.
- Yang, X., L.H. Castilla, X. Xu, C. Li, J. Gotay, M. Weinstein, P.P. Liu, and C.X. Deng. 1999. Angiogenesis defects and mesenchymal apoptosis in mice lacking SMAD5. *Development.* 126:1571-80.
- Yang, X., C. Li, X. Xu, and C. Deng. 1998. The tumor suppressor SMAD4/DPC4 is essential for epiblast proliferation and mesoderm induction in mice. *Proc Natl Acad Sci U S A.* 95:3667-72.
- Yao, D., M. Ehrlich, Y.I. Henis, and E.B. Leof. 2002. Transforming growth factor-beta receptors interact with AP2 by direct binding to beta2 subunit. *Mol. Biol. Cell.* 13:4001-12.
- Yi, S.E., A. Daluiski, R. Pederson, V. Rosen, and K.M. Lyons. 2000. The type I BMP receptor BMPRII is required for chondrogenesis in the mouse limb. *Development.* 127:621-30.
- Yokouchi, Y., K.J. Vogan, R.V. Pearce, 2nd, and C.J. Tabin. 1999. Antagonistic signaling by Caronte, a novel Cerberus-related gene, establishes left-right asymmetric gene expression. *Cell.* 98:573-83.
- Yoshida, Y., S. Matsuda, and T. Yamamoto. 1997. Cloning and characterization of the mouse tob gene. *Gene.* 191:109-13.
- Yoshida, Y., S. Tanaka, H. Umemori, O. Minowa, M. Usui, N. Ikematsu, E. Hosoda, T. Imamura, J. Kuno, T. Yamashita, K. Miyazono, M. Noda, T. Noda, and T. Yamamoto. 2000. Negative regulation of BMP/Smad signaling by Tob in osteoblasts. *Cell.* 103:1085-97.
- Young, R.A., and R.W. Davis. 1983. Efficient isolation of genes by using antibody probes. *Proc Natl Acad Sci U S A.* 80:1194-8.
- Zawel, L., J.L. Dai, P. Buckhaults, S. Zhou, K.W. Kinzler, B. Vogelstein, and S.E. Kern. 1998. Human Smad3 and Smad4 are sequence-specific transcription activators. *Mol Cell.* 1:611-7.
- Zhang, H., and A. Bradley. 1996. Mice deficient for BMP2 are nonviable and have defects in amnion/chorion and cardiac development. *Development.* 122:2977-86.
- Zhang, Y., C. Chang, D.J. Gehling, A. Hemmati-Brivanlou, and R. Derynck. 2001. Regulation of Smad degradation and activity by Smurf2, an E3 ubiquitin ligase. *Proc Natl Acad Sci U S A.* 98:974-9.
- Zhao, Y.Y., Y. Liu, R.V. Stan, L. Fan, Y. Gu, N. Dalton, P.H. Chu, K. Peterson, J. Ross, Jr., and K.R. Chien. 2002. Defects in caveolin-1 cause dilated cardiomyopathy and pulmonary hypertension in knockout mice. *Proc Natl Acad Sci U S A.* 99:11375-80.
- Zhou, X.P., K. Woodford-Richens, R. Lehtonen, K. Kurose, M. Aldred, H. Hampel, V. Launonen, S. Virta, R. Pilarski, R. Salovaara, W.F. Bodmer, B.A. Conrad, M. Dunlop, S.V. Hodgson, T. Iwama, H. Jarvinen, I. Kellokumpu, J.C. Kim, B. Leggett, D. Markie, J.P. Mecklin, K. Neale, R. Phillips, J. Piris, P. Rozen, R.S. Houlston, L.A. Aaltonen, I.P. Tomlinson, and C. Eng. 2001. Germline mutations in BMPRII/ALK3 cause a subset of cases of juvenile polyposis syndrome and of Cowden and Bannayan-Riley-Ruvalcaba syndromes. *Am J Hum Genet.* 69:704-11.
- Zhu, H., P. Kavsak, S. Abdollah, J.L. Wrana, and G.H. Thomsen. 1999. A SMAD ubiquitin ligase targets the BMP pathway and affects embryonic pattern formation. *Nature.* 400:687-93.
- Zimmerman, L.B., J.M. De Jesus-Escobar, and R.M. Harland. 1996. The Spemann organizer signal noggin binds and inactivates bone morphogenetic protein 4. *Cell.* 86:599-606.

A 1 ABBREVIATIONS

Chemicals/Materials

AA	Acrylamid	HEPES	N-2-hydroxyethylpiperazine-2'-ethansulfonic acid
Amp	Ampicillin	HHB	HANKS-HEPES-buffer
APS	ammonium persulfate	HRP	Horseradish peroxidase
ATP	adenosine triphosphate	LB	Luria bertani
BAA	N,N'-Methylenbisacrylamid	LM	Lovastatin/Mevalonate
BCA	Bicinchoninic acid	LPDS	Lipoprotein-deficient serum
BSA	Bovine serum albumin	Luminol	3-Aminophthalhydrazide
CHAPS	3-[(3-cholamydopropyl)dimethyl-ammonio]-1-propanesulfonate	M β CD	Methyl- β -cyclodextrin
CP	Chlorpromazine	MMLV	Mouse Moloney murine leukemia virus
DEAE	Diethylaminoethyl	PBS	Phosphate buffered saline
dH ₂ O	deionized water	PEI	Polyethylenimine
DMEM	Dulbecco's modified eagle medium	PFA	paraformaldehyde
DMSO	Dimethylsulfoxid	PMSF	Phenylmethylsulfonylfluorid
dNTP	2'-Desoxy-nucleosid-5'-triphosphate	pNPP	p-nitrophenyl-phosphate
DTT	Dithiothreitol	RNase	Ribonuclease
EDTA	Ethylendiammintetraacetate	SDS	Sodium dodecylsulfate
EGFP	enhanced green fluorescent protein	<i>Taq</i>	<i>Thermophilus aquaticus</i>
EtBr	Ethidiumbromide	TBS	TRIS buffered saline
EtOH	Ethanol	TCA	Trichlor acetic acid
FCS	fetal calf serum	TEMED	N,N,N',N'-Tetramethyl-ethylendiamine
GFP	green fluorescent protein	TRIS	TRIS-(hydroxymethyl)-aminomethane
HA	hemagglutinin	Triton X-100	4-(1,1,3,3-Tetramethylbutyl)cyclohexyl-polyethylene glycol

Terms

A β	amyloid-beta	dyn2	dynamamin 2
ADP	Adenosine Diphosphate	ECL	enhanced chemoluminescence
ActRI/II	Activin type I/II receptor	EEA1	Early Endosomal Antigen 1
ALK	Activin-like kinase	EGF	Epidermal Growth Factor
ALP	Alkaline phosphatase	EGFR	EGF receptor
AMH	Anti Mullerian Hormone	EM	electronmicroscopy
AP	assembly protein	eNOS	endothelial nitric oxide synthase
APP	amyloid precursor protein	Eps15	EGFR pathway substrate clone 15
ARF6	ADP-ribosylation factor 6	Eps15R	Eps15-related protein
ATP	Adenosine Triphosphate	ERK	extracellular signal-related kinase
BAMBI	BMP and Activin membrane bound inhibitor	FGF	Fibroblast Growth Factor
BISC	BMP2-induced signaling complex	Fig.	Figure
BMP	Bone morphogenetic protein	FOP	Fibrodysplasia Ossificans Progressiva
BRI/BRII	BMP type I/II receptor	FRAP	Fluorescence recovery after photobleaching
BRE	BMP-responsive element	GAP	GTPase activating protein
CamKII	Ca ²⁺ /calmodulin-dependent kinase	GDF	Growth and differentiation factor
cav	caveolin	GED	GTPase effector domain
CBP	CREB-binding protein	GPI	Glycosylphosphatidylinositol
CCP	clathrin-coated pit	G-protein	GTP-binding protein
CCV	clathrin-coated vesicle	GS-box	glycine/serine rich region
cdc42	cell division cycle 42 (G-protein)	GSL	glycosphingolipid
CME	clathrin-mediated endocytosis	GST	Glutathione S-Transferase
CMV	Cytomegalovirus	GTP	Guanosine triphosphate
CREB	cAMP response element binding protein	HPLC	High performance liquid chromatography
CSD	caveolin scaffolding domain	Id1	inhibitor of differentiation 1
CTB	cholera toxin-B subunit	I-EM	immuno-electronmicroscopy
dab-2	Disabled-2	IF	immunofluorescence
DAN	differential screening-selected gene aberrant in neuroblastoma	Ig	Immunoglobulin
DNA	Deoxyribonucleic acid	IL2R β	Interleukin 2 receptor β
Dpp	Decapentaplegic	IP	immunoprecipitation
DRM	detergent-resistant membrane	JAK	Janus kinase

Appendix

ds	double stranded	JNK	c-Jun N-terminal kinase
JPS	Juvenile Polyposis	RNA	Ribonucleic acid
ld	liquid (phase)	RNAi	RNA interference
LDL	low-density lipoprotein	RT-PCR	reverse transcriptase-PCR
LF	long form (of BRII)	SARA	Smad anchor for receptor activation
lo	liquid-ordered (phase)	SBE	Smad-binding element
MAD	Mother against Dpp	SF	short form (of BRII)
MAPK	mitogen-activated protein kinase	Shh	sonic hedgehog
MEF	mouse embryonic fibroblast	siRNA	small interfering RNA
MEKK	MAP/ERK kinase	skip	c-ski-interacting protein
MH	MAD-homology (domain)	Smurf	Smad ubiquitination regulatory factor
MIS	Mullerian inhibiting substance	sno	c-ski-related novel protein
MKK	MAP kinase kinase	sog	short gastrulation
mRNA	messenger RNA	SOST	Sclerostin
NES	nuclear export signal	STAT	signal transducer and activator of transcription
NLS	nuclear localization sequence	SUMO	small ubiquitin-related modifier
NMDA	N-methyl-D-aspartate	SV40	Simian Virus 40
NMT	N-myristoyltransferase	TAB	TAK binding protein
OD	optical density	TAK1	TGF- β activated kinase 1
PAGE	Polyacrylamide gelelectrophoresis	TC	truncation
PAK	p21-activated kinase	Tfn	transferrin
PCR	Polymerase chain reaction	TGF- β	Transforming growth factor- β
PDGF	platelet-derived growth factor	TK	thymidine kinase
PFC	preformed complex	Tld	Tolloid
PH	pleckstrin homology (domain)	Tob	transducer of Erb-B2
pH	power of hydrogen	Tsg	twisted gastrulation
PI3K	Phosphatidylinositol-3-kinase	UV	ultraviolet
PKC/PKD	protein kinase C/D	VIP-21	Vesicular integral-membrane protein of 21 kD
PPH	primary pulmonary hypertension	WB	western blot
PRD	proline/arginine rich domain	wnt	wingless-type MMTV integration site family
Ras	rat sarcoma (G-protein, proto-oncogene)	Wt	wildtype
RISC	RNA-induced silencing complex	XIAP	X-chromosome linked inhibitor of apoptosis
RLTK	Renilla luciferase with thymidine kinase promoter		

Units

bp	basepairs	min	minutes
°C	degree Celsius	ml	milliliter
g	gram	mM	millimolar
h	hours	nM	nanomolar
k	kilo-	RLU	relative light units
kb	Kilobases	rpm	rounds per minute
kD	Kilodalton	RT	room temperature
l	Liter	S	seconds
μ	micro	V	Volt
M	molar		

A 2 SEQUENCES OF RECEPTOR CONSTRUCTS AND OLIGONUCLEOTIDES

BRII-LF, BRII-SF and BRII-TC1 (Nohe et al., 2002)

Homo sapiens BRII protein sequence (NCBI accession: Q13873)

```
1-26 signal sequence                27-1038 mature protein chain
1   mtsslqrpwrvpwlpwtillvstaaasqnqerlcafkdpyqqdlgigesr
51  ishengtilcskgstcyglwekskgdinlvkqgcwshigdpqechyeecv
101 vtttppsiqnqgyrfccstdlcnvnftenfpppdttplspphsfnrde
    151-171 transmembrane domain
151 iialasvsvlavlivalfgyrmltgdrkqglhsmnmmeaaasepsldl
    27-202 BRII-TC1                203-504 kinase domain
201 dnllklleligrgrgygavykgslderpvavkvfsfanrqnfinekniyrvp
251 lmehdniaarfivgdervtadgrmeyllvmeyypngslckylslhtsdwvs
301 scrlahsvtrglaylhtelprgdhykpaishrdlnsrnvlvknegtcviv
351 dfglsmrltgnrlvrpgeednaaisevgtiryapevlegavnlrdeca
401 lkqvdmyalgliyweifmrctdlfpgesvpeyqmafqt evgnhptfedmq
451 vlvsrekqrpkfpeawkenslavrsketiedcdwqdaearltaqcaer
    27-530 BRII-SF
501 maelmmiwernksvsptvnpstamqnerllshnrrvpkigpydyssss
551 yiedsihhtdsivknissehsmstpltigeknrnsinyerqqaqarips
601 petsvtslstntttnttngltpstgmttisempypdetnlhttnvaqsig
651 ptpvclqlteedletnkldpkevdknlkessdenlmehslkqfsgpdpls
701 stsssllypliklaveatgqqdftqtangqaclipdvlptqiypkqqn
```


cav-1 human specific primers for PCR reaction (see 4.1.1)

Product size: 164 bp

huCav1/F = oah20: 5' - tct cta cac cgt tcc cat cc -3'

huCav1/R = oah21: 5' - caa tct tga cca cgt cat cg -3'

cav-1 mouse specific primers for PCR reaction (see 4.1.1)

Differentiation between cav-1 α - and - β -isoforms is possible (Kogo and Fujimoto, 2000).

FL (=cav-1 α)-specific

Product size: 551 bp

a-start/F = oah07: 5' - acg atg tct ggg ggc aaa tac -3'

stop/R = oah11: 5' - tca tat ctc ttt ctg cgt gct gat -3'

5' V (= cav-1 β)-specific

Product size: 574 bp

5' V/F2 = oah09: 5' - ctt ttc ttc cca ccg ctg ttg c -3'

stop/R = oah11: 5' - tca tat ctc ttt ctg cgt gct gat -3'

DANKSAGUNG

Ich möchte Prof. Petra Knaus dafür danken, dass Du mich für dieses Thema begeistert hast sowie für Deine positive Grundstimmung! Außerdem gabst Du mir die Möglichkeit, an verschiedenen Konferenzen teilzunehmen und Kollaborationen zu anderen Gruppen aufzubauen. Vielen Dank für diese Erfahrungen!

Ich danke Prof. W. Sebald sehr für die Unterstützung vor allem im letzten Jahr meiner Promotion und dafür, dass ich – fast wie zuvor – im 313er Lab arbeiten konnte!

Prof. G. Krohne danke ich sehr herzlich für die Übernahme des Zweitgutachtens und immer wieder sehr hilfreiche Tipps sowie ein offenes Ohr bei der Umsetzung der elektronenmikroskopischen Studien.

Ein herzliches Dankeschön geht an Prof. E. Conzelmann, für interessante Diskussionen über Membranen und Trennungsmethoden sowie einige Abende gemeinsamer Laborarbeit.

For fruitful collaborations I like to thank Prof. Y. Henis, Keren Bitton-Worms, Maya Mouler Rechtman, Prof. G. Harms and Dr. A. Noskov. I am especially thankful to Yoav because you really cared about me and my work and had such an inspiring and motivating impact on me! Thanks a lot!

Bettina Lakeit, Ulli Borst und Wolfgang Hädelt danke ich von Herzen, vor allem für Euren unermüdlichen Einsatz, organisatorische Probleme so unbürokratisch wie möglich und mit vollem persönlichen Einsatz zu lösen!

Tausend Dank an Simone Hillgärtner und Nadine Yurdagül-Hemmrich! Ich weiß nicht, wo ich ohne Euch wäre – auf alle Fälle wäre alles viel langsamer vorangegangen! Ganz zu schweigen von unserer Freundschaft, die sich entwickelt hat und die ich sehr schätze!

Elisabeth Meyer-Natus und Daniela Bunsen danke ich sehr für die Präparation der Proben für die Elektronenmikroskopie. Danke für viele nützliche Ratschläge und die Zeit, die Ihr mir und meiner Arbeit gewidmet habt!

Meine Arbeit haben im Labor einige besondere Menschen begleitet und beeinflusst, denen ich im Speziellen danken möchte. Raphaela Schwappacher, Valeska Wenzel, Dr. Sylke Hassel und Dr. Marei Sammar haben mich in all meinen Vorhaben unterstützt, mit mir wissenschaftlich und privat diskutiert und hatten immer ein offenes Ohr für mich! Eure Meinung war und ist mir immer besonders wichtig. Ich schätze jeden von Euch sehr!

Guys, we are the weirdest herd, I've ever seen...!

Meinen Freundinnen Heike Busse und Simone Baumeister gilt großer Dank! Während Heikes telefonischer Beistand unersetzlich ist, danke ich Simone vor allem für praktische Hilfen und Ablenkung vom manchmal frustrierenden Laboralltag! D A N K E !

Ganz zum Schluss kommen immer die allerwichtigsten Personen! Mein Dank kennt keine Worte für meinen Ehemann Steffen Reichert, meine Eltern Ulla und Thomas Hartung und meinen Bruder Stefan Hartung! Nicht jeder hat solch ein liebendes und unterstützendes, familiäres Umfeld und ich fühle mich privilegiert und stolz, Euch zu haben!

LEBENS LAUF

Persönliche Daten

Anke Hartung

geboren am 18.03.1974 in Bleicherode

verheiratet

Anstellungen

- 05/02 – 08/05 Wissenschaftliche Mitarbeiterin, Promotion
Julius-Maximilians Universität, Würzburg
Physiologische Chemie II, Biozentrum
- 04/01 – 10/01 Wissenschaftliche Mitarbeiterin, Diplomarbeit
Aventis Pharma Deutschland GmbH, Frankfurt
Disease Group “Thrombosis and Degenerative Joint Diseases”
- 11/99 – 03/00 Wissenschaftliche Mitarbeiterin, Praktikum
Aventis Pharma Deutschland GmbH, Frankfurt
Disease Group “Thrombosis and Degenerative Joint Diseases”

Ausbildung

- 05/02 – heute Promotionsstudium Biologie
Julius-Maximilians Universität, Würzburg
Physiologische Chemie II, Biozentrum
Dissertation: Localization of BMP receptors in distinct plasma membrane
domains and its impact on BMP signaling
- 04/98 – 03/02 Studium der Biologie (Biochemie, Pharmazeutische Biologie, Molekulare
Pflanzenphysiologie)
Julius-Maximilians Universität, Würzburg
Abschluss: Diplom
Diplomarbeit: Etablierung einer Col2A1-Promotor-Linie zur Genexpression
in chondrozytären Zellen
- 11/94 – 03/98 Studium des Gymnasiallehramts (Biologie, Chemie)
Julius-Maximilians Universität, Würzburg
Abschluss: Zwischenprüfung
- 12/89 - 07/94 Julius Echter Gymnasium, Eisenfeld
Abschluss: Allgemeine Hochschulreife

SCHRIFTENVERZEICHNIS

Publications

Hartung, A., Bitton-Worms, K., Mouler Rechtman, M., Wenzel, V., Börgermann, J., Hassel, S., Henis, Y.I., Knaus, P.: Different routes of BMP receptor endocytosis influence BMP signaling
submitted

Sammar, M., Stricker, S., Schwabe, G.C., Sieber, C., Hartung, A., Hanke, M., Oishi, I., Pohl, J., Minami, Y., Sebald, W., Mundlos, S., Knaus, P. (2004): Modulation of GDF5/BRI-b signalling through interaction with the tyrosine kinase receptor Ror2 *Genes Cells* **9(12)**:1227-38

Hassel, S., Schmitt, S., Hartung, A., Roth, M., Nohe, A., Peterson, N., Ehrlich, M., Henis, Y.I., Sebald, W., Knaus, P. (2003): Initiation of Smad-dependent and Smad-independent signaling via distinct BMP-receptor complexes *J Bone Joint Surg Am* **85 Suppl.3**:44-51

Oral presentations

Hartung, A., Worms, K., Noskov, A., Wenzel, V., Harms, G.S., Henis, Y., Knaus, P. (2005): Localization of BMP receptors in specific plasma membrane domains *1st German Workshop on TGF-beta, Kloster Weltenburg (Kelheim)*, 22.-24.04.2005

Hartung, A. (2003): BMP-receptor assembly in distinct plasma membrane domains *Jahrestagung des Internationalen Graduiertenprogramms "Molecular Biology and Medicine of the Lung"*, **Rauischholzhausen**, 04.-06.08.2003

Poster presentations

Hartung, A., Börgermann, J., Worms, K., Noskov, A., Wenzel, V., Harms, G.S., Henis, Y., Knaus, P. (2005): Localization of BMP receptors in specific plasma membrane microdomains *7th Young Scientist Meeting der Deutschen Gesellschaft für Zellbiologie "Vesicular Trafficking"*, **Jena**, 22.-24.09.2005

Hartung, A., Worms, K., Wenzel, V., Henis, Y., Knaus, P. (2005): Localization of BMP receptors in specific plasma membrane microdomains *Deutsche Gesellschaft für Zellbiologie Meeting*, **Heidelberg**, 16.-19.03.2005

Hartung, A., Hassel, S., Noskov, A., Harms, G.S., Knaus, P. (2004): Localization of BMP receptors in specific plasma membrane microdomains *FASEB conference "Protein Lipidation, Signaling and Membrane Domains"*, **Tucson**, 24.-29.07.2004

Hartung, A., Hassel, S., Henis, Y.I., Knaus, P. (2004): Initiation of Smad-dependent and Smad-independent signaling via distinct BMP-receptor complexes and plasma membrane domains *Strategies in Tissue Engineering*, **Würzburg**, 17.-19.06.2004

Hartung, A., Hassel, S., Henis, Y.I., Knaus, P. (2004): Initiation of Smad-dependent and Smad-independent signaling via distinct BMP-receptor complexes and plasma membrane domains *Deutsche Gesellschaft für Zellbiologie Meeting*, **Berlin**, 24.-27.03.2004

Hassel, S., Hartung, A., Schwappacher, R., Schmitt, S., Nohe, A., Souchelytskyi, S., Henis, Y.I., Sebald, W., Knaus, P. (2003): BMP receptor oligomerization determines the initiation of different signalling cascades *FASEB conference "The TGF- β Superfamily: Signalling & Development"*, **Tucson**, 12.-17.07.2003

Hassel, S., Hartung, A., Schmitt, S., Nohe, A., Souchelytskyi, S., Henis, Y.I., Sebald, W., Knaus, P. (2002): BMP receptor oligomerization determines the initiation of different signalling cascades *Gordon Research Conference "Peptide Growth Factors"*, **New Hampshire**, 2002

Hassel, S., Hartung, A., Schmitt, S., Nohe, A., Henis, Y.I., Sebald, W., Knaus, P. (2002): Initiation of Smad-dependent and Smad-independent signalling via distinct BMP-receptor complexes *4th International Conference on Bone Morphogenetic Proteins*, **Sacramento**, 2002

ERKLÄRUNG

Hiermit erkläre ich ehrenwörtlich, dass ich die vorliegende Dissertation in allen Teilen selbständig angefertigt und keine anderen als die von mir angegebenen Quellen und Hilfsmittel verwendet habe.

Ich erkläre weiterhin, dass ich diese Dissertation weder in gleicher noch in ähnlicher Form in anderen Prüfungsverfahren vorgelegt habe.

Ich habe außer den mit dem Zulassungsgesuch urkundlich vorgelegten Graden keine weiteren akademischen Grade erworben oder zu erwerben versucht.

San Diego, im Februar 2006